Dissertation

Zur Erlangung des Doktorgrades der Fakultät für Chemie und Pharmazie der Ludwig-Maximilians-Universität München

Targeted RNAi and pDNA based therapy for gastrointestinal tumors

Arzu Cengizeroglu
aus Augsburg
2012

Dissertation

Zur Erlangung des Doktorgrades der Fakultät für Chemie und Pharmazie der Ludwig-Maximilians-Universität München

Targeted RNAi and pDNA based therapy for gastrointestinal tumors

vorgelegt von
Arzu Cengizeroglu
aus Augsburg, Deutschland
2012

Erklärung

Diese Dissertation wurde im Sinne von § 7 Abs. 1,2 bzw. 4 bis 7 der Promotionsordnung vom 28. November 2011 von Professor Dr. Ernst Wagner von der Fakultät für Chemie und Pharmazie vertreten.

Eidesstattliche Versicherung

Diese Dissertation wurde selbständig, ohne unerlaubte Hilfe erarbeitet.

München, am 02.03.2012

……
(Unterschrift des Autors)

Dissertation eingereicht am 16.01.2012

1. Gutacher: Prof. Dr. Ernst Wagner

2. Gutacher: PD Dr. Manfred Ogris

Mündliche Prüfung am 01.03.2012

Ever tried.

Ever failed.

No matter.

TRY AGAIN

Fail again.

Fail better.

Samuel Beckett

dedicated to my family and partner
in love and gratitude

1. Table of contents

2. Introduction

2.1. Nucleic acid-based therapy - progress and prospects

The idea of human gene therapy – viral and non-viral – came into existence in the early 1970ies[2-4]. A four-year old girl became the first gene therapy patient on Sept. 14th, 1990 at the NIH Clinical Centre, who was treated with autologous T cells genetically-corrected by retroviral-mediated insertion of a normal ADA gene[5]. As a result of this first successful treatment other clinical trials were initiated[6, 7]. The original idea of nucleic-based therapy, where the correction of defective genes in genetic as well as acquired diseases either in an *ex vivo* or an *in vivo* approach was attemtpted, has been further developed. Generally, therapy approaches can be divided in direct compensation of genetic defects or target gene silencing – of genes which are either pathogenic or essential for cell viability. Worldwide more than 2000 clinical trials on nucleic acid-based therapeutics are being executed with disease patterns covering as diverse fields as inherent genetic diseases like severe combined immunodeficiency (SCID) and acquired diseases like HIV infection. The main focus of clinical gene therapies, though, lies on the treatment of cancer, with a majority of clinical trials targeting epigenetic and genetic alterations of tumor suppressors and oncogenes[8] – the cause of malignant diseases. Cancer cells have defects in the regulatory control systems regulating normal cell proliferation and homeostasis. Most cancers are diverse in the mutations they accumulate and their steps towards acquiring a malignant phenotype. Nonetheless, common characteristics found in certain types of cancer – especially in colorectal cancer – offer promising intervention points for therapeutic attempts. Generally, the treatment of solid tumors relies on surgical removal followed by a combinatorial radio-and/chemotherapy, whereas with highly aggressive cancer phenotypes, where apart from the primary tumor, lesions occur in non-adjacent organs a systemic treatment is the only viable option. Therapeutic effects in cancer treatment are accomplished by designing therapies that correct the cancer-associated molecular defects, target the differences of tumor cells that set them apart from normal tissue or the delivery of toxic substances locally to tumor cells[9-11]. In particular, treating cancers resistant to currently available modalities or to customize cancer treatment based on the molecular properties of the tumor with a special focus on tumor initiating cells, has been the goal of many clinical studies[12-15]. The therapeutic approach shifted from altering the original gene material to interfering with protein synthesis utilizing small interfering RNA (siRNA) by translational arrest in order to posttranscriptionally silence protein expression by specific degradation of messenger RNA (mRNA)[16]. This naturally occuring phenomenon of RNA interference (RNAi) was first described by Andrew Fire and Craig Mello in 1998 in Nature in which they studied specific genetic interference by double-stranded RNA in *Caenorhabditis elegans*[17], in comparison further experiments with cultured Drosophila cells utilizing short synthetic dsRNAs elicited a

non-specific response induced by a interferon-driven immune response[18]. In contrast, studies using 21-23bp synthetic dsRNAs attained sequence specific RNA interference without evoking significant side effects[19]. The mechanism of RNAi is based on regulating gene expression by degrading target mRNA in the cytoplasm, while plasmid DNA based gene therapy – in order to achieve therapeutic gene expression or stable integration into the host's genome – has to reach the nucleus (Fig.1).

The RNAi approach interferes with the mRNA metabolism in the cytosol, the siRNAs are incorporated into a multi-protein complex known as RNA-induced silencing complex (RISC) and during this process the passenger strand is released whereas the guide strand binds to the Ago2 protein[20, 21]. If the nucleotide sequence of the guide strand is complementary to a sequence within the mRNA of the target gene, this strand is used by the RISC as template to destroy the matching counterpart (Fig.1). These technologies became immensly important and the idea of creating highly specific knock-down systems without significant side effects for determination of new therapeutic targets by harnessing RNAi for biomedical research and drug development, has been the main focus of many researchers worldwide. In general, nucleic acid-based therapies either utilizing plasmid DNA or small interfering RNA share similar inherent problems which need to be overcome in order to improve efficiency, biosafety as well as the overall therapeutic value. Nucleic acids are highly hydrophilic, thus are not able to penetrate lipid cell membranes and are subject to fast degradation by nucleases once applied into the blood stream[22-24]. Thus, for small interfering RNA as well as plasmid DNA (pDNA) successful application and delivery with the least toxicity and without inducing an immune response poses an important aspect of the nucleic-acid based therapeutic approach. For instance, pDNA can be delivered alone by injection into muscle tissue or via hydrodynamic delivery, but in most cases requires a carrier system which provide for shielding, targeting and cellular uptake.

The strategies for delivery of nucleic acids can generally be divided into two major groups – viral vector mediated gene delivery and non-viral gene delivery approaches. Viral vector systems are based on the most basic properties of wildtype viruses, with a streamlined genome capable of harbouring genetic material of considerable size. The main advantage is the highly efficient cellular uptake and intracellular delivery of therapeutic genes to the nucleus. Despite the efficacy of viral vectors, with only a few particles capable of transduction, the inflammatory and immune host response of many viral vector systems remains a biosafety issue. Insertional mutagenesis has been described for lentiviral vectors bearing the risk of oncogenic deregulation. Those biosafety concerns together with limitations like low transgene loading size and high costs have encouraged researchers to focus on non-viral vector systems, since they exhibit low immunogenicity due to lack of viral proteins eliciting an immune response. The disadvantage of non-viral vectors, is their low efficiency in gene delivery which can only be partly

compensated for in a dose-dependent manner. Amongst non-viral gene delivery reagents, linear polyethyleniminie (LPEI) has been widely used for its versatility and comparatively high transfection efficiency[25-29]. For gene delivery purposes LPEI has already been used for efficient transfer of genetic material *in vivo* into a wide variety of organs such as lung[30, 31], brain[27, 32], pancreas[33], retina[34], bladder[35] as well as tumors[33, 35, 36]. Mannosylated derivatives of linear PEI have even reached the clinic as delivery reagent for the treatment of bladder cancer[36] and human immunodeficiency virus (HIV) therapy[37, 38], respectively. Nonetheless, in terms of gene delivery efficiency the properties and outstanding features of viral vectors are still to be met by non-viral transfection systems.

These vectors are usually composed of cationic lipids or cationic polymers – both capable of condensing DNA by electrostatic interaction with the negatively charged DNA phosphate groups to create either lipoplexes or polyplexes. Thus, DNA is protected from degradation and due to an excess of positive charges, complexes are able to interact with the negatively charged cell membrane. After attaching to the glycocalyx of the cell membrane, the complexes are internalized via endocytosis. Within the acidic endosomes, the delivery vectors act as "proton sponge" by buffering the pH which leads to endosomal swelling and rupture allowing DNA to eventually enter the nucleus[39]. Once released in the cytoplasm of the target cell, the pDNA construct has to be able to ensure long-lasting transgene expression at therapeutic levels. What is decisive here is the optimal plasmid design in addition to improved delivery strategies, this is equally true for siRNA application. Unlike pDNA, siRNAs do not require reaching the nucleus to develop their full effect. Delivery strategies for siRNAs focus on their stabilization, in particular during circulation in the blood stream. Once the target cell is reached, proper endosomal release and the incorporation in the RISC complex are necessary for a therapeutic effect. New designs for small interfering RNA from recent publications and promising results from preclinical studies[40, 41] yielded sticky siRNA (ssiRNA) as a new class of interfering RNAs. For the creation of ssiRNAs, the 3‘-overhangs of siRNAs are extended with short complementary (dA)5-8/(dT)5-8 3’ sequences which are able to form long double-stranded reversible RNA concatemers in the presence of a polycationic transfection polymers like PEI. The concatemers form stable nanoparticles reminiscent of DNA/PEI complexes, and show higher silencing efficiency in preclinical models as compared to non oligomerized siRNA[41, 42]. Thus, these sticky siRNA therapeutics show great promise as potential drug canidated for a wide variety of pathologies, since the formation of reversible concatemers increases stability of complexes in the presence of blood or serum and ultimately leads to enhanced delivery efficiency of siRNA.

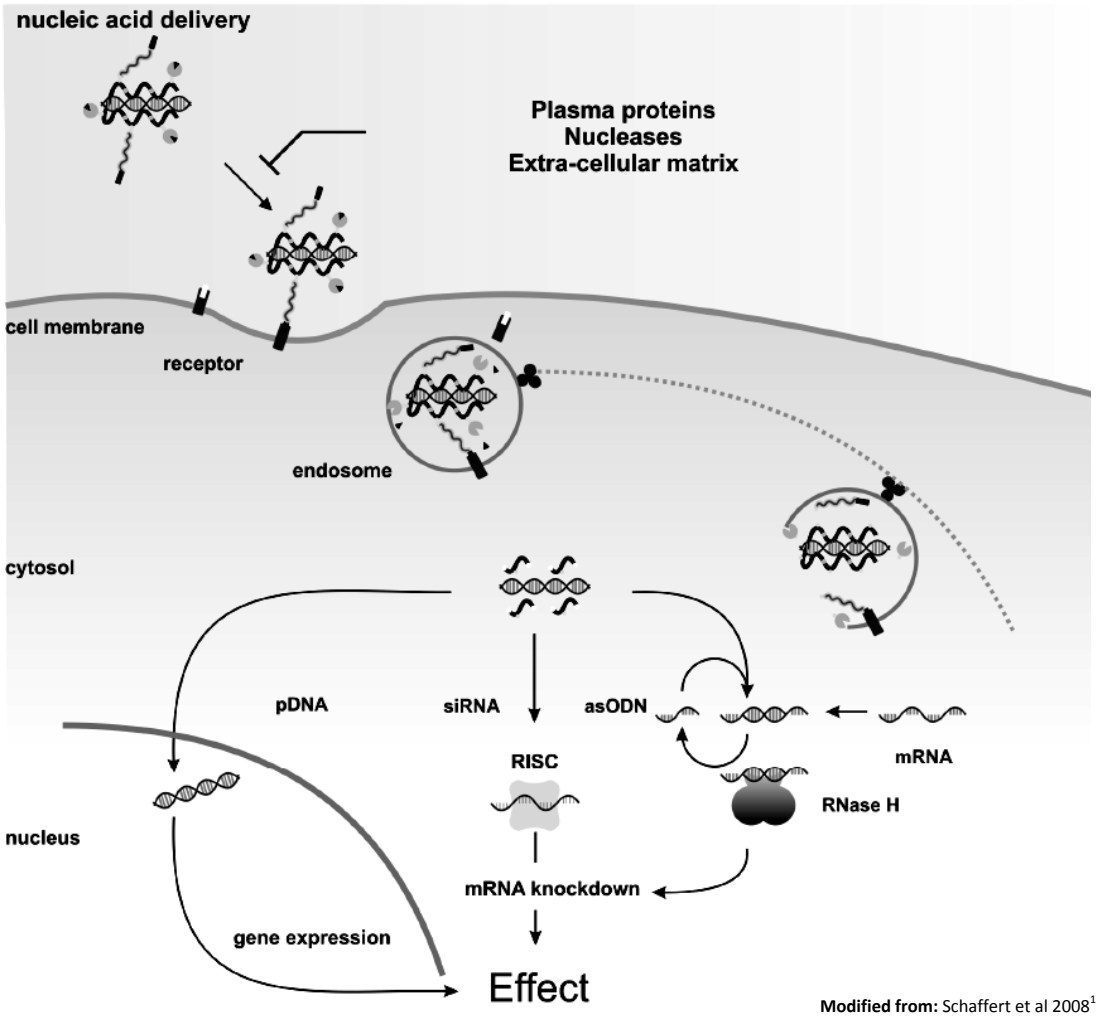

Modified from: Schaffert et al 2008[1]

Fig.1 Overview of plasmid DNA and small interfering RNA delivery

Nucleic acid compounds complexed with transfection polymers harbouring targeting ligands dock to the cell by ligand-receptor interaction and are internalized into an endosomal vesicle. Along the microtubule scaffold of the cell endosomes are actively transported to the vicinity of the nucleus. Particle release into the cytoplasm is triggered by an acidic pH-shift in endosomes which leads to the disruption of the endosomal membrane. Depending on the nucleic acid type, administered amounts of small interfering RNA (siRNA) or antisense oligodeoxynucleotides (asODN) are unpacked and processed in the cytosol, whereas plasmid DNA (pDNA) has to enter the nucleus to reach its full potential.

In order to identifiy the most promising therapeutic targets within these tumor cells, we have to gain a profound understanding of the underlying mutations and molecular alterations occuring in colorectal cancer cells. In particular, the sequential events driving the transition of normal colonic tissue to malignant carcinomas are the main focus of our therapeutic approach to treat colorectal carcinomas. The main focus of this experimental work was the attempt to specifically and with high efficacy deliver various nucleic acid containing transfection complexes into cancer cell of gastrointestinal origin with a greater focus on colorectal cancer.

2.2. Pathogenesis of colorectal cancer

Colorectal and hepatocellular cancer both belong to the group of gastrointestinal carcinoid tumors, which forms in the lining of the gastrointestinal tract. This group of neoplasia comprises esophageal cancer, gastric cancer, hepatocellular carcinoma, gallbladder cancer, pancreatic cancer, colorectal cancer and anal cancer[43]. Gastrointestinal cancer, in particular colorectal cancer, is one of the most common and deadly malignancies globally and responsible for a large fraction of cancer deaths[44]. In 2008 colorectal cancer was the third most common cancer in both sexes with over 1.2 Mio new cases worldwide[45]. Colorectal carcinomas (CRCs) both occur sporadically usually around the age of 65 and hereditarily at an earlier age with 5-15% of colorectal cancers being inherited[46, 47]. A heritable predisposition to colorectal cancer represents familial adenomatous polyposis (FAP) characterized by germline mutations in the adenomatous polyposis coli (APC) gene and hereditary nonpolyposis colorectal cancer (HNPCC) characterized by germline mutations in mismatch (MMR) genes (e.g. hMSH2, hMLH1)[46-49]. The majority of sporadic colorectal cancers, as well as FAP, evolve according to the adenomacarcinoma sequence proposed by Fearon and Vogelstein[50]. After the initial pathologic transformation of normal colonic epithelium to benign adenomas or adenomatous polyps, a series of genetic alterations leads to the occurence of invasive carcinomas. Generally mutations sequentially occur in one oncogene (K-ras) and three tumor suppressor genes (APC, SMAD4 and p53). According to the Knudson's two-hit hypothesis[51], oncogenes like K-ras require a genetic event in one allele, whereas the tumor suppressor genes require genetic alterations in both alleles[46]. Eventually, the event triggering the adenoma-carcinoma sequence and thus leading to the development of malignant cancers is the aberrant activation of the wnt signaling pathway[52-54]. The current model for the canonical wnt-pathway (for details see chapter 2.3) postulates that wild-type APC binds nuclear β-catenin and exports it to the cytoplasm[55-57], where it is phosphorylated, subsequently ubiquitinated and therefore targeted for proteosomal degradation[58, 59] (Fig.2). Mutations in APC prevent degradation of β-catenin, leading to its accumulation in the nucleus, where it functions in association with the HMG box protein T-cell factor 4 (TCF4) as a transcriptional co-activator and consequently enables the expression of various genes (e.g. c-MYC[60] or Cyclin D1[61, 62]) controlled by promoters with TCF4 binding sites[63, 64]. Target genes of the wnt-pathway in turn activate cell proliferation, enhance migration and reduce adhesion. Proceeding in the adenoma-carcinoma sequence, alterations in tumor suppressor genes SMAD4 and p53 occur. The SMAD4 protein mediates the inhibitory transforming growth factor β (TGF- β) signaling pathway which is responsible for suppressing cell growth[65], the inactivation of SMAD4 results in affected cells becoming insusceptible to TGF-β-mediated growth suppression[66]. Inactivation of tumor suppressor gene p53 allows for survival of aberrant cells[67], since it usually mediates growth arrest or induction of apoptosis following various cellular stress[68].

In comparison to FAP, HNPCC and about 15 % percent of sporadic colorectal cancers develop as a consequence of mutations in one or more of the three mismatch repair genes hMSH2, hMLH1 and hPMS2, which are usually functioning to maintain genetic stability. This in turn leads to an accumulation of genetic alterations in oncogenes and tumor suppressor genes among others, which accelerates tumor progression[46]. So far, a major obstacle for further investigations of colorectal cancers for the development of successful therapy strategies is the lack of suitable *in vitro* and *in vivo* models to study interference with the wnt/β-catenin pathway in cell culture as well as in a suitable mouse tumor model. For *in vitro* studies, primary cultures of colorectal cancer cells with similar properties and phenotypes as the original malignant materials are desireable. In this work, eight low passage colon cancer cells lines originating directly from the clinic were utilized[69]. Only 5 - 10 passages after harvesting the primary tumor cells from the patients were required for the generation of such low passage cell lines. Thereby accumulation of alterations due to long-term cultivation was avoided. Despite the succesful investigation of CRCs in the past decade, there still is an urgent demand for therapeutic targets and *in vivo* models closely reflecting characteristics of tumor cells, which would facilitate the investigation of cancers and especially development of successful novel therapy strategies.

2.3. The canonical wnt/β-catenin/TCF-signaling pathway

The canonical wnt/β-catenin pathway regulates cell fate decisions during development of vertebrates and invertebrates. The wnt-ligand is a secreted glycoprotein that binds to Frizzled receptors, which triggers a cascade resulting in displacement of the multifunctional kinase GSK-3β from the APC/Axin/GSK-3β-complex. In the absence of wnt-signal (*Off-state*), β-catenin, an integral cell-cell adhesion adaptor protein as well as transcriptional co-regulator, is targeted for degradation by the APC/Axin/GSK-3β-complex (Fig.2). Appropriate phosphorylation of β-catenin by coordinated action of CK1 and GSK-3β leads to its ubiquitination and proteasomal degradation through the β-TrCP/SKP complex[70-72].

In the presence of wnt binding (*On-state*), Dishevelled (Dvl) is activated by phosphorylation and poly-ubiquitination, which in turn recruits GSK-3β away from the degradation complex (Fig.2). This allows for stabilization of β-catenin levels, nuclear translocation and recruitment to the LEF/TCF DNA-binding factors where it acts as an activator for transcription by displacement of Groucho-HDAC co-repressors. Importantly, point-mutations in β-catenin lead to its deregulated stabilization[73]. APC and Axin mutations also have been documented in some tumors, underscoring the deregulation of this pathway in human cancer. During development, the wnt/β-catenin pathway integrates signals from many other pathways including Retinoic acid, FGF, TGF-β, and BMP in many different cell-types and tissues[74].

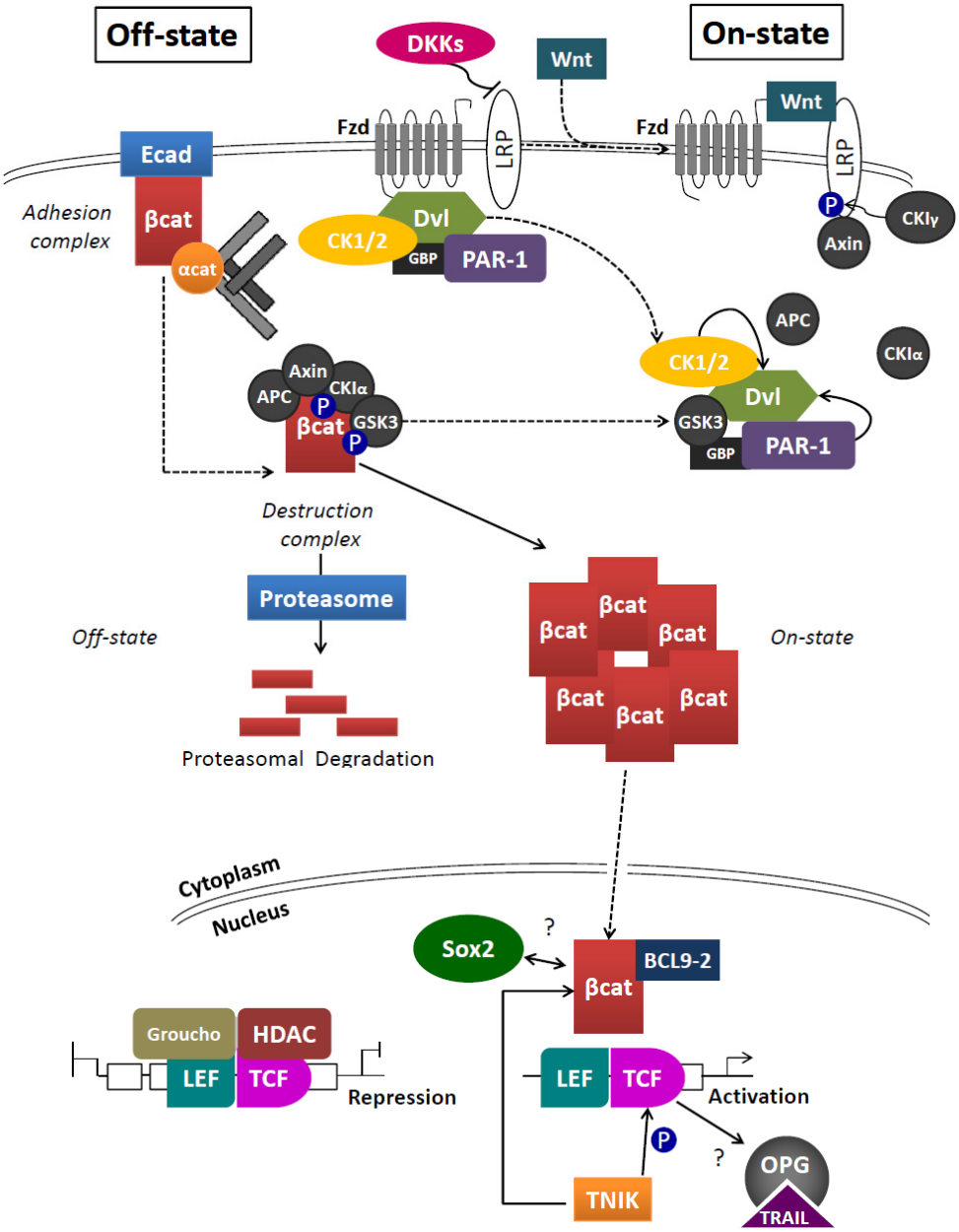

Fig.2 The canonical wnt/β-catenin/TCF-signaling pathway

In the absence of wnt signaling (Off-state), β-catenin proteins are synthesized but rapidly ubiquitinylated and proteasomally degraded. When wnt ligands engage the frizzeled (Fzd) receptors (On-state), β-catenin phosphorylation by a multi-protein complex is inhibited and β-catenin degradation disrupted. Consequently, β-catenin accumulates and translocates to the nucleus, where it forms a complex with transcription factors and serves as a transcriptional co-activator, thus inducing transcription of wnt target genes.

The temporal order and combination of mutations in human cancers appear to be relevant to tumor progression. Despite the complexities of genetic alteration available to developing colorectal cancer cells, activation of the wnt pathway remains the common denominator, and inhibiting its output remains a goal for therapeutic intervention[75].

2.3.1. Deregulation of wnt-signaling in colorectal cancer

The molecular mechanisms driving the transition of normal colonic mucosa to adenocarinoma are well investigated and depend on aberrant wnt signaling[50, 76-79]. In non-transformed cells the wnt pathway is thightly controlled with low cytoplasmic levels of β-catenin, where only upon activation of the Frizzled receptors by wnt ligands the nuclear translocation of β-catenin is induced by disrupting a multi-protein complex responsible for marking transcriptional regualtor β-catenin for proteosomal degradation. In an active wnt pathway scenario, high levels of β-catenin in the nucleus interact with the T-cell factor/lymphoid enhancer factor (TCF/LEF) family of transcription factors, which in turn activates expression of specific wnt target genes[60, 62]. Around 90% of sporadic colon cancers show aberrant wnt signaling activity, with 80% harbouring APC gene mutations[80-82], whereas less frequently cancer formation can be induced by mutations in the CTNNB1[75, 83] or Axin 2 gene[84]. On the cellular and molecular level, 80% of early colon adenomas start with a loss-of-function mutation in the adenomatosis polyposis coli (APC) gene and 10-15% with an activating mutation in the β-catenin gene. The canonical function of APC, a tumor suppressor gene which generally operates as a "gatekeeper" to prevent tumor growth, is targeting the oncogenic protein β-catenin for degradation and thereby regulating wnt signaling. Identification of the interaction of APC with the proto-oncogene β-catenin has linked colorectal carcinogenesis to the wnt signal transduction pathway. The wnt signaling pathway, named for its most upstream ligand, the glycoprotein wnt, controls cell fate decisions and plays a fundamental role in both gastrointestinal development and colorectal carcinogenesis[76, 85, 86]. If the first step of the two-hit hypothesis has already taken place because of an inherited APC mutation, further mutations (e.g. in p53 or KRAS) to APC-mutated cells are more likely to cause cancer than they would in non-mutated epithelial cells. APC, Axin2 and β-catenin mutations result in a defective β-catenin degradation complex and as a consequence nuclear accumulation of β-catenin and thus chronic transcriptional activation of wnt target genes. Some of the genes activated via the wnt pathway are likely to contribute directly to tumorigenesis. To induce cancer formation, a sequential accumulation of somatic gene mutations has to occur[87]. In most instances, before progression into malignant, invasive and metastatic cancers occurs at least four to five key genes must harbour mutations[88]: for instance in most cases of colorectal cancer, APC gene mutations marks an early event of tumor formation[89], whereas TP53 mutations usually appear as a late event[50]. The most common mutations deregulating and constantly activating wnt-signaling are mutations in the APC gene, identified as the basis for familial adenomatous polyposis (FAP)[90, 91]. In the majority of sporadic colorectal tumors they appear early in tumorigenesis. APC was positioned as a negative regulator of wnt signaling[92]. This was confirmed by findings indicating that wild type APC facilitated the destabilization of the β-catenin protein, whereas wnt had the contrary effect. Mutations in β-catenin demonstrated an oncogenic relationship between

β-catenin and APC, since the mutated version prevented its regulation by APC[80, 83, 93]. In further studies, Axin was identified as an additional member of the β-catenin regulatory complex and found to be mutated in human cancers[94]. Hence, with the discovery of a well-described pathway like the wnt/β-catenin pathway including its extracellular ligands, cell surface receptors, intracellular transducers and transcription factors that activate and repress genes that contribute to neoplasia, we can now utilize this knowledge to target vital parts of this signaling pathway.

Pathway activation involves interaction of a wnt ligand with a seven-transmembrane Frizzled molecule and an LRP5 or LRP6 co-receptor (Fig.2). The ensuing phosphorylation of the LRP co-receptor generates direct binding sites for Axin, which is thereby recruited to the plasma membrane and ultimately degraded. The APC–Axin complex is disrupted along with its ability to mark β-catenin for destruction through its phosphorylation and targeting to the proteosome. The stabilized β-catenin interacts with the T-cell factor (TCF) and lymphoid enhancer factor (LEF) transcription factors in a manner that displaces genetic repressors and recruits coactivators. There are many ways for cancers to co-opt this program, insusceptible to extracellular cues and relentlessly driving the expression of genes governing growth, survival and cell fate determination.

2.3.2. β-catenin – adhesion or transcription?

The key component of wnt signaling is β-catenin, an integral cell-cell adhesion adaptor protein as well as a transcriptional co-regulator. In unstimulated cells (*Off-state*), free cytoplasmic β-catenin is targeted for degradation by a multiprotein machine including APC, Axin and the multifunctional glycogen synthase kinase 3β (GSK-3β). Interaction between Axin and GSK-3β facilitates phosphorylation of β-catenin by GSK-3β[95]. In this way β-catenin is marked for ubiquitination and ultimately proteasomal degradation[96, 97], thus controlling overall levels of β-catenin.

β-catenin functions both in cell adhesion and transcription. Choosing properly between these functions is crucial for normal development, and the incorrect choice can lead to cancer. Wnt-induced β-catenin conformational changes favor assembly into transcription complexes activating wnt target genes, whereas α-catenin-associated β-catenin appears to favor adhesion. Additionally, phosphorylation dissociates β-catenin from adhesion complexes while promoting wnt-related transcription. The interactions of β-catenin with adhesion, transcriptionand destruction complexes ensure proper tissue architecture and cell-fate decisions during normal development. Misguided interaction decisions can be oncogenic, since failure to destroy cytoplasmic β-catenin plays a role in most colorectal cancers. Axin, APC, E-cadherin and TCF bind to overlapping, although non-identical, sites in the central Armadillo (Arm) repeats of β–catenin[98-101], thus there is a potential for competitive binding interactions. Like all

protein–protein interactions, β-catenin interaction choices are likely based on protein interaction affinities and the concentrations of β-catenin and its partners. It accumulates in the cytoplams and is captured by the destruction complex and destroyed, when wnt signaling is absent. Thus, now β-catenin is available to activate transcription, as free cytoplasmic β-catenin rises, it enters the nucleus and binds to TCF to initiate transcription of wnt-responsive genes. Upon β-catenin binding, a cascade of genes are activated responsible for various steps in tumorigenesis - enhancing blood and nutrient supply to tumors via VEGF expression, tumor invasion and formation of metastasis in distant organs, self-sufficiency of growth signals as well as evasion of apoptosis both allowing for rapid tumor growth and failure of terminal differentiation (Fig.3).

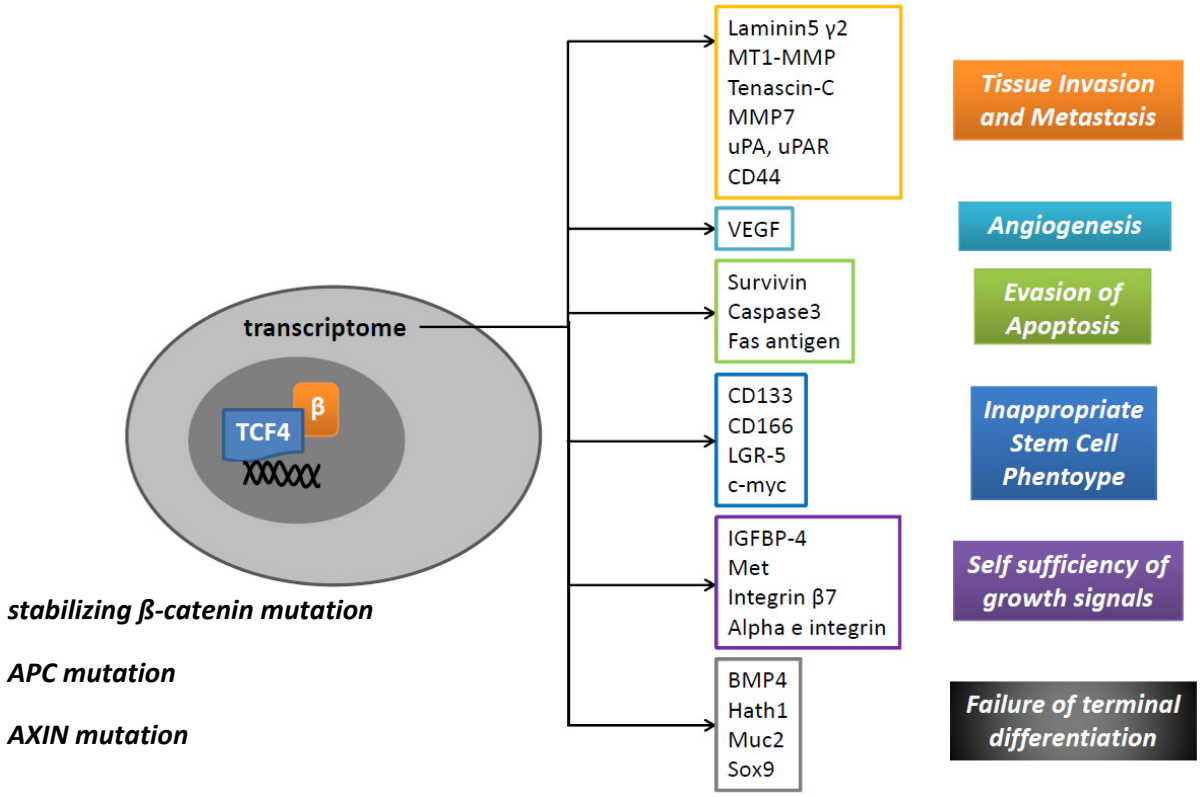

Adapted from: Hannahan D, Weinberg RA. The hallmarks of cancer. Cell 2000; 100:57-70

Fig.3 β-catenin-induced transcriptome

Nuclear accumulation of ß-catenin is initiated by either a stabilizing ß-catenin mutation, an APC or an AXIN mutation rendering the destruction complex, which otherwise targets ß-catenin for degradation, ineffective. In the nucleus, ß-catenin binds DNA together with the transcription factors TCF/LEF-1 (T-cell factor/lymphocyte enhancing factor-1) and subsequently induces transcription of a variety of genes, which contribute to aggressive progression of tumor growth, apoptosis evasion and metastasis.

Understanding the dynamics of protein interaction networks during normal processes and disease especially of β-catenin regulation is essential. With extensive knowledge about β-catenin and its role in the wnt-pathway, novel therapeutic approaches to treat colorectal cancer can be developed. We primarily focused on developing specific nucleic acid delivery strategies targeting wnt-signaling.

2.4. Therapeutic approaches for colorectal carcinoma

Colorectal cancer is one of the most common cancers worldwide and despite improvements in surgery, radio- and chemotherapy the overall five year survival is around 50%. Therefore, there is an obvious need for novel treatment approaches. Gene therapy is a promising new modality of treatment which can be used in combination with existing therapies. Convential treatment of colorectal cancer usually comprises surgery, followed by radio- and chemotherapy. Current gene therapy strategies usually involve the use of interventional genetic techniques to enhance the immunological response to a tumor or to deliver cytotoxic agents to tumor cells. In general, corrective gene therapy approaches involve either the introduction of tumor suppressor genes or the inactivation of proto-oncogenes. Gene therapy has the potential of solving the problems of chemotherapeutic strategies and could be either regarded as an alternative to conventional treatment or utilized in a combinatorial therapy approach.

2.4.1. Gene delivery strategies and existing gene therapy for CRC

Efficient gene delivery options for colorectal cancers have often been theorized, with clear requirements for targeting, shielding and loading capacity. In this thesis, non-viral vectors for nucleic acid delivery were utilized. These transfection complexes offer a higher loading capacity for DNA than viral vector systems and can be modified for specific targeting, as has been shown in preclinical studies as well as *in vivo* studies[102-105]. For *in vivo* gene delivery, defined particles avoiding interaction with blood components and non-target cells are required. For this purpose existing established linear and branched PEI polymers were modified to enhance gene delivery efficancy[106, 107]. The high protonation level at physiological pH of this polymer is responsible for its excellent DNA complexing ability which makes it a potent transfection agent. Furthermore, delivery vectors should be able to ensure highly specific cell targeting and selective expression for an *in vivo* therapy approach. The epidermal growth factor receptor (EGFR), a receptor with four transmembranes and intrinsic tyrosine kinase activity, induces via downstream signaling proliferation, enhanced cell migration and evasion of apoptosis upon ligand binding[108]. Although EGFR is present on all epithelial and stromal cells, overexpression of this receptor as well as a mutated variant of the EGFR yielding constitutive tyrosine kinase activity are commonly found in solid tumors[109]. In a recent publication, levels of EGFR in CRC were analyzed: EGFR reactivity was positive for 143 patients (97%) and high for 118 (80%). According to multivariate analysis, EGFR overexpression was significantly associated with tumor stage showing higher percentage of EGFR overexpression in T3 than T4 (P=0.003), yet $EGFR^{high}$ tumors were not associated with overall survival[110]. This makes EGFR a viable for target for therapeutic attempts, we utilized a fully synthetic peptide GE11, which targets the EGFR without inducing receptor activity as described previously[108]. The genetic changes which lead to the development of colorectal cancer are well described and, therefore, may be

amenable to correction. Replacement of tumor suppressor genes such as p53 has been shown to reverse phenotypic changes in animal models and has been licensed for human use in clinical trials. Prophylactic treatment with tumor suppressor genes for individuals at high risk of developing colorectal cancer, such as those with familial adenomatous polyposis, may prove beneficial in preventing or delaying the onset of malignant change. Colorectal cancer is a disease which can be attacked by a number of genetic mechanisms in order to kill tumor cells directly, prevent further growth and enhance the anti-tumor immune response. Gene therapy for colorectal cancer has reached the stage of clinical trials for patients with disseminated disease. The main focus of this work is corrective gene therapy in the form of inactivation of proto-oncogenes with antisense and selective apoptosis-induction using a cancer-specific promoter.

2.4.2. Transcriptional targeting of tumor cells

Specific expression of transgenes in tumor cells has been repeatedly attempted via tissue or cancer cell specific promoters[111-113], the underlying idea focuses on the utilization of therapeutically relevant genes for cancer-specific and thus safe treatment. This depends on achieving efficient and targeted gene expression. In this work, we utilized a tumor specific vector system targeting cell lines with deregulated wnt/β-catenin signaling. In 2001, Lipinski and co-workers developed a synthetic β-catenin responsive promoter, CTP1, to selectively drive strong gene expression in colon cancer cell lines. They were able to demonstrate similar expression levels of CTP1 driven genes in established β-catenin-deregulated tumor cells compared to those of the non-tissue-specific CMV promoter. In addition, only low CTP1-mediated expression in normal cells could be observed[114]. Lipinski and co-workers developed the promoter further regarding basal promoter, the number of Tcf binding sites and the distance between these and the basal promoter. Finally, in 2004, they presented the optimized version of CTP1, CTP4 (Fig.4), which is highly tumor specific and highly active[113].

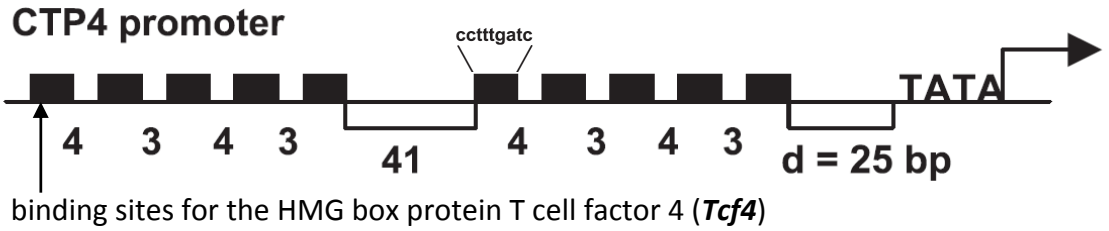

Adapted from: Lipinski et al. 2004

Fig. 1 Composition of the CTP4 promoter

Each black box represents binding sites for the HMG box protein T cell factor 4 (TCF4) and numbers indicate the base pairs between the Tcf sites and the distance from the end of the most proximal site to the start of the TATA box. The CTP4 promoter comprises two times five TCF binding sites seperated by a 41 base pair gap and a 25 base pair distance between the last binding site and the TATA box.

The first synthetic Tcf-responsive promoters described were those of Korinek and colleagues[80]. They comprised three Tcf consensus sites with either the basal c-fos (pTOPFLASH) or the tk promoter (pTOPCAT) and have been used by many investigators working in this field. Lipinski et al. attempted to improve the existing TOPFLASH system. Transcriptional targeting restricts transcription of transgenes to tumor cells and prevents normal tissue toxicities related with other cancer treatment approaches like chemotherapy or radiation[115, 116]. Ideally, tumor-specific promoters should be highly active in tumor cells and have little or no activity in normal cell. The benefit of such a highly specific system can be utilized for various purposes, in this work the CTP4 promoter as part of a Firefly Luciferase expression casette was introduced lentivirally into a range of colorectal cancer cell lines and one hepatocellular cell line in order to create a wnt-dependent screening system.

2.4.3. Potential therapeutic targets in wnt-signaling

The quest for safe, effective nucleic acids that block the effects of aberrant wnt signaling activity in colorectal cancer has been widely discussed in recent years. Due to the complexity of the wnt-pathway it is amenable to therapeutic intervention at various levels, ranging from inhibiting receptor-ligand interaction to disruption of TCF-β-catenin complex formation and inactivation of target genes in the nucleus. In this work, we focused on interfering with molecular structures directly associated with the wnt-pathway and with a defined function like β-catenin and TCF as proof-of-principle and other targets with known or still uncertain contribution to the wnt-signaling pathway – TNIK, OPG, Sox2 and PAR-1.

According to Mahmoudi et al. the Traf2 and Nck-interacting kinase (TNIK) is an essential activator of wnt target genes. TNIK is localized in the nuclei of wnt active intestinal crypts and recruited to promoters of wnt target genes in mouse crypts and in colorectal cancer cells in a β-catenin-dependent manner[117]. TNIK interacts directly with both β-catenin and TCF4 and phosphorylates TCF4 which results in TCF/LEF-driven transcriptional activation wnt target genes. Their results indicated that siRNA depletion of TNIK followed by expression array analysis shows the critical function of TNIK as an essential and specific activator of wnt target genes. Similar observations were made by Shitashige et al., they identified TNIK as an activating kinase for TCF4, which is essential for colorectal cancer growth[118].

Osteoprotegerin (OPG) was first described as a key factor inhibiting the differentiation and activation of osteoclasts, thus essential for bone resorption. As an additional function OPG also acts as a decoy receptor and binds to TRAIL, neutralizing its function. The group of DeToni identified OPG being regulated by β-catenin and capable of mediating resistance to TRAIL-Induced apoptosis in colon cancer[119]. By silencing β-catenin with siRNA an increase in sensitivity to TRAIL-induced apoptosis was observed which supports the role of β-catenin/TCF4 as a regulator of OPG and underlines the

importance of this pathway in providing cancer cells with growth as well as survival signals allowing for proliferation and evasion from apoptosis.

The SRY-related HMG-box (SOX) 2 family of transcription factors (Sox2) are involved in regulation of embryonic development and in determination of cell fate. Besides, Sox2 is required for stem-cell maintenance in the central nervous system and also regulates gene expression in the stomach. Sox2 is one of the four factors (Oct3/4, Sox2, Klf4 and c-myc) that can reprogram human somatic cells to pluripotent stem cells that exhibit the essential characteristics of embryonic stem cells[120]. Several groups could show a functional connection between colorectal cancer and the expression of Sox2. For instance, expression of Sox2 correlates with distant recurrence and poor prognosis of rectal cancer patients treated with preoperative CRT. It is postulated, that correlations among these genes may be associated with tumor regrowth and metastatic relapse after CRT[121]. Additionally, Fang et al. demonstrated that expression levels of Sox2 mRNA and protein were frequently overexpressed in primary colorectal cancer tissue[122], thus a promising target for siRNA-mediated knock-down.

Protease-activated receptors (PAR) are seven-transmembrane spanning domain G protein-coupled receptors comprising four receptors named PAR1, PAR2, PAR3 and PAR4. The protease-activated receptor 1 (PAR-1), has been correlated with the malignant phenotype in colon cancer[123]. PAR-1 potentiates wnt activation of the β-catenin pathway but blocks the JNK pathway. Suppressing endogenous PAR-1 function inhibits wnt signalling through β-catenin in mammalian cells, and Xenopus and Drosophila embryos[124]. PAR-1 seems to be a positive regulator of the β-catenin pathway and an inhibitor of the JNK pathway. These findings show that PAR-1, a regulator of polarity, is also a modulator of wnt-β-catenin signalling, indicating a link between two important developmental pathways.

2.5. Aims of the thesis

The idea of developing gene therapy specifically tailored for the treatment of malignant disease has been discussed in many publications and can only be achieved if very selective pathways or proteins/nucleic acids which are exclusively expressed in tumor cells or non-transformed cells are utilized. Since aberrant activation is the major driving force in colorectal cancers, we propose several methods targeting this particular pathway either by RNA interference (RNAi)-mediated depletion of novel therapeutic targets which we describe in this work as well as established players of the wnt-pathway. The unique aberrant deregulation in the wnt/β-catenin signaling pathway is utilized to develop a targeted therapy approach (Fig.5).

The idea was to start with a primary screen for potentially therapeutic targets in order to pinpoint their role in wnt-signaling (Fig.5, top left panel). Based on this target evaluation, which functions as a prevalidation tool the effect of siRNA-mediated knock-down of all target cell lines had to be further analyzed in a number of biological assays (Fig.5, lower panel). For this purpose a colony formation and cell motility/invasion assay had to be conducted for all relevant target cell lines. The effect on proliferation of all potential therapeutic targets should be determined, by using a ubiquitous promoter stably transduced in all cell lines. Upon siRNA mediated knock-down, the reduced levels of FLuc can be correlated with diminished proliferation rates. If the data of all assays points in a way that conveys reduced levels of proliferation, invasive behavior and aggressiveness (Fig.5, lower panel), a viable candidate is found for a treatment attempt *in vivo*.

As an additional aim, the tumor-selectivity of the CTP4-promoter was to be employed in the delivery of the cytotoxic protein diphteria toxin A (DTA) in colorectal cancer target cells, as part of a plasmid DNA based gene therapy approach (Fig.5, upper right panel). The selectivity of the novel CpG-depleted DNA constructs encoding for DTA had to first be verified *in vitro* and then tested in an orthotopic dissemination tumor model.

For *in vivo* testing of both siRNA and pDNA formulations, we had to establish a tumor dissemination model in NMRI nude mice. After the standardization of the mouse model, we will have to utilize siRNA targeting a therapeutic target verified *in vitro* as well as a CTP4-controlled pDNA construct expressing Diphteria toxin subunit A targeting wnt-deregulated colorectal cancer cells (Fig.5, lower right panel).

Both, specific siRNA aimed at therapeutic targets retrieved from the *in vitro* screen, as well as pDNA encoding for cytotoxic protein DTA prevalidated in cell culture, should be utilized for nucleic acid delivery in an orthotopic liver dissemination model.

Fig.5 Overview experimental strategy of the PhD Thesis

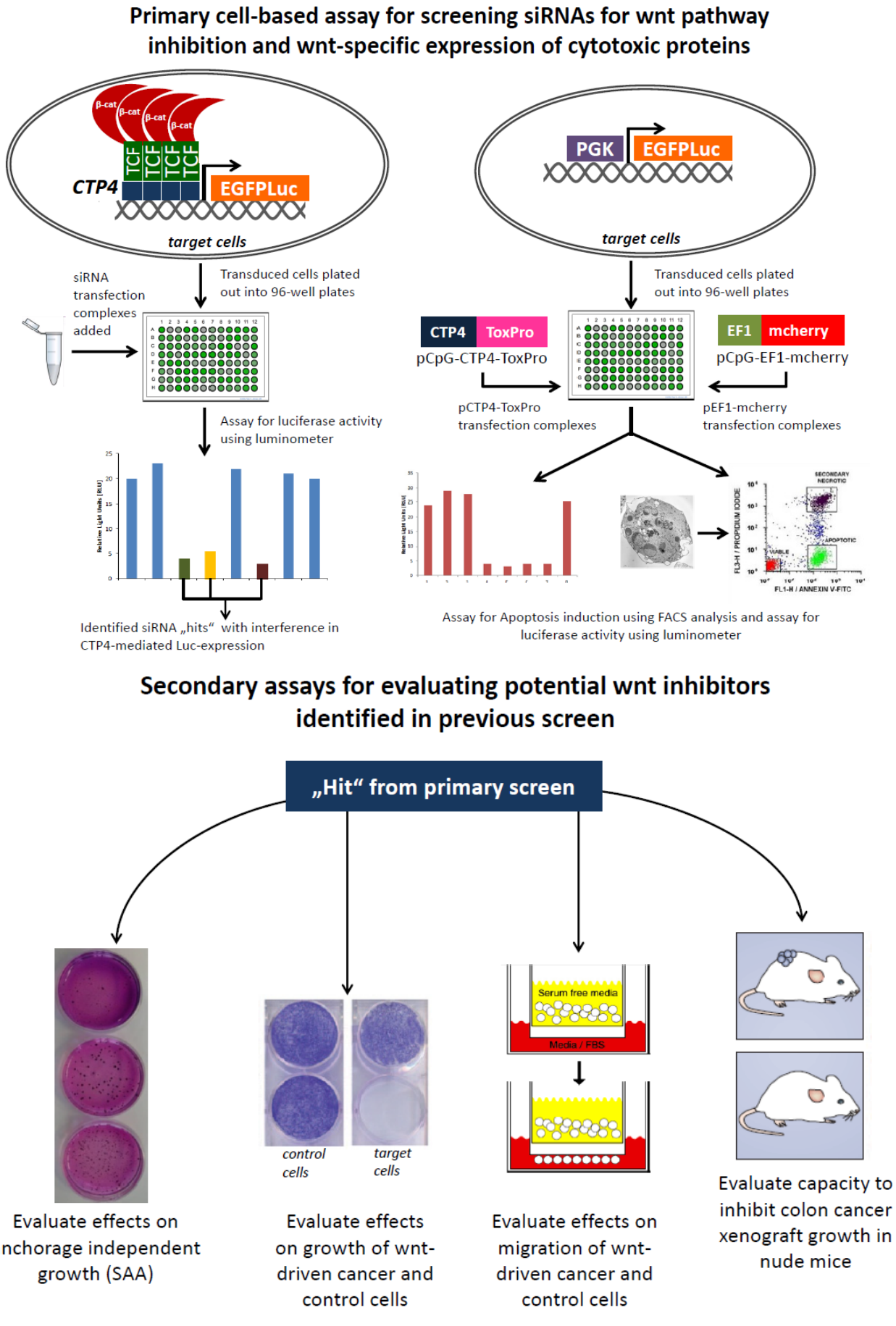

3. Material and Methods

3.1. Methods of molecular cloning and propagation of plasmids

3.1.1. Restriction digestion of plasmid DNA

For all cloning experiments 500ng plasmid DNA was incubated 1 hour with 1 unit of restriction enzyme (Fermentas, Waltham/MA, USA) per µg DNA in the appropriate restriction enzyme buffer according to manufacturer's recommendations. Success of digestion was verified by agarose gel electrophoresis, correct DNA fragments were excised from agarose gels with a sharp scalpel. Agarose was dissolved and DNA was purified using the QIAquick Gel Extraction Kit (Qiagen, Hilden, Germany) according to manufacturer's recommendations.

3.1.2 Ligation, transformation of E.coli and preparation of plasmid DNA

A molar ratio of 1:8 of purified, digested and dephosphorylated vector DNA (200ng) and the designated insert DNA were used for sticky end ligations. All ligations were carried out using 1 – 3 units T4 DNA Ligase from Rapid DNA Ligation Kit (Fermentas, Waltham/MA, USA) with overnight incubation at 16°C in a final volume of 20 - 50 µL. Competent E.coli bacteria (DH5α, DB3.1 or dam$^-$ ER2925) were thawed on ice, mixed with 50-200 ng DNA from the ligation cocktail and incubated on ice for 30 minutes, then heat-pulsed at 42°C for 45 seconds and subsequently incubated on ice for 1-2 minutes. 1 ml of LB-medium was added prior incubation at 37°C for 1-2 hours while shaking continuously. Bacteria were streaked on antibiotic LB-Agar plates (LB-medium with 1.5% Agar) containing 50 µg/ml ampicillin, kanamycin or zeocin (Roche, Mannheim, Germany) and incubated at 37°C overnight for the selection of the transformants. All plasmid DNA preparations were carried out depending on the volume of the bacterial culture either with QIAprep Spin Miniprep Kit (for cultures up to 5mL), a EndoFree Plasmid Maxi Kit (for cultures up to 600mL) or a EndoFree Plasmid Giga Kit (for cultures up to 3 L) (Qiagen, Hilden, Germany) according to manufacturer's instructions. Verification of all cloned plasmids was performed by sequencing new constructs employing GATC Biotech (Constance, Germany), luciferase- and fluoresecence transgene harbouring plasmids were tested by transfection for their functionality.

3.1.3 Cloning strategies

Luciferase reporter gene plasmids

pPGK-EGFPLuc (encoding a fusion of enhanced green fluorescent protein (EGFP) and GL3 Firefly Luciferase under the control of the phosphoglycerate kinase promoter). The CMV promoter was cut out with HindIII/NcoI from the pCMV-EGFPLuc construct and replaced with the PGK promoter, which was

PCR amplified from pAAVS1-PGKEGFP-HSVtkNEO (a gift from T.Cathomen) inserting a HindIII restriction site.

pCTP4-Luc (encoding GL3 Firefly Luciferase under the control of the artificial β-catenin-dependent promoter CTP4) was a gift from Dr.Kai Lipinski[113, 114].

pCTP4-EGFPLuc (encoding a fusion of EGFP and GL3 Firefly Luciferase under the control of the artificial β-catenin-dependent promoter CTP4). EGFPLuc was removed from pCMV-EGFPLuc by the restriction enzymes NcoI and XbaI and cloned into the expression vector pCTP4-Luc[113] digested with the same restriction enzymes, thereby replacing the Luc fragment. For preparation of plasmid DNA, the dam$^-$ bacteria ER2925 were used.

pCMV-Luc (encoding GL3 Firefly Luciferase under the control of the cytgomegalovirus promoter) described in Plank et al. (1992) was produced endotoxin-free by Elim Biopharmaceuticals (San Francisco, CA, USA) or Aldevron (Fargo, ND, USA).

pGL3 basic (encoding GL3 Firefly Luciferase under the control of no promoter) was purchased from Promega (Madison, USA).

Plasmids encoding therapeutic genes

pCpG-hCMVenh-CTP4-Apoptin (encoding the chicken anemia virus protein apoptin under the control of the CTP4 promoter in a CpG-free backbone). Chicken anemia virus, subunit VP3 (Apoptin) cDNA is based on the published sequence (nucleotide ID NM FR850030.1) was synthesized by Geneart (Regensburg, Germany). The sequence was designed for optimized codon usage in mouse, cryptic splicing sites were removed. The Apoptin cDNA fragment was cut out by digestion with NheI/BglII and cloned into the pCpG-mcs (purchased from InvivoGen, California, USA) expression vector, where the murine CMV enhancer was replaced with the human version, precut with NcoI/XbaI. Additionally the EF1 alpha promoter was replaced with the CTP4-promoter using SpeI and XhoI.

pCpG-hCMVenh-CTP4-DTA (encoding the A chain of the diphtheria toxin (DTA) under the control of the CTP4 promoter in a CpG-free backbone). The DTA fragment was cut out from the pH19-DTA (kindly provided by Abraham Hochberg) construct with NcoI/BamHI and cloned into the pCpG-mcs (purchased from InvivoGen, California, USA) expression vector, where the murine CMV enhancer was replaced with the human version, precut with NcoI/XbaI. Additionally the EF1 alpha promoter was replaced with the CTP4-promoter using SpeI and XhoI.

pCpG-hCMVenh-ΔCTP4-DTA (encoding the A chain of the diphtheria toxin (DTA) in a CpG-free backbone). The CTP4 promoter from the pCpG-hCMVenh-CTP4-DTA construct was cut out using XhoI and re-ligated to remove the promoter region.

3.2. Establishing stable Luciferase cell lines via lentiviral transduction

Target cells were seeded in T25 cell culture flasks at a density of 100,000 cells 24 h prior to transduction with a lentiviral vector encoding a PGK-EGFPLuc and CTP4-EGFPLuc cassette. The cDNA from vectors pEGFPLuc (Clontech, Mountain View, CA USA) and pCTP4-EGFPLuc was excised and cloned into the vector pHIV7/SF-GFP[125] for the production of lentiviral vectors in cooperation with Dr.Martina Anton (Institute of Experimental Oncology and Therapy Research, TUM). The pHIV7/SF-GFP transfection vector incorporates the PGK promoter in the expression casette, only for the CTP4-EGFPLuc expression casette the PGK promoter was removed. Transduction was performed with 1 mL virus supernatant in the presence of 8µg/ml hexadimethrine bromide (Polybrene®) (Sigma-Aldrich, St.Louis, USA), 24 h thereafter cells were transferred into T75 flask. After two rounds of splitting, a p24 ELISA was performed to ensure the absence of any lentiviral particles. Transduced target cells were washed twice with PBS, harvested and collected in 1mL PBS/10%FBS. Transduced target cells were sorted with a MoFlo cell sorter (Beckman Coulter) to obtain a homogenous cell population of eGFP-positive cells. In order to discriminate viable from dead cells, to exclude doublets and to ensure a homogenously high expression of eGFP, cells were appropriately gated by forward/side scatter as well as pulse width. Per sample at least 500,000 gated events were collected for further cultivation to establish a purified cell population.

3.3. *In vitro* studies

3.3.1. Cell lines and cell culture conditions

LS174T (colorectal adenocarcinoma, ATCC-CL188), COGA-2 (rectal adenocarcinoma) and COGA-12 (coecum adenocarcinoma)[69] were cultured in RPMI 1640 (Biochrom, Berlin, Germany). SW480 (colorectal adenocarcinoma, ATCC-CCL-228) and Hela (cervix adenocarcinoma, ATCC-CCL-2) cells were cultured in DMEM (Biochrom, Berlin, Germany), whereas HepG2 (hepatocellular carcinoma, ATCC-HB-8065) cells were propagated in DMEM:Ham's F12 (1:1). All cell culture media was supplemented with 10% fetal bovine serum (Biochrom, Berlin, Germany) and 2mM L-Alanyl-L-Glutamin (Biochrom, Berlin, Germany). All cultured cells were grown at 37°C in 5% CO_2 in humidified atmosphere. Additional cell lines utilized in this study are shown in Table 1. All cells were cultured in T75 or T150 flasks as well as various plates purchased from TPP AG (Trasadingen, Switzerland). In order to harvest cell, they were shortly washed with 0.05 % trypsin/0.02 % EDTA in PBS solution (Invitrogen, Karlsruhe, Germany) and

subsequently incubated with fresh trypsin/EDTA solution at 37°C. After the detachment of the cells trypsin was inhibited by addition of serum containing growth medium. EDTA was removed by centrifugation at 180 g to 500 g and subsequently uptake of the cell pellet in fresh growth medium.

Table 1: Cell lines

Cell line	Description origin	Culture medium	ATCC No.
BT-549	Human breast cancer	RPMI 1640 Medium + 10% FBS + 0.023 IU/ml insulin	300132 , Cell line service (CLS, Eppelheim, Germany)
HuH 7	Human hepatocellular carcinoma	Ham's F12:DMEM medium + 10% FBS	JCRB0403, Japanese Cancer Research Resources Bank, Tokyo, Japan
L-wnt3A	wnt3A producing cell line	RPMI 1640 Medium + 10% FBS	CRL-2647**,** American type culture collection (ATCC, Manassas, USA)
A549	Human lung carcinoma	DMEM medium + 10% FBS	CCL-185, ATCC
MCF7	Human breast adenocarcinoma	RPMI 1640 medium + 10% FBS	HTB-22, ATCC
PC-3	Human prostate cancer	RPMI 1640 medium + 10% FBS	CRL-1435, ATCC
KB	Human cervix carcinoma	RPMI 1640 medium + 10% FBS	CCL-17, ATCC
U87	Human glioblastoma	DMEM medium + 10% FBS	HTB-14, ATCC
HEK293	Human embryonic kidney cells	DMEM medium + 10% FBS	CRL-1573, ATCC
K562	Human erythromyeloblastoid leukemia	RPMI 1640 medium + 10% FBS	CCL-243, ATCC
DU145	Human prostate cancer	RPMI 1640 medium + 10% FBS	HTB-81, ATCC

3.3.2. Plasmid DNA transfection

For transfection approaches with plasmid DNA depending on the size of transfection vessel 1-5x10^4 cells were seeded 24 hours prior to transfection in 200 – 2000µL medium. In a 96-well format 5x10^3 cells were plated in 200µL cell culture medium per well, before transfection medium was removed and replaced with 80µL fresh medium. The complexes for transfection were formed with 500-800ng plasmid DNA and a linear polythylenimine or conjugate consisting of LPEI coupled to an EGFR targeting peptide via polyethylene glycol spacer. As a non-targeted control, LPEI-PEG-Cys with a distal cysteine was used[108]. Polyplexes were formed at a molar ratio of PEI nitrogen to RNA phosphate (N/P) ratio of 6 in HBG buffer (HEPES(4-(2-hydroxyethyl)-1-piperazineethanesulfonic acid) buffered glucose: 20mM HEPES,

5% *w/v* glucose, pH 7.4) for 30 minutes at room temperature. An aliquot of 20µL complexes were added directly to the cells and medium was replaced with 200µL fresh culture medium after 8 hours. Transfection efficiency was evaluated 24, 48 and 72 hours after treatment employing a Firefly Luciferase reporter gene expression assay (as described in 3.5.) and FACS analysis of EGFP and mcherry expression (as described in 3.3.4.). Gene transfer was performed using two to five wells/group and experiments were at least repeated twice.

3.3.3. small interfering RNA transfection

All target cells were seeded in 96-well plates (TPP, Trasadingen, Switzerland) at a density of $5x10^3$ cells per well 24h prior to transfection. Transfection polyplexes were generated by diluting siRNA duplexes targeting one of the following genes Osteoprotegerin (OPG; Ambion, Austin/TX, USA), Traf2 and Nck-interacting kinase (TNIK; Ambion, Austin/TX, USA), β-catenin (β-cat, Thermo Scientific, Waltham/MA, USA), protease-activated receptor-1 (PAR-1, Ambion, Austin/TX, USA), T-cell factor 4 (TCF-4; Ambion, Austin/TX, USA), sex determining region Y-box 2 (Sox-2; Thermo Scientific, Waltham/MA, USA), or control siRNA; non-specific control duplex (Thermo Scientific, Waltham/MA, USA) to a concentration of 800ng siRNA per 96-well and mixing it with a modified PEI compound (brPEISucc) described previously[106] at N/P of 15 in HBG buffer. For improved *in vivo* application targeting PAR-1 an established method for polyplex stabilization was utilized, extending the 3'-overhangs of target siRNA with 8 complementary (dA)/(dT) nucleotides in order to create sticky siRNA (ssiRNA). For „sticky" siRNA targeting PAR-1 or a scrambled version of PAR-1 LPEI-PEG-GE11 was utilized at an N/P ratio of 6, where ssiRNA form long double-stranded RNA concatemers in the presence of PEI. For both types of siRNA transfection complexes prepared were added to the cells in 100µL fresh culture medium. Target siRNA was diluted to a final concentration of 50µg siRNA/250µL polyplexes with brPEISucc at an N/P ratio of 15 for *in vivo* studies. Mixing of transfection complexes were prepared in the following manner for all animal experiments: The required amount of HBG for all reactions was pipetted first, then the desired amount of either brPEISucc for siRNA or LPEI-PEG-GE11 for ssiRNA were calculated and added to the HBG. Finally siRNA and ssiRNA for all reactions were added to the prepared HBG/BPEISucc or HBG/LPEI-PEG-GE11 dilutions. The mixture of transfection polyplexes then was allowed to complex for at least 30 minutes. All results are shown with Relative Light Units (RLU) corresponding to the luminescence signal emitted by 10,000 cells/well.

3.3.4. Flow cytometry via fluorescence-activated cell sorting (FACS)

The analysis of fluorescent protein expressed from different transfected constructs was performed using flow cytometry. Using the forward and side scatter channel every particle of a cell suspension can be analyzed for their size as well as the granularity within a particle in order to differentiate different cell types in a heterogenous sample. The medium was aspirated from target cells, washed with PBS and harvested with trypsin/EDTA. The cell number was determined and up to $1x10^7$ cells were then transferred to a 5 ml round-bottom tube, washed twice with PBS and then resuspended in 750 µL FACS-buffer (10% v/v FBS in PBS) and kept on ice until analysis. Prior to acquisition with a Cyan™ ADP flow cytometer (DakoCytomation, Copenhagen, Denmark), 1 µl of the fluorescent DNA stain DAPI (4',6-Diamidino-2-phenylindole from Sigma-Aldrich, St. Louis, USA; 0.5 mg/ml) was added to each sample to enable discrimination between viable and dead cells. DAPI emission was detected at the violet 1 channel (excitation: 405 nm, beamsplitter: 484 nm, emission filter: 450/50nm) and EGFP fluorescence was excited at 488 nm and emission was detected using a 530/40 nm bandpass filter and a 575/25 nm bandpass filter. A total of $5x10^4$ gated events per sample were collected. To exclude cell debris and cell agglomerates, cells were appropriately gated by forward versus side scatter and pulse width. The percentage of EGFP-positive cells was determined by diagonal gating[126].

3.3.5. Biological assays

3.3.5.1. Tetrazolium-based colorimetric assay (MTT)

A tetrazolium-based colorimetric assay (MTT) is a rapid method for the assessment cytotoxicity, the working principle rests upon the observation that viable cells have the ability to metabolize a water-soluble tetrazolium dye 3-(4,5-dimethylthiazol-2-yl)-2,5-diphenyl tetrazolium bromide (MTT), into an insoluble formazan salt. For the MTT-assay cells were seeded in 96-well microtiter plates and transfection, at the same conditions as described previously, was performed. The cell density was chosen according to the cell type and rate of cell growth (~ 5,000 – 20,000 cells/well). Depending on read-out time of each experiment, transfected 96-well plates were placed in the cell culture incubator for 24 - 72h, at the end of which the viability tests were performed including untreated controls and background blanks used as reference. After transfection in a 96 well plate, a 10 µL aliquot of a 5 mg/mL solution of MTT dissolved in sterile PBS was added to each well reaching a final concentration of 0.5 mg MTT/ml. After incubation for 1-2 h at 37°C, the medium was completely removed and the samples were frozen at -80°C for at least 1 h. The purple formazan product was dissolved in 100 µl/well dimethyl sulfoxide (DMSO, Sigma-Aldrich, Steinheim, Germany) while shaking continuously and quantified by a microplate reader Spectrafluor Plus (Tecan Austria GmbH, Grödig, Austria) at 590 nm with a background

correction at 630 nm. Cell viability in terms of cell respiration activity normalized to the reference data (%) is expressed as:

$$\% \text{ viability} = \frac{(A_{sample} - A_{blank})}{(A_{reference} - A_{blank})} \times 100$$

3.3.5.2. Soft agar assay for colony formation

The soft agar assay for colony formation is an achorage independent growth assay in soft agar, which is considered the most stringent assay for detecting malignant transformation of cells. For this colony formation assay 24 hours after siRNA transfection 5,000 cells were collected and seeded in a 1.5mL layer of 0.7% agar (w/v) in either RPMI1640-10%FBS, Ham'sF12:DMEM-10%FBS or DMEM-10%FBS (cell agar layer) in a 60mm dish (Nunc, Roskilde, Denmark) which contains a 1.5mL base agar layer of 1.0% agar (w/v) in the corresponding cell culture medium. The base agar layer added to each well prevented cells from attaching and forming a monolayer on the plastic substrate. 1.5mL cell suspension was poured on top of the base agar layer, allowed to solidify and incubated at 37°C/5% CO_2 for 15 days. Following this incubation period, colony formation was analyzed by staining cells with yellow tetrazolium MTT (3-(4,5-dimethylthiazolyl-2)-2,5-diphenyltetrazolium bromide) for one hour and quantifiying the number of colonies formed per well. Using a Zeiss Axiovert 200 microscope (Carl Zeiss, Jena, Germany) cell colonies of > 10 cells were counted and absolute counts are presented.

3.3.5.3 . AnnexinV-FITC flow cytometric analysis of apoptosis

AnnexinV-FTIC is used to quantitatively determine the percentage of cells within a population actively undergoing apoptosis. In an early phase of apoptosis, the membrane of apoptotic cells phospholipid phosphatidylserine (PS) is translocated from the inner leaflet of the plasma membrane to the outer leaflet, thereby exposing PS to the external environment. Annexin V is a 36kDa calcium-dependent phospholipid-binding protein that has a high affinity for PS, and is useful for identifying apoptotic cells with exposed PS. Staining with AnnexinV-FITC is typically used in conjunction with a vital dye in this case DAPI (4',6-diamidino-2-phenylindole). Viable cells with intact membranes exclude DAPI, whereas the membranes of dead and damaged cells are permeable to DAPI. For sample preparation, 1-5x10^6 cells were harvested by trypsin/EDTA 24, 48 or 72 hours post transfection or start of treatment, washed once with PBS and resuspended in 500 µl of AnnexinV binding buffer (BioVision, California, USA). AnnexinV-FITC (BioVision, California, USA) was added at 1 µg/ml each and incubated for 10 minutes at room temperature. Shortly before acquiring samples using a Cyan^{TM} ADP flow cytometer, 1 µl of the fluorescent DNA stain DAPI (Sigma-Aldrich; 0.5 mg/ml) was added to each sample to enable

discrimination between viable, apoptotic and necrotic cells. Annexin V-Cy5 fluorescence was excited at 633 nm and emission was detected using a 680±30 nm bandpass filter and DAPI emission was detected at the violet 1 channel (excitation: 405 nm, beamsplitter: 484 nm, emission filter: 450/50nm). To exclude cell debris and doublets, cells were appropriately gated by forward versus side scatter and pulse width. A total of $5x10^4$ gated events per sample were collected. Cells that stain positive for AnnexinV-FITC and negative for DAPI are undergoing apoptosis. Cells that stain positive for both AnnexinV-FITC and DAPI are either in the end stage of apoptosis, are undergoing necrosis, or are already dead. Cells that stain negative for both AnnexinV-FITC and DAPI are alive and not undergoing measurable apoptosis.

3.3.5.4. Migration assay – Boyden chamber

Invasion through the extracellular matrix (ECM) is an important step in tumor metastasis. Cancer cells initiate invasion by adhering to and spreading along the blood vessel wall. Microporous membrane inserts are widely used for cell migration and invasion assays. Invasion/migration behavior of siRNA transfected cells was determined using a QCM™ 96-well Cell Invasion Assay according to manufacturer's instructions. In brief, treated cells were loaded in a well with an 8µm pore size polycarbonate membrane deprived of chemo-attractants. Invading cell migrate through and attach to the bottom of membrane, non-invading cells remain above. Invaded cells were detached, lysed and mixed with a green-fluorescent dye which exhibits strong fluorescence enhancement when bound to cellular nucleic acids. Results were expressed as percentage of invaded cells compared to control siRNA treated target cells.

3.4. *In vivo* studies

3.4.1. Orthotopic tumor dissemination model

All animal procedures were approved and controlled by the local ethics committee and carried out according to the guidelines of the German law of protection of animal life. Animals were kept in individually vented cages with a 12 h day/night cycle; water and chow were provided ad libitum. For the LS174T orthotopic liver metastasis model 5 week old female NMRI-nu/nu mice (n=20) were injected with $7,5x10^5$ LS174T CTP4-EGFPLuc cells in 50µL PBS into the spleen. Growth of metastases was analyzed by BLI measurement of Luciferase activity carried out as previously described[127]. In short, *in vivo* imaging was performed using the IVIS Lumina Imaging System (Caliper Life Sciences GmbH), treated mice were anesthetized by i.p. injection of xylazin/ketamin (0.375 ml/0.635 ml in PBS, respectively). Ten minutes after i.p. injection of 300 mg/kg luciferin (Promega, Hilden, Germany) the bioluminescence

signal was collected for one to three minutes. Reflected light pictures were taken during illumination with four white LED. Image acquisition and processing was carried out using Living Image 2.60.1 - IGOR Pro 4.09 Software. Bioluminescent imaging was performed as single picture imaging at day 3 after tumor injection and as sequence imaging at day 6, 8 and 10 after tumor cell injection. At day 13 mice were sacrificed and the liver as well as the spleen of each mouse was collected for analysis.

3.4.2. Size and Zetapotential measurements

Particle size of sticky siRNA and pDNA formulations was measured by laser-light scattering using a Zetasizer Nano ZS (Malvern Instruments, Worcestershire, U.K.). For particle size measurement complexes were formed for 30-40 minutes at room temperature, containing 20 µg nucleic acid and the corresponding amount of polymer in HBG buffer. For estimation of zetapotential, polyplexes were diluted with 10 mM NaCl at a nucleic acid concentration of 20µg/ml, and particle charge was determined. The data represent the mean of at least three measurements.

3.4.3. Plasmid DNA and small interfering RNA transfection

Transfection polyplexes for *in vivo* applications were formed by diluting either plasmid DNA or small interfering RNA as well as sticky siRNA with 50µg nucleic acids per mouse and injection. For siRNA transfection PEI-SUC-10 was utilized at N/P of 15 in HBG buffer and for pDNA as well as sticky siRNA LPEI-PEG-GE11 was incorporated in transfection complexes with an N/P ratio of 6 in physiological HBG buffer. In the β-catenin siRNA transfection experiment two injections with 50µg siRNA per mouse (n=6) into the tail vein were conducted, the PAR-1 and PAR-1 scrambled sticky siRNA as wells pCpG-hCMVenh-CTP4-DTA experiments three injections were employed intravenously (n=7) with 48 hour gaps in between. In all cases experiments were terminated on day 14 after tumor inoculation.

3.4.4. Bioluminescence imaging (BLI)

For live examination of Luciferase expression *in vivo* mice were anaesthetized by administration of isoflurane in oxygen and intraperitoneally injected with 100µl D-luciferin (60mg/ml, Promega, Madison/WI, USA) diluted in PBS. After 10 minutes the mice were imaged for bioluminescence in an IVIS Lumina imaging system (Caliper Life Sciences, Rüsselheim, Germany) in a light-tight chamber on an adjustable, heat-controlled stage. For quantification of the BLI signal, a region of interest (ROI) was laid covering the analyzed area and the signal measured as emitted photons/second. The acquisition time was set depending on the bioluminescence intensity. Data were analyzed using the Xenogen Living Image 4.0 software.

3.4.5. Tumor tissue isolation

On the day the animal experiments were terminated the liver and spleen of all test mice were surgically removed and snap frozen on dry ice, homogenized with mortar and pestle cooled with liquid nitrogen and aliquots of the powder either lysed in 200 µL Promgea cell lysis buffer (Promega, Madison/WI, USA) or in 150 µL lysis buffer from the miRCURY™ RNA Isolation Kit (Exigon, Vedbaek, Denmark). Luciferase activity was determined from protein extracted from lysed tumor tissue, with background signal (100–200 RLU) subtracted from each value and transfection efficacy expressed as relative light units (RLU) per mg protein. Protein content was determined by a modified BCA assay as in 3.7.

3.5. Luciferase reporter gene assay

For *in vitro* transfections Luciferase activity was quantified in cell lysates by adding 55µL lysis buffer (diluted 1:10, Promega, Mannheim, Germany) to each well either 24, 48 or 72 hours after transfection. After 30 minutes incubation and flash-freezing plates at -80°C, 35µL of lysed cell suspension were measured in a Centro LB 960 plate luminoter reader (Berthold Technologies, Bad Wildbad, Germany) with 10 seconds integration after automatic injection of 100µL freshly prepared luciferin substrate solution using the Luciferase Assay system (Promega, Mannheim, Germany). Luciferase reporter gene expression was expressed as relative light units (RLU) per seeded cells measured in at least triplicates. Two ng of recombinant Luciferase (Promega, Mannheim, Germany) correspond to 10^7 light units (RLU). Values were adjusted to account for the HBG treated control cells and are stated as mean ± standard error of mean (s.e.m.) of relative light units (RLU) per $5x10^3$ seeded cells on a logarithmic scale.

3.6. RNA isolation and quantitiative reverse transcriptase polymerase chain reation

For qPCR analysis of all relevant therapeutic targets, total RNA was isolated from all samples with the miRCURY™ RNA Isolation Kit (Exigon, Vedbaek, Denmark*)* and 500ng each transcribed into cDNA using the Transcriptor High Fidelity cDNA Synthesis Kit (Roche, Basel, Switzerland) according to manufacture's instructions. Samples were analyzed in duplicates from the same reverse transcriptase reaction and normalized to the housekeeping gene GAPDH. Primers for all targets were designed using the Universal ProbeLibrary Assay Design Center from Roche by performing a species-selective intron spanning assay and in order to find an optimal combination of a Universal ProbeLibrary probe and a gene-specific primer set (all primers ordered from Metabion, Martinsried, Germany. For sequences see Supplementary Information). Analysis was performed in the LightCycler® 480 Real-Time PCR System and qPCR reaction were mixed and run according to manufacturer's recommendations.

3.7. Protein analysis and Western Blot

Protein extracts were collected from LS174T cells 48 hours after siRNA transfection. The combined cell suspension from quadruplicates was lysed with 100µL lysis buffer (Promega, Mannheim, Germany) supplemented with a protease inhibitor cocktail tablet (Roche, Basel, Switzerland) by vortexing cells for total cell lysate preparation. After collecting the supernatant of the cell lysates, protein concentrations were determined using a BCA protein assay according to manufacturer's instructions (Thermo Scientific, Waltham/MA, USA) with bovine serum albumin as standard. Equal amounts of protein were denaturized by incubation at 95°C for 5 minutes in reducing conditions using dithiothreitol and β-mercaptoethanol (Sigma-Aldrich, St.Louis, USA) seperated on a 10% SDS-polyacrylamide gel with the mini-PROTEAN electrophoresis module assembly (Bio-Rad, Hercules/CA, USA) and blotted on a nitrocellulose (NC) membrane. The NC membrane was incubated 1h at RT in 5% w/v non-fat milk powder dissolved in TBST to block unspecific antibody binding sites and immunoreacted overnight at 4°C with a mouse monoclonal antibody against β-catenin (1:5,000, Cell Signaling Technology, Danvers/MA, USA) and a HRP conjugated horse anti-mouse secondary antibody (1:8,000, Vector Lab Inc., Burlingame/CA, USA). To standardize protein amount, the immunostaining procedure was repeated for α-tubulin housekeeping protein visualization employing an anti-α-tubulin antibody (1:5,000, Sigma-Aldrich). In a separate tube, 1.5mL/membrane ECL solutions were mixed in a 1:1 ratio, dispersed onto membranes and protein detected by autoradiography.

3.8. Immunfluorescence and immunohistological evaluation

Immunfluorescence cultured cell lines. Cells were seeded in chamber slides (Nunc, Roskilde, Denmark) at a density of 20,000 cells per chamber 24 hours prior transfection. After siRNA transfection (as described for target cells in 96-well format) cells were incubated 48 hours before cells were fixed with 4% paraformaldehyde in PBS for 15 minutes at room temperature. In order ensure staining of nuclear β-catenin, fixed cells were permeablized with 100% methanol for 10 minutes at -20°C and finally rinsed in PBS for 5 minutes before blocking specimen in blocking buffer (1X PBS/5% normal goat serum) for 60 minutes. Chamber slides then were incubated with a diluted primary antibody solution (β-catenin 1:100 in 1XPBS/1% BSA/ 0.3%Triton X-100) at 4°C over night. After rinsing each chamber three times in PBS, specimens were incubated with an Alexa488-conjugated secondary antibody solution (Alexa488/goat-anti-mouse IgG 1:200 in 1XPBS/1% BSA/0.3% Triton X-100) for 2 hours at RT in the dark. All samples were examined immediately using appropriate excitation wavelength on an Axiovert 200 fluorescence microscope equipped with a Zeiss Axiocam camera. Alexa488 fluorescence was excited using a 485 ± 11nm bandpass filter and emission was detected using a 530 ± 15nm bandpass filter. Transmitted light images were collected using differential interference contrast (DIC). Digital image recording and image analysis were performed with the Axiovision 4.6 software (Zeiss).The images were taken first as bright

field pictures and additionally with the appropriate filter a fluorescence image visualizing eGFP expression or DAPI staining, usually at a 20-fold magnification with a CCD-camera (Zeiss Axiocam, Oberkochen, Germany).

Immunohistochemical analysis. From liver tumor tissue five µm sections were formaline fixed and paraffin embedded, liver tissue samples were collected 13d after tumor inoculation for the detection of Luciferase and β-catenin. Five µm sections were mounted on Super Frost® Plus slides (Thermo Scientific, Waltham/MA, USA) and antigen retrieval for Luciferase staining was achieved with Pronase E (Sigma-Aldrich) diluted in 0.5 M Tris buffer (0.1% w/v) for 20 minutes at room temperature; β-catenin antigen retrieval was performed in a steamer with sodium citrate buffer (10 mM sodium citrate, pH 6.0) for 20 minutes. Endogenous peroxidase activity was quenched by treatment with 1% H_2O_2 for 30 minutes. Slides were incubated over night at 4°C with an anti-luciferase goat polyclonal horseradishperoxidase (HRP) conjugated antibody (Abcam, 1:50 in Tris-buffered saline (TBS)/0.3% BSA (TBS-B)) and an β-catenin mouse monoclonal antibody (BD Biosciences Pharmingen, diluton 1:50 in TBS-B), respectively. For β-catenin staining, a biotinylated secondary anti-mouse antibody was prepared using a rabbit ABC kit (VECTASTAIN ® Elite ABC system, Vector). Immunoreactivity was visualized with the chromogen 3-amino-9-ethyl-carbazole (AEC) (AEC single solution, Invitrogen) for 20 minutes. Slides were evaluated on a Zeiss Axiovert 200 microscope (Carl Zeiss, Jena, Germany) using a 20x DIC objective.

3.9. Confocal laser scanning microscopy

For laser scanning microscopy (LSM) studies, five µm sections of tumor-bearing liver samples mounted on Super Frost ® Plus slides (Thermo Scientific, Waltham/MA, USA) were stained for β-catenin with an Alexa488-labelled secondary antibody as described in 3.9. and incubated with DAPI (1 µg/ml) in PBS in order to stain the nuclei of the paraffin embedded liver tissue samples. Cell imaging was performed with a confocal laser scanning microscope (LSM 510 META; Carl Zeiss, Jena, Germany) equipped with an argon and two helium/neon lasers delivering light at 488, 543, and 633 nm, respectively, as well as an argon laser emitting ultraviolet light at 364 nm. Light was collectedthrough a 63 · 1.4 NA oil immersion objective (Carl Zeiss). Data acquisition was performed in multitrack mode (Alexa 488: excitation at 488 nm, emission at 505–530nm bandpass; DAPI: excitation at 364 nm, emission at 385–470nm bandpass). Data were analyzed with AxioVision 4.6 software (Carl Zeiss).

3.10 Statistical analysis

Results are shown as mean ± s.e.m., with number of experiments indicated. Statistical significance was determined by paired student's t-test. Probability values < 0.05 were considered as statistically significant are marked with a single asterisk, < 0.005 by double asterisks and < 0.0005 by triple asterisks.

4. Results

4.1. Therapeutic siRNA target evaluation

4.1.1. Cell line screen for wnt-deregulation

To determine the activity of the tissue-specific CTP4 promoter, 15 different cancer cell lines and ten low passage human colon cancer cell lines (Coga) were transiently transfected with Luciferase plasmids pCTP4-Luc, pCMV-Luc, pGL3 basic and LPEI-PEG-GE11 as a transfection reagent. Based on the comparison to a strong constitutively active viral promoter CMV (pCMV-Luc) and a DNA construct harbouring the identical transgene without a promoter (pGL3 basic), the relative expression levels were expressed as Relative Light Units [RLU] per 10,000 transfected cells (Fig. 6). The tested cell lines feature a range of oncogenic and tumor-suppressive mutations characteristic from the tumor tissue they originated from. Since the transfection conditions were the same for each group, the expression levels were comparable. Nonetheless, transfection efficencies within testes cell lines may vary and many cell lines have never been tested for their deregulation in the wnt/β-catenin pathway.

The cell lines without non-deregulated wnt/β-catenin pathway showed CTP4-activity comparable to the background level of the pGL3 basic control, showing the absence of „leakiness“ by the CTP4 promoter (Fig. 6A). In contrast, the wnt/β-catenin deregulated SW480 and LS174T cells showed a 2.6-time and a 5-time higher transgene expression driven by CTP4 compared to the CMV promoter, respectively, demonstrating the high and specific expression efficiency of the promoter. Interestingly, with HepG2 hepatocellular carcinoma cells the CTP4-promoter exceeds the CMV promoter by 1.7-fold, whereas Huh7 cells – also a hepatocellular carcinoma cell line – show no deregulation and thus no CTP4-activity at all (88-fold less active than CMV). Since Hela cells showed high expression levels for CMV-Luc, but 2040-fold less activity for the CTP4 promoter, they were chosen as a non-colorectal control cell line. Next, we asked if the expression levels for CTP4-driven transgene expression also high for our Coga cell lines (Fig. 6B). The Luciferase expression obtained with the CTP4 promoter construct only surpasses the CMV promoter transfected group in two cell lines, namely Coga2 and Coga12, where the difference in expression were very similar (1.86-fold of CMV for Coga2 and 1.82-fold of CMV for Coga12).

Taken together, the above data confirm high efficiency and specificity of the CTP4-promoter in established tumor cell lines and low passage human colorectal cancer cell lines. In the following, SW480, LS174T, HepG2, Coga2, Coga12 were used as CTP4-permissive and HeLa cells as nonpermissive control cells, in order to reflect the target screen in many different cancer cell lines of gastrointestinal origin.

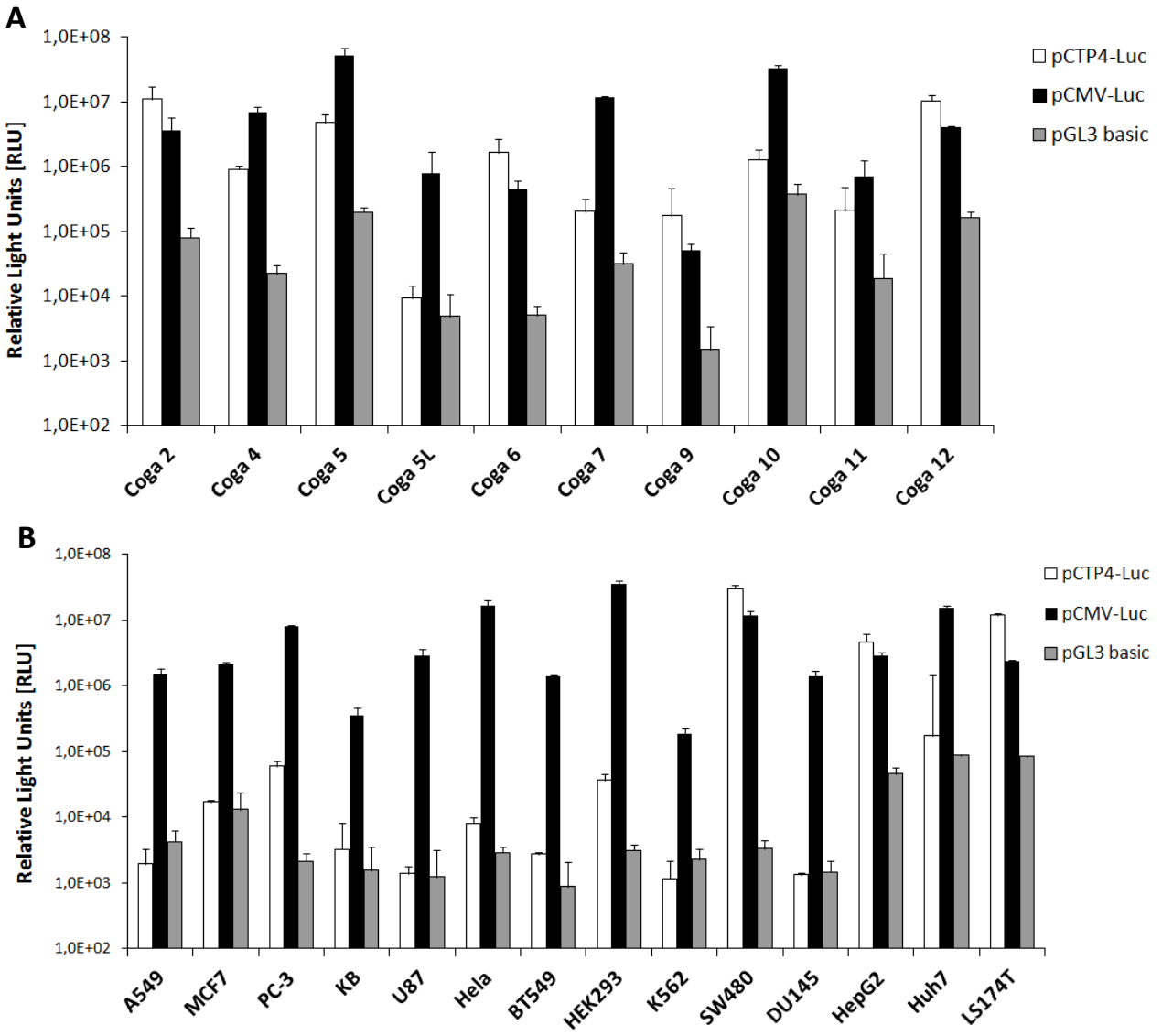

Fig.6 Cell line screening for wnt/β-catenin deregulation in various human cancer cell lines and low passage colon carcinoma cells

(A) Low passage colon carcinoma cells[69] were transfected with constructs both encoding for a Firefly Luciferase (FLuc), one driven by the CTP4-promoter, the other harboring the same backbone driven by the ubiquitously active CMV-promoter and finally with a promoterless FLuc control plasmid (pGL3 basic) using 500ng of each plasmid and LPEI-PEG-GE11 at N/P ratio 6 in a 96-well format. (B) Cancer cell lines originating from various tumor types were also transfected with the same constructs and under the same conditions as indicated for Coga cells. The values are representative means of triplicates of at least two independent experiments and are stated as mean ± s.e.m of relative light units (RLU) per 10,000 cells measured 48 hours after transfection.

4.1.2. qPCR screen in target cell lines for potential therapeutic targets

In order to analyze the expression levels of a selected group of potential therapeutic targets, a RT-qPCR evaluation of all target cell lines for potentially tumorigenicity-related wnt-targets (TCF4, β-catenin, TNIK, PAR-1, OPG and Sox2) was performed. With increased levels of our postulated therapeutic targets, the possibility of therapeutically relevant siRNA-mediated knock-down is given and can be validated in further experiments. As reference, expression levels of indicated target genes in Hela cells were taken into consideration for final evaluation. Cell lines utilized for analysis, were LS174T, SW480, Coga12, Coga2 and HepG2 cells, as they were identified in the previous cell line screen to pinpoint cell lines deregulated in the wnt/β-catenin pathway.

The LS174T cell line exhibited high levels of all targets examined apart from OPG (Fig.7), the expression of β-catenin correlated well with the level of CTP4-activity (Fig.6 B). In SW480 cells β-catenin levels are 33-times higher than the mRNA levels observed in Hela cells, which accounts for the exceptionally high CTP4-activity (see also Fig.6 B). The OPG levels clearly exceed control cell line amount only in SW480 cells which is consistent with previously published data[119]. Hela cells had only low levels of all wnt-related targets, with only Sox2 expression exceeding the levels of Coga2 and HepG2 cells. Exceedingly high levels of TNIK and PAR-1 were examined throughout all target cell lines investigated compared to the non-deregulated control, with LS174T cells showing the highest levels in both targets. For PAR-1, LS174T demonstrate an increase in expression levels of 44-fold compared to control cell line, whereas for TNIK levels a 29-fold expression increment was observed. Based on these results the LS174T cell line was identified as a suitable candidate for TNIK or PAR-1 siRNA targeting.

Althogether, these results suggest that the postulated therapeutic targets can be of relevance in gastrointestinal tumorigenesis, since they are mainly up-regulated in colorectal and hepatocellular cancer cell lines. All in all, potentially therapeutic target genes are overexpressed in SW480, LS174T, HepG2, Coga2 and Coga12, but were not signicantly increased in the non-colorectal control cell line Hela.

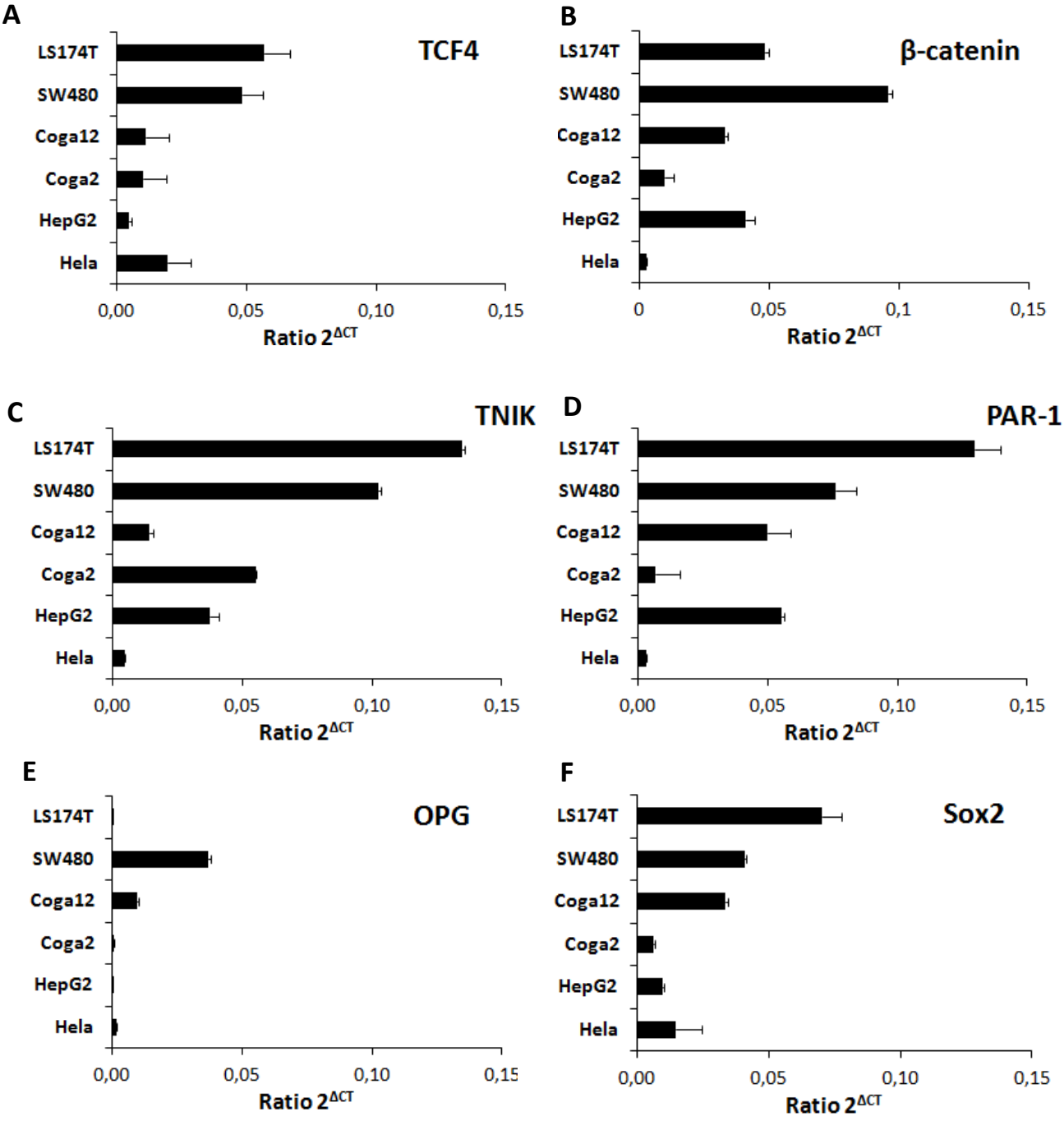

Fig.7 RT-qPCR evaluation of all target cell lines for all potentially tumorigenicity-related targets

Four different colorectal carcinoma cell lines (LS174T, SW480, Coga12 and Coga2), a hepatocellular carcinoma cell line (HepG2) and as a non-wnt/β-catenin deregulated control a cervix carcinoma cell line (Hela) were screened for (A) TCF4, (B) β-catenin, (C) TNIK, (D) PAR-1, (E) OPG or (F) Sox2 via quantitative RT-qPCR. For TCF4, β-catenin, TNIK, PAR-1, OPG and Sox2 expression, the means of triplicates ± s.e.m. were calculated from two independent experiments. Histograms represent the mRNA level of each therapeutic target as ratio of target CT normalized with CT of the housekeeper GAPDH.

4.1.3. Therapeutic siRNA transfection in stably transduced target cell lines

We wanted to establish a screening system with Luciferase transgene expression depending solely on accessible TCF4-binding sites, thus treatment with different siRNAs would contribute to changes in wnt-activity and finally in decreased Firefly Luciferase expression levels. For this approach, LS174T, Hela, HepG2, Coga2, Coga12 and SW480 cells were stably transduced with recombinant lentiviral vectors harbouring either a CTP4-EGFPLuc or a PGK-EGFPLuc expression casette resulting in CTP4-Luc and PGK-Luc cell lines, respectively. After establishment of the transgenic cell lines, they were transfected with TCF4, β-catenin, TNIK, PAR-1, OPG and Sox2 siRNA using brPEISucc at an N/P ratio of 15.

To rule out effects not related to wnt-pathway regulation, cells with either CTP4- and PGK-driven Luc expression casettes were transfected simultaneously, so the degree of siRNA-mediated knock-down in transgene expression will reflect the involvement of the therapeutic target investigated. For PGK-EGFPLuc cells the knock-down achieved in FLuc activity was generally not as prominent as for CTP4-Luc cells. In PGK-EGFPLuc cells, reduced levels of transgene expression ranged between 38% and 89% compared to control-siRNA treated cells (Fig.8 A – E). Througout all target transfections, CTP4-EGFPLuc cells showed more profound knock-down levels, with expression levels of FLuc compared to control-siRNA treated cells ranging between 11% and 86%. The highest reduction in transgene expression could be observed with β-catenin, PAR-1 and TCF4 siRNA in CTP4-Luc cells. In LS174T cells β-catenin knock-down reduced FLuc levels to 13% (Fig.8 D). The TCF4, PAR-1 and Sox2 levels in LS174T cells are reduced to similar levels as β-catenin mediated knock-down (Fig.8 D). Similarly, β-catenin knock-down in Coga2, Coga12, HepG2 and SW480 cells led to the highest knock-down in CTP4-Luc cells (Fig.8 A,B,C,E). The only target which did not achieve significant knock-down in CTP4-Luc cells, compared to PGK-Luc cells was OPG (Fig.8 A-E).

To put it all together, by comparing the results from CTP4 versus the PGK driven EGFPLuc, the specific siRNA-meditated knock-down can be determined. Reduction of CTP4-driven transgene expression is attributed to specific wnt-related interference, whereas diminished PGK-driven Luc expression correlated with reduced proliferation rates. The stable introduction of a CTP4-driven FLuc for therapeutic target screening could be achieved. The extent of reduced transgene expression provides a possible insight into the involvement of investigated therapeutic targets in the wnt/β-catenin-pathway as well as the value of investigated potentially therapeutic structures as therapeutic targets especially for siRNA treatment.

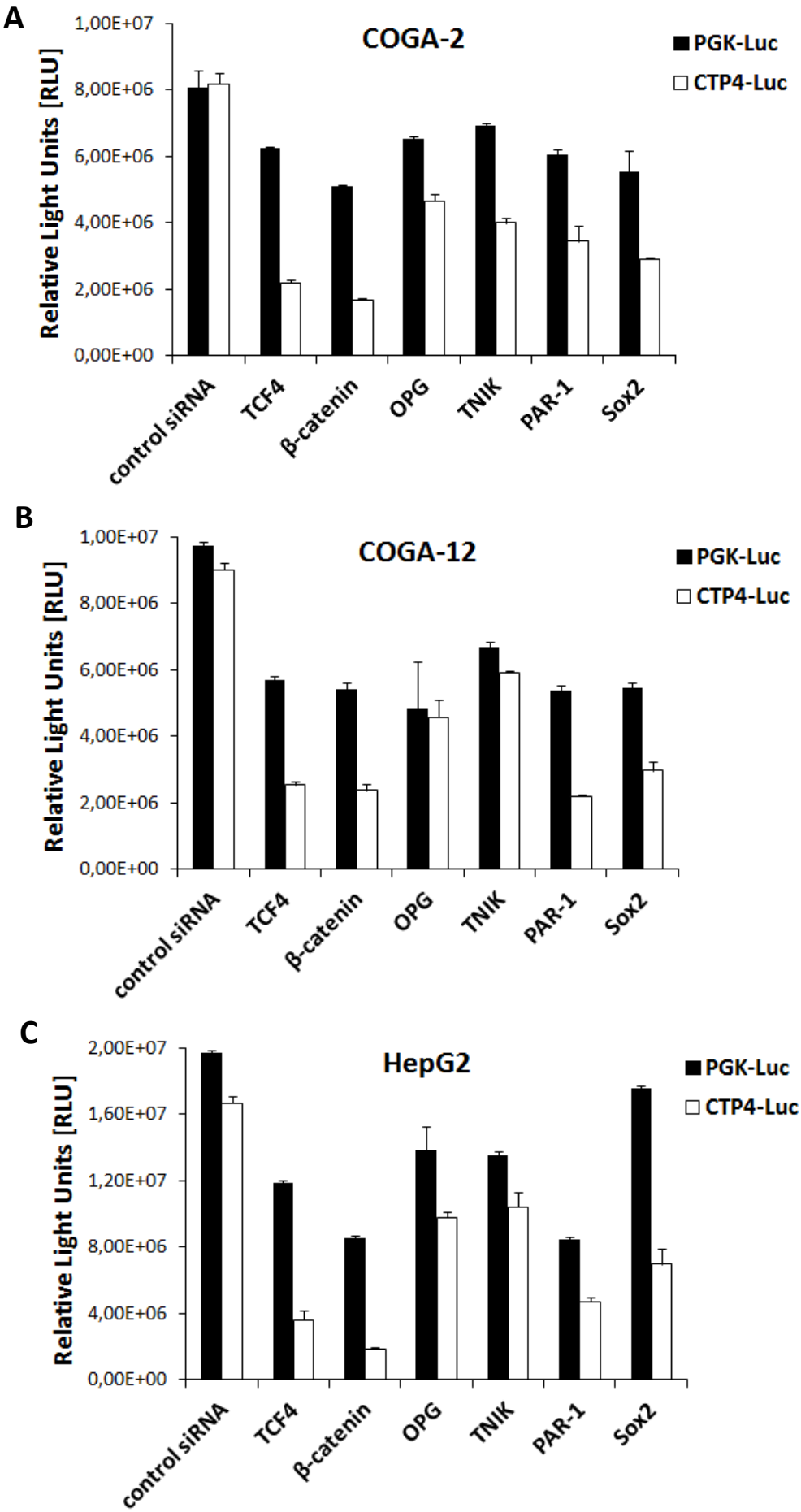
A
COGA-2
PGK-Luc
CTP4-Luc
Relative Light Units [RLU]
1,00E+07
8,00E+06
6,00E+06
4,00E+06
2,00E+06
0,00E+00
control siRNA
TCF4
β-catenin
OPG
TNIK
PAR-1
Sox2
B
COGA-12
PGK-Luc
CTP4-Luc
Relative Light Units [RLU]
1,00E+07
8,00E+06
6,00E+06
4,00E+06
2,00E+06
0,00E+00
control siRNA
TCF4
β-catenin
OPG
TNIK
PAR-1
Sox2
C
HepG2
PGK-Luc
CTP4-Luc
Relative Light Units [RLU]
2,00E+07
1,60E+07
1,20E+07
8,00E+06
4,00E+06
0,00E+00
control siRNA
TCF4
β-catenin
OPG
TNIK
PAR-1
Sox2

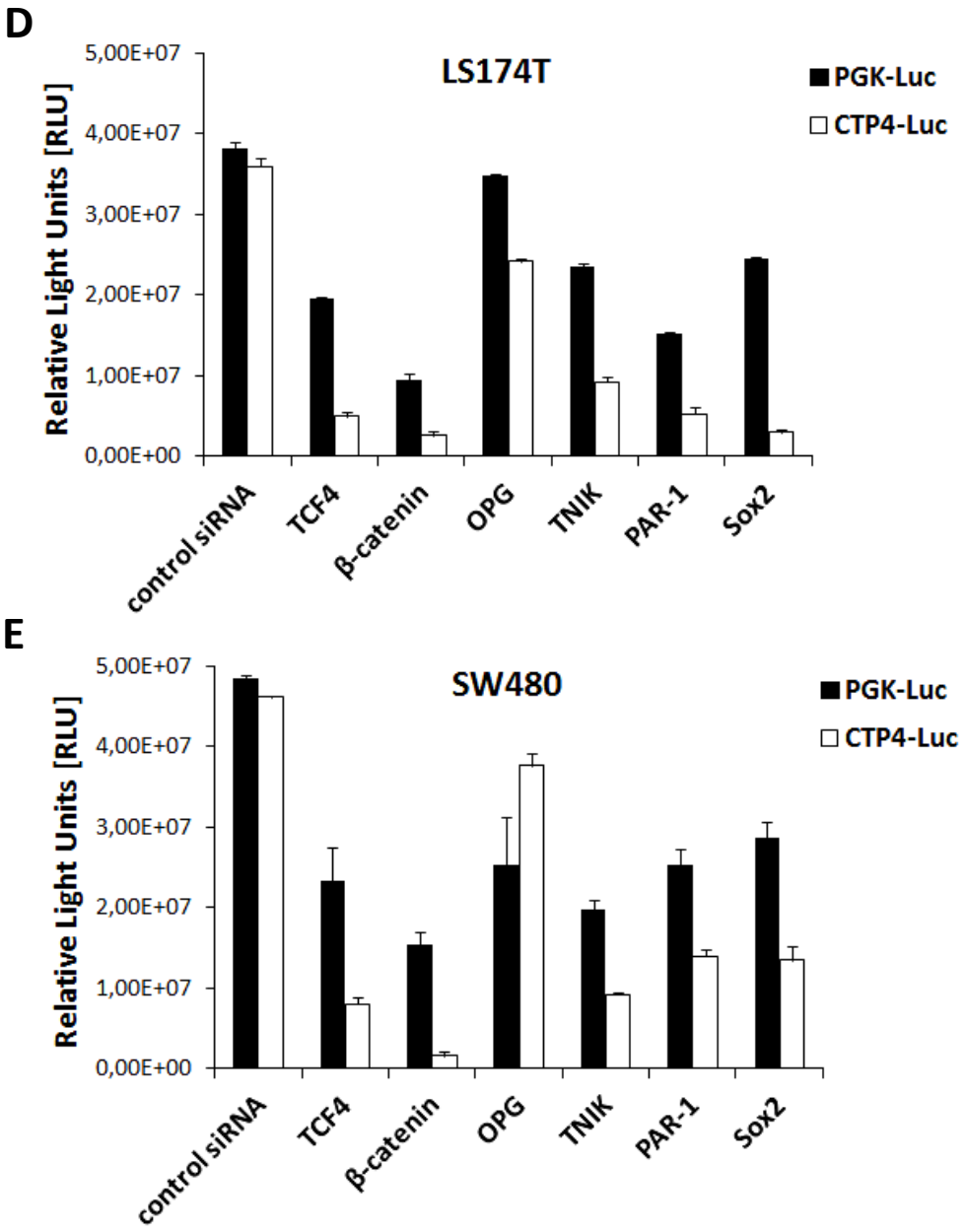

Fig.8 Stably transduced CTP4-Luc and PGK-Luc cells transfected with potential tumorigenicity - related targets siRNA

Target cell lines Coga2 (A), Coga12 (B), HepG2 (C), LS174T (D) and SW480 (E) stably transduced either with a CTP4-EGFPLuc (CTP4-Luc, empty bars) or a PGK-EGFPLuc (PGK-Luc, full bars) casette, were transfected with 500ng siRNA complexed with brPEISucc (N/P of 15) per 96-well targeting either TCF4, β-catenin, OPG, TNIK, PAR-1 or Sox2. The values are representative means of triplicates of at least two independent experiments and are stated as mean ± s.e.m. of relative light units (RLU) per 10,000 cells measured 48 hours after transfection.

4.1.4. siRNA-mediated knock-down validation in LS174T cells

In order to confirm the actual reduction of mRNA and protein levels from targeted molecular structures, RT-qPCR and a Western Blot analysis of LS174T cells transfected with β-catenin siRNA and brPEISucc (N/P of 15) were performed 48 hours after transfection. Specific knock-down of β-catenin mRNA as well as protein could be confirmed and LS174T cells were utilized for all *in vivo* experiments.

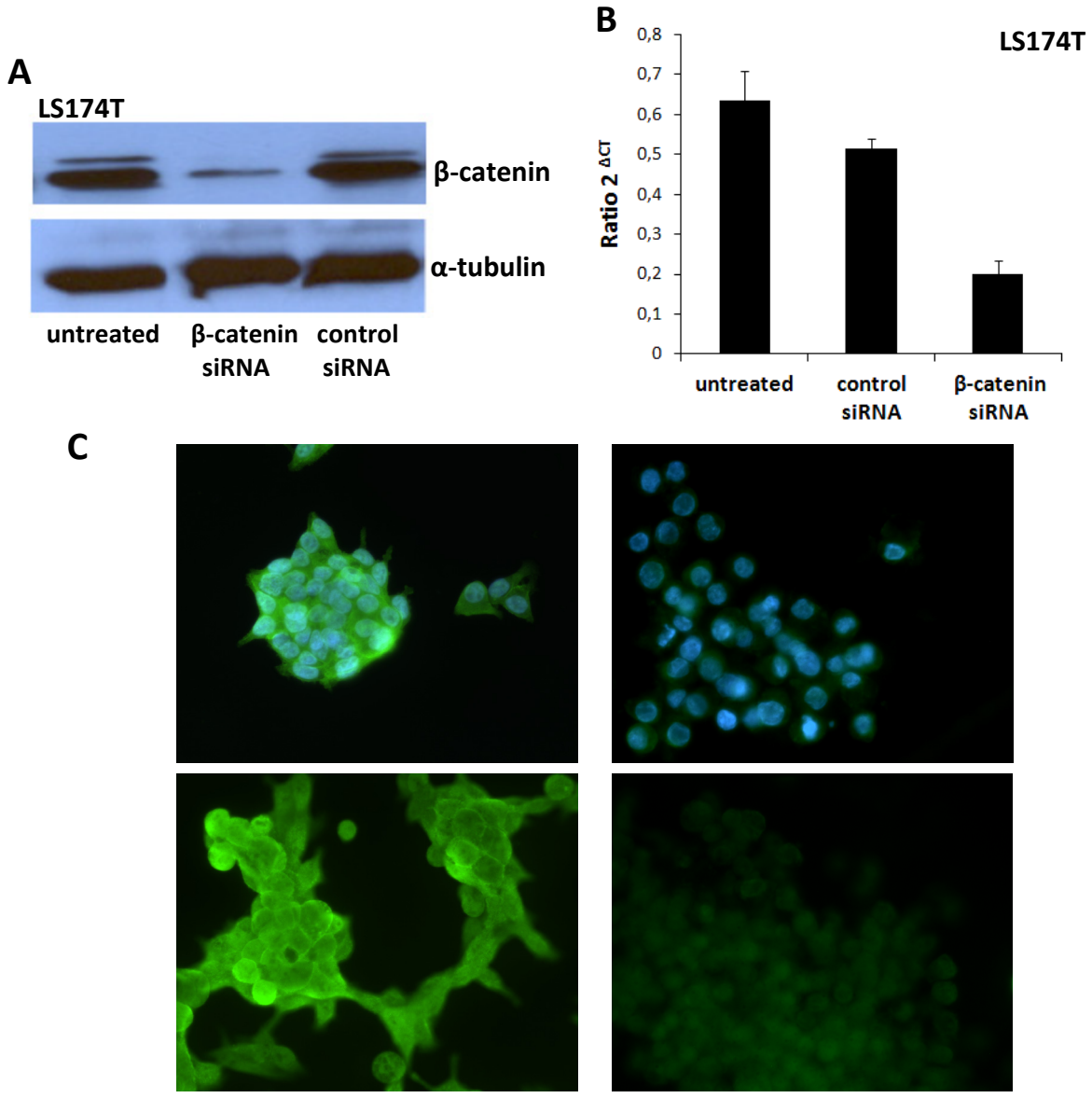

Fig.9 LS174T cells β-catenin level after siRNA-mediated knock-down

From LS174T cells transfected with β-catenin siRNA an exempelary RT-qPCR and a Western Blot were performed with RNA and protein extract from quadruplicates of transfected cells 48 hours after transfection. (A) Western Blot of β-catenin, control siRNA treated and untreated cells. (B) qPCR of β-catenin mRNA levels in untreated, control siRNA or β-catenin siRNA transfected LS174T cells. (C) Immunfluorescence of β-catenin in LS174T cells stained with an Alexa488 labelled secondary antibody.

4.2. Biological monitoring of identified therapeutic targets

4.2.1. Determination of anchorage independent growth in a soft agar assay

Effect of tumorigenicity-related wnt-target siRNA on cell anchorage independent growth for all target cell lines was analyzed with a soft agar assay. Growth in soft agar after siRNA transfection of LS174T, SW480, Coga12, Coga2, HepG2 and Hela cells was examined. Cells were transfected with 500ng of siRNA per 96-well complexed with brPEISucc at an N/P ratio of 15, 24 hours later cells were collected, re-seeded in 60mm dishes and cultured in soft agar for 15 days. Subsequently, colonies of at least 10 cells were counted and a significant decrease in 10 cell – colonies, was evident throughout all cell lines (apart from control cell line Hela) for β-catenin and PAR-1 (Fig.10 A-D). Representative cultures of β-catenin and control siRNA-treated as well as untreated LS174T cells are shown (Fig.10 B) For OPG siRNA-treated cells, only SW480 cells showed significantly reduced numbers of colonies. PAR-1, β-catenin and TNIK showed highly significant growth reduction in all target cell lines. None of the investigated potentially therapeutic targets had a profound effect on Hela cells which served as a control cell line.

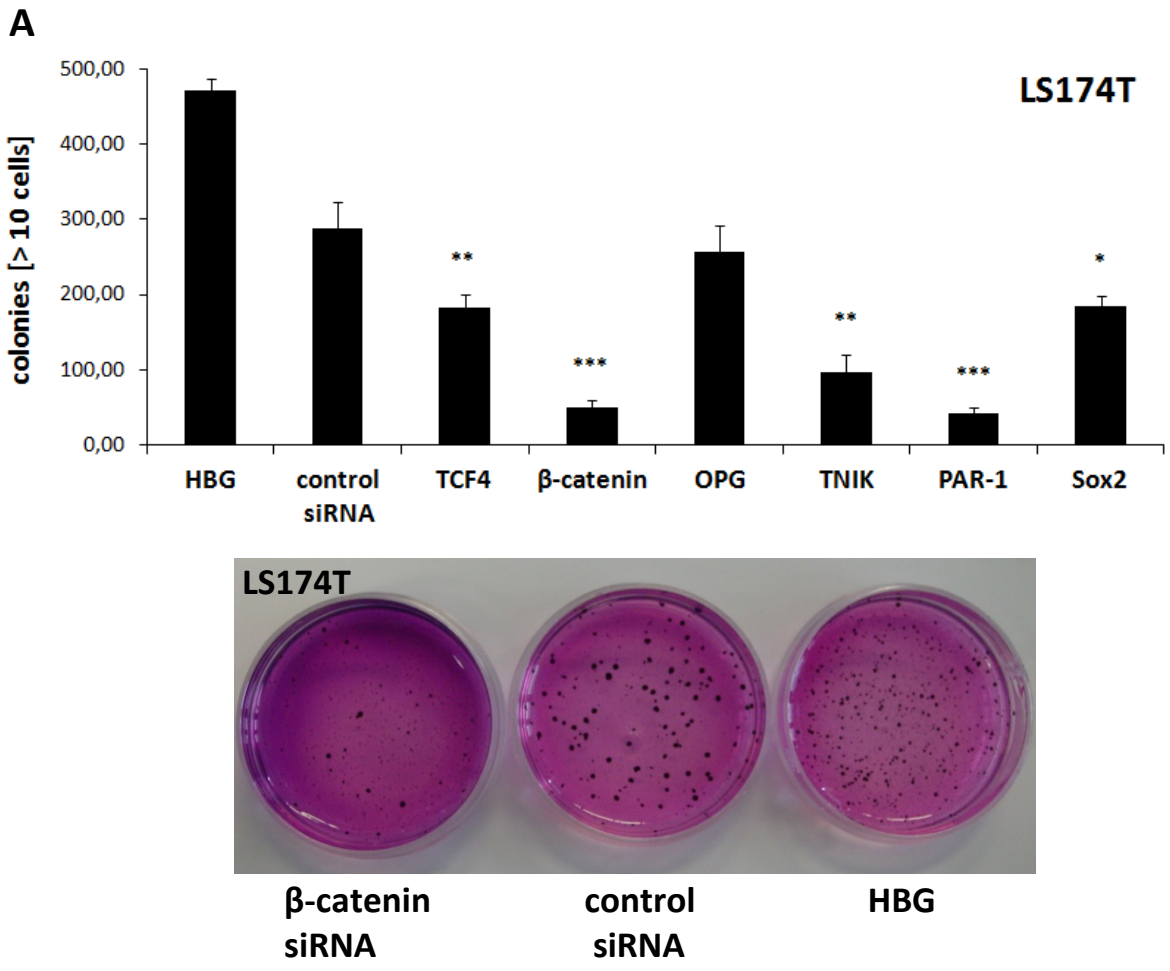

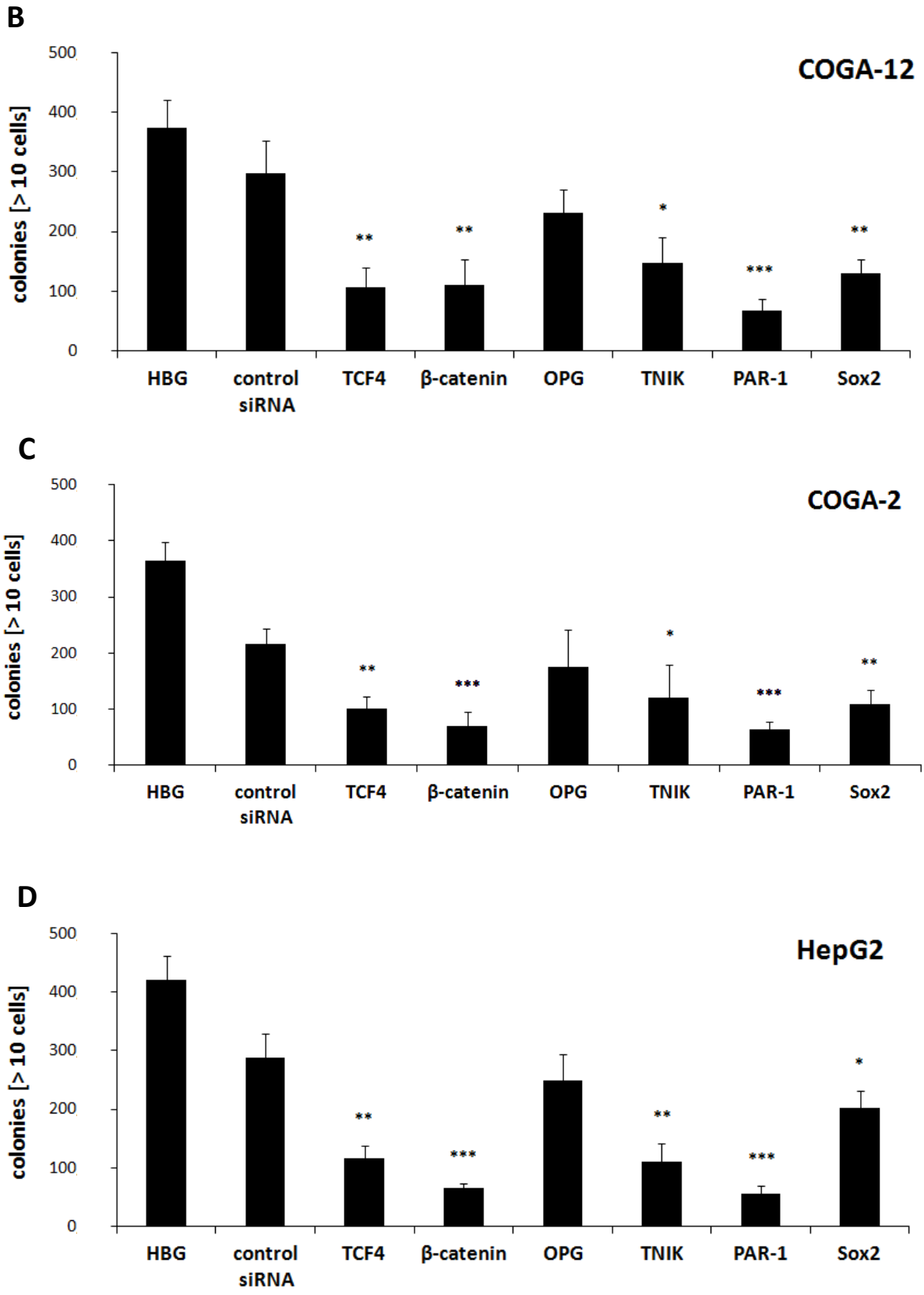
B
COGA-12
colonies [> 10 cells]
500
400
300
200
100
0
**
**
*
***
**
HBG
control siRNA
TCF4
β-catenin
OPG
TNIK
PAR-1
Sox2
C
COGA-2
colonies [> 10 cells]
500
400
300
200
100
0
**
***
*
***
**
HBG
control siRNA
TCF4
β-catenin
OPG
TNIK
PAR-1
Sox2
D
HepG2
colonies [> 10 cells]
500
400
300
200
100
0
**
***
**
***
*
HBG
control siRNA
TCF4
β-catenin
OPG
TNIK
PAR-1
Sox2

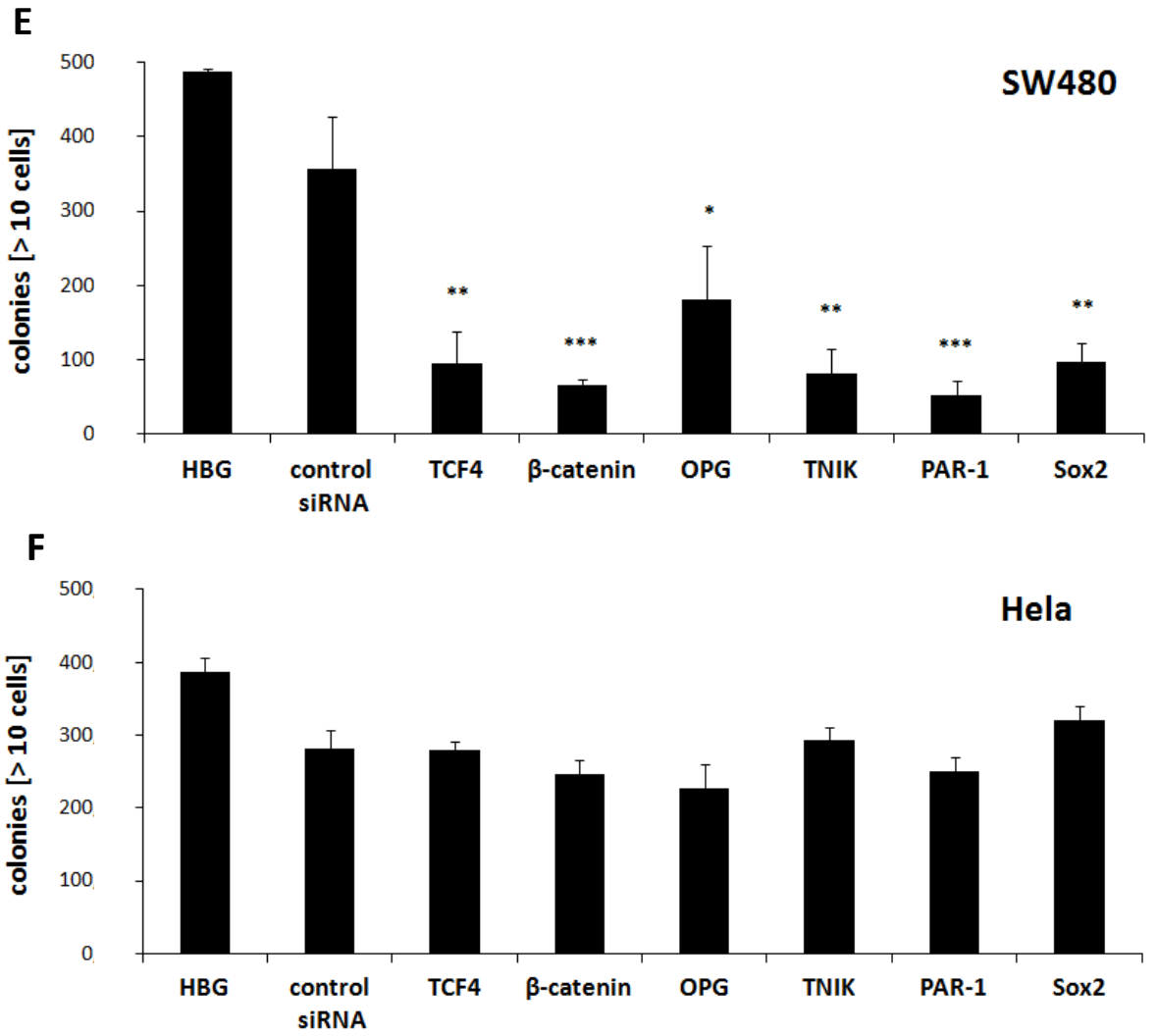

Fig.10 Soft agar colony formation assay for all target cell lines after transfection with tumorigenicity-related target siRNA

Four different colorectal carcinoma cell lines LS174T (A), SW480 (E), Coga12 (B) and Coga2 (C), a hepatocellular carcinoma cell line HepG2 (D) and as a non-wnt/β-catenin deregulated control a cervix carcinoma cell line Hela (F) were treated with 500ng of either TCF4, β-catenin, TNIK, PAR-1, OPG or Sox2 siRNA per 96-well complexed with brPEISucc at an N/P ratio of 15, after 24 hours cells were seeded in a soft agar layer for colony formation and observed for 14 days. At the end of incubation period, 10 cell – colonies were stained with MTT-reagent and number of colonies of triplicates determined. For statistical analysis a paired student's t-test comparing the treated to control siRNA treated specimen. Data represents mean ± s.e.m with * = significantly different from respective controls ($p<0.05$), ** = $p < 0.005$ and *** = $p < 0.0005$.

4.2.2. Determination of invasion potential in a transwell assay

Invasion through the extracellular matrix (ECM) is an important step in tumor metastasis. Cancer cells initiate invasion by adhering to and spreading along the blood vessel wall. Proteolytic enzymes, such as MMP collagenases, dissolve tiny holes in the sheath-like covering (basement membrane) surronding the blood vessels to allow cancer cells to invade[128].

In order to evaluate invasion of tumor cells through a basement membrane model, the QCM™ 96-well Cell Invasion Assay was utilized. This kit utilizes 96-well inserts with an 8µm pore size polycarbonate membrane coated with a thin layer of ECMatrix™, a reconstituted basement membrane matrix of proteins derived from the Engelberth Holm-Swarm (EHS) mouse tumor[129-132]. Target cell lines were treated with target siRNAs complexed with brPEISucc at an N/P ratio of 15; 24 hours after transfection treated cells were seeded into the upper chamber with cell culture medium lacking fetal bovine serum (FBS). The lower chamber contained FBS which acted as a chemoattractant for cells in the upper chamber. Invading cells migrate through and attach to the bottom of the membrane, while non-invading cells remain above. After invaded cells are detached and lysed, the cell lysate is stained with a fluorescent dye which exhibits strong fluorescence enhancement when bound to cellular nucleic acids.

For LS174T cells β-catenin, PAR-1 and TNIK evoked the strongest decrease in migration (Fig.11). Nonetheless, all examined targets show a profound effect on all target cell lines, apart from OPG. The latter only reduced migrations to a significant extend in SW480 cells, which concurs with increased OPG levels in this cell line (see also Fig.7). In LS174T cells β-catenin, TNIK, PAR-1 and Sox2 siRNA knockdown contributed almost equally to invasive behavior (Fig.11). In the control cell line Hela only TCF4- and Sox2 siRNA treated cells demonstrate a slight decrease in migrated cells, all remaining approaches showed no evident effect on Hela cells.

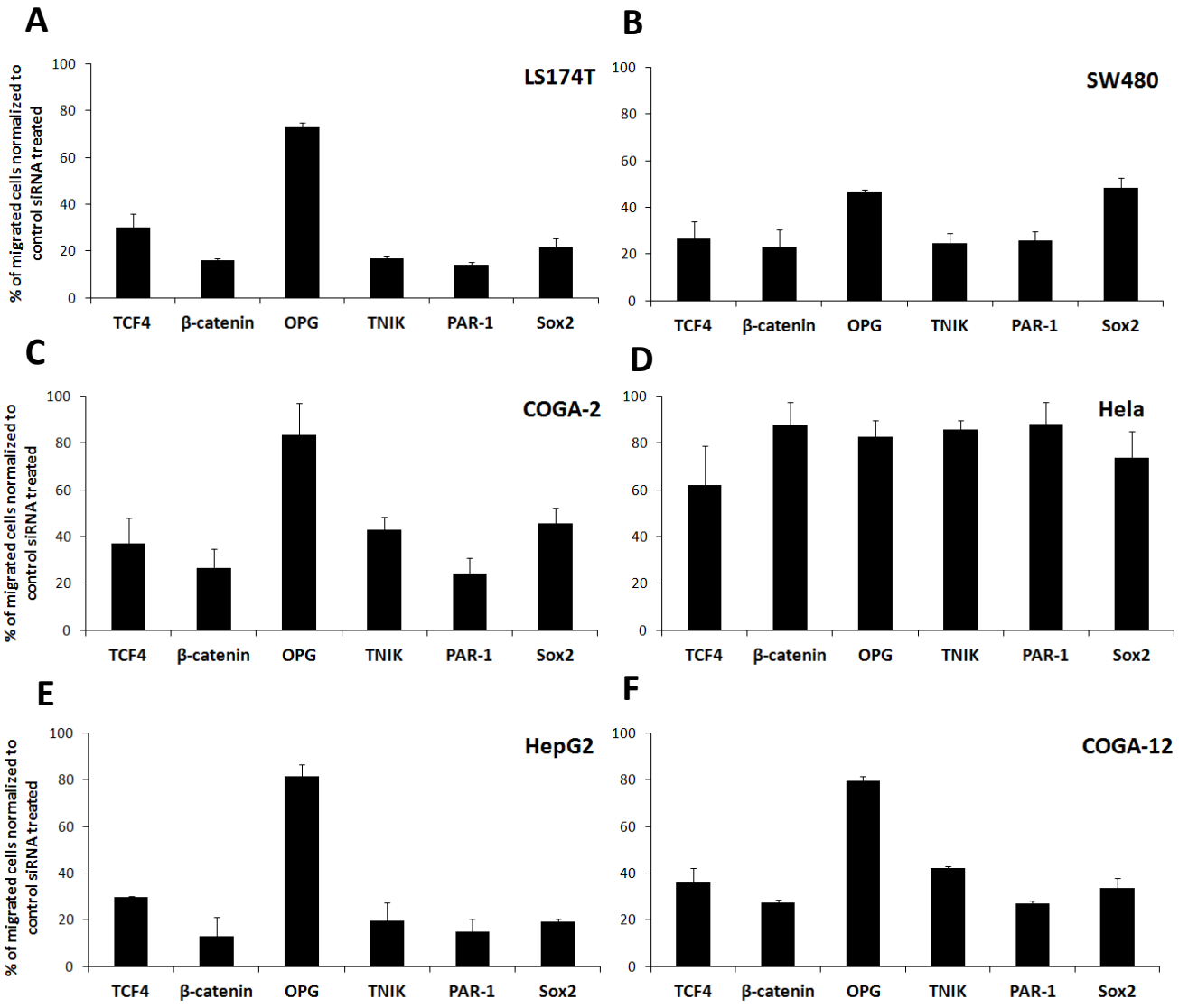

Fig.11 Invasion assay for all target cell lines after transfection with tumorigenicity-related target siRNA

Four different colorectal carcinoma cell lines LS174T (A), SW480 (B), Coga2 (C) and Coga12 (F), a hepatocellular carcinoma cell line HepG2 (E) and as a non-wnt/β-catenin deregulated control a cervix carcinoma cell line Hela (D) were treated with 500ng of either TCF4, β-catenin, TNIK, PAR-1, OPG or Sox2 siRNA complexed with brPEISucc at an N/P ratio of 15, after 24 hours cells were seeded in 8µm Boyden chamber. Migration behavior induced by creating a chemo-attractant gradient and migrated cells of each triplicate were measured according to the manufacturer's instructions. Results are represented as percentage of migrated cells normalized to control siRNA treated cells. The values are representative means of triplicates ± s.e.m of at least two independent experiments.

4.3. Transactivation of wnt-signaling in target and non-deregulated control cell lines

In order to verify that wnt-signaling can be induced LS174T, SW480, HepG2, Coga2, Coga12, Hela and HEK293 were either transfected with 500ng plasmid DNA using LPEI-PEG-GE11 at an N/P ratio of 6 encoding a dominant negative mutant of TCF4 (dnTCF4), a β-catenin mutant with a C-to-A missense mutation that changes Ser33 to Tyr (β-catenin S'33Y) or control transfections were carried out with a plasmid encoding a red fluorescence protein (mcherry). Alternatively, cell were treated with GSK3 inhibitor LiCl (25mM), recombinant wnt3a protein dissolved in cell culture medium at 30µg/mL (rec wnt3a) and supernatant from L-wnt3A cells expressing wnt3a (wnt3a SN). Target cells lines used were stably transduced with a CTP4-EGFPLuc expression cassette, while Hela and HEK293 cells as non-deregulated control cell lines were stably transfected with linearized CTP4-EGFPLuc and a homogenous cell population created with zeocin selection pressure.

Control cell lines Hela- and HEK293 CTP4-EGFPLuc cells show no measurable transgene expression levels (Fig.12 A & B), Transfections with dnTCF4 or mcherry plasmid have no wnt stimulatory effect as expected (RLU at background level), whereas β-catenin S'33Y transfection or treatment with LiCl increase CTP4 driven Luc activity by 32200- and 32000-fold in Hela as well as 1700- and 16000-fold in HEK293 cells, respectively. The direct comparison of wnt3a-protein treated cells in control cell lines shows an increase in transgene expression of 7300-fold in Hela cells compared to the untreated control (Fig.12 A & B). Interestingly the L-wnt3A derived supernatant has no wnt-inducing effect in either the control or the target cell lines. The expression levels of treated target cell lines did not exceed the untreated control Luciferase expression, except for LiCl treated Coga2 cells (115-fold increase) (Fig.12 D). Transfection with mcherry reduces transgene expression due to the temporary toxic effect of the transfection reagent, while transfection with dnTCF4 pDNA successfully reduces wnt-activity in all target cell lines. In contrast, β-catenin S'33Y transfection has no stimulatory effect although theoretically the wnt-pathway should be induced.

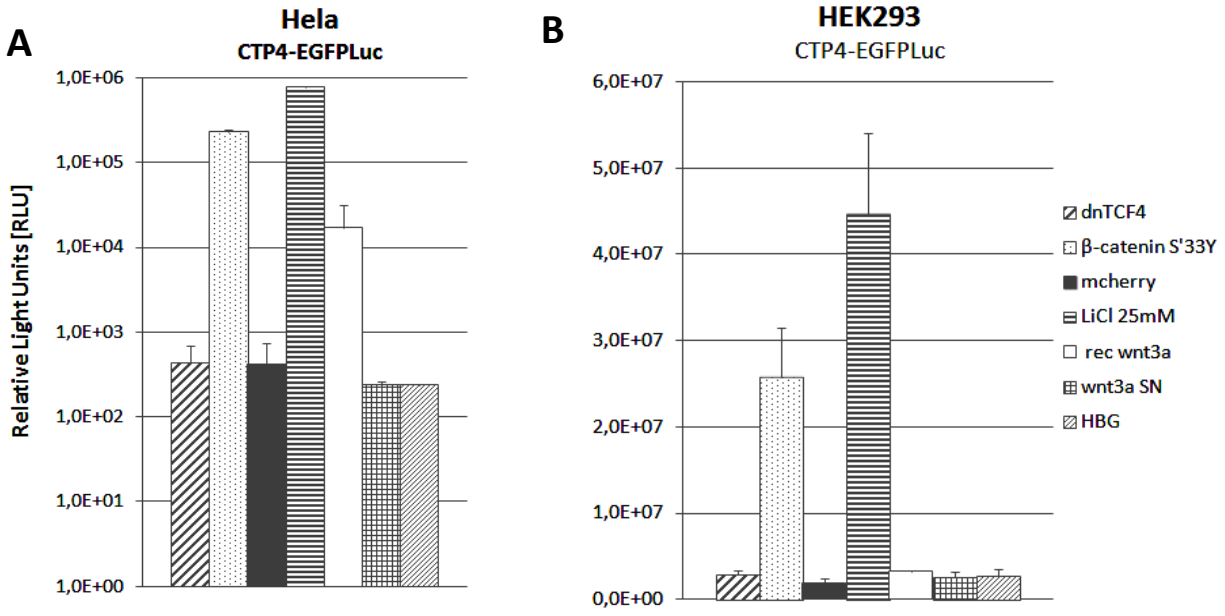

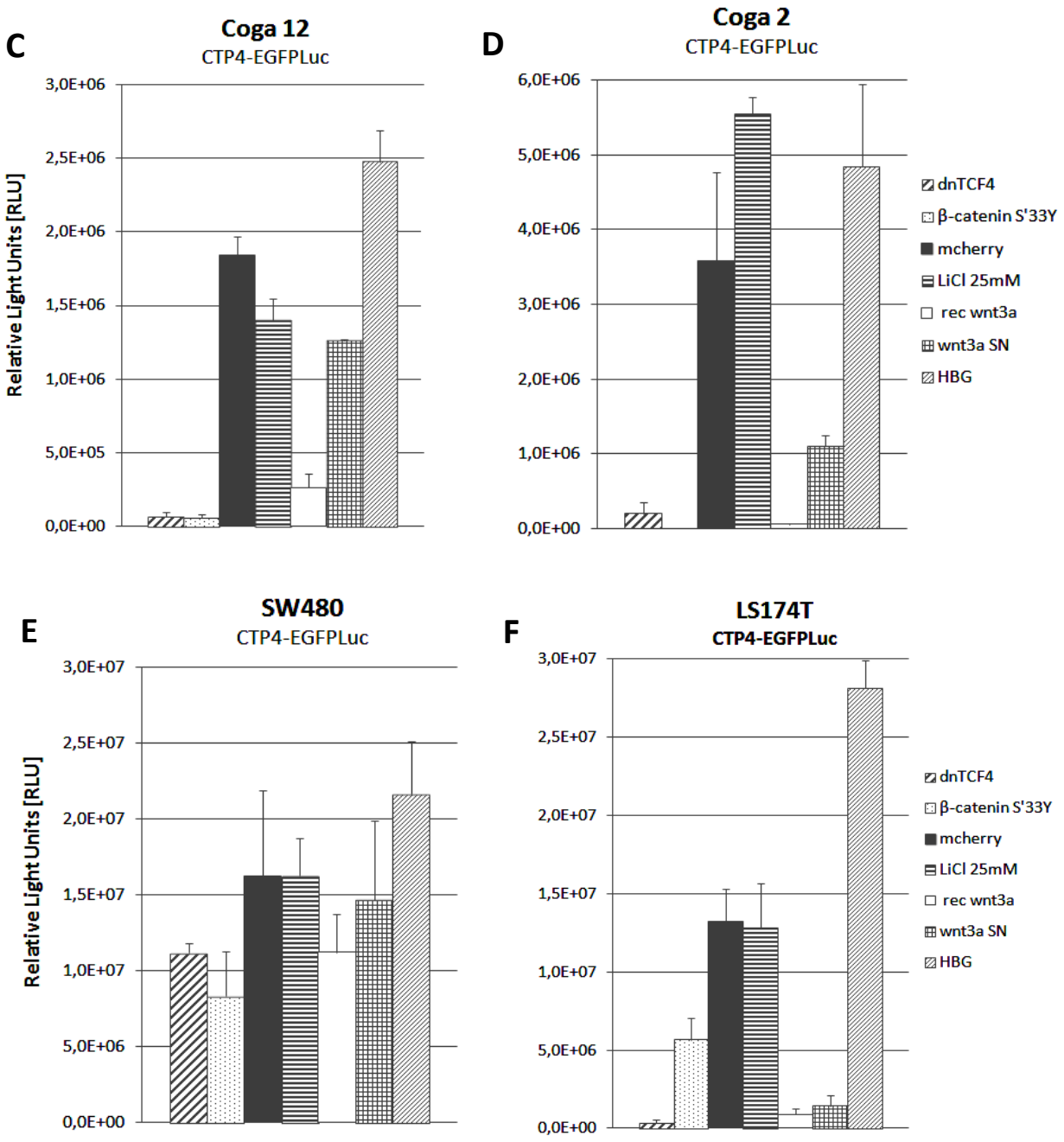

Fig.12 Wnt-pathway induction of target and control cell lines

Transfection of non-deregulated cell lines Hela (A) and HEK293 (B), as well as target cell lines Coga12 (C), Coga2 (D), SW480 (E) and LS174T (F) cells with pDNA complexed with LPEI-PEG-GE11 N/P of 6 encoding either dnTCF4, β-catenin S‘33Y, mcherry or treatment with LiCL or wnt3a. Firefly Luciferase activity driven by the CTP4 promoter stably introduced into all cell lines was quantified 48 hours after treatment. The values are representative means of triplicates of at least two independent experiments and are stated as mean ± s.e.m. of relative light units (RLU) per 10,000 cells measured 48 hours after transfection.

4.4. Targeted delivery of plasmid DNA encoding cytotoxic proteins

4.4.1. Transfection efficiency of target cells

The previous sections confirmed the selectivity of the CTP4 promoter for β-catenin deregulated tumor cell lines. In addition, the strong deregulation in various cell lines derived from gastrointestinal tumors was determined. With the objective to achieve maximum selectivity to exclusively kill cells with a deregulated wnt/β-catenin pathway, plasmids were cloned with a CpG-free backbone harbouring two different cytotoxic proteins – either Apoptin or Diptheria Toxin Subunit A (DTA). Since the major limiting factor to the apoptosis induction ability is the transfection efficiency of the target cell lines, we chose a dual strategy, where target cells were - in the same experimental setting – transfected with plasmid DNA expressing fluorescent protein mcherry for transfection efficiency determination in addition to DTA or Apoptin pDNA transfection. In the following, the results from transfections with 500ng pCpG-hCMVenh-EF1-mcherry pDNA complexed with LPEI-PEG-GE11 at an N/P ratio of 6 per well of 10,000 seeded cells are shown.

Transfection efficiency of Coga2 cells peaked at 21 % as determined by flow cytometry 48 hours after gene delivery, the range of red fluorescence in transfected cells varied from light fluorescence evident after 24 hours to high expression of mcherry protein after 48 and 72 hours (data not shown). Coga12 reach a transfectability of 49%, which is higher than transfection efficiency in Coga2. LS174T cells, despite their unique morphology of growing in loose clumps still reach a transfection efficacy of 40%. Of SW480 and HepG2 cells almost 60% can be transfected (Fig.13). In comparison, the most efficient gene delivery was achieved with HEK293 cells (88%) and Hela cells (65%). In all cases, transfected cells were strongly fluorescent indicating high levels of mcherry in those target cells where gene delivery was successful.

To sum up, all previously identified target cell lines could successfully be transfected with a transgene (in this case mcherry as proof of principle) with varying efficiencies under the control of a ubiquitously active and strong promoter.

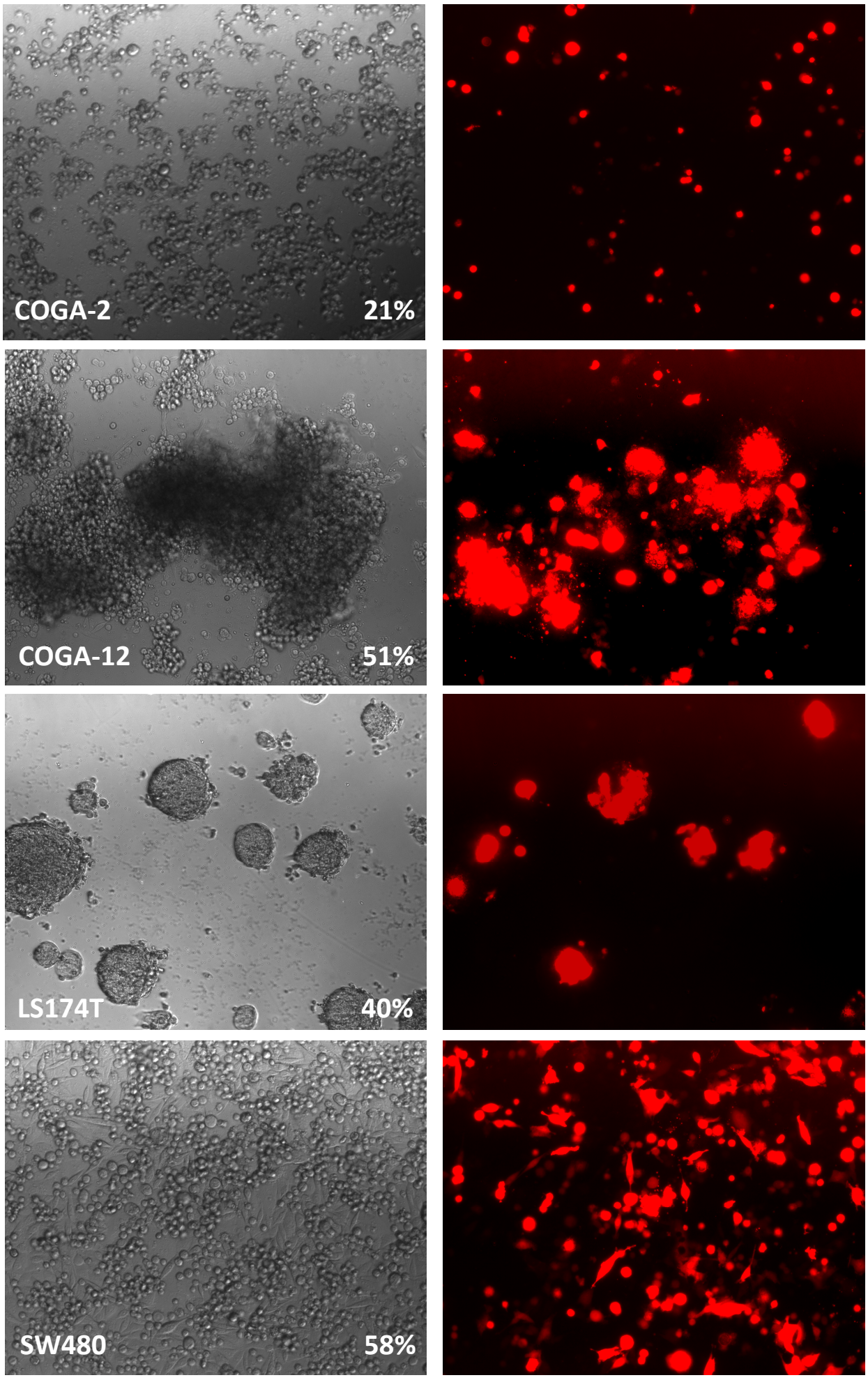
COGA-2
21%
COGA-12
51%
LS174T
40%
SW480
58%

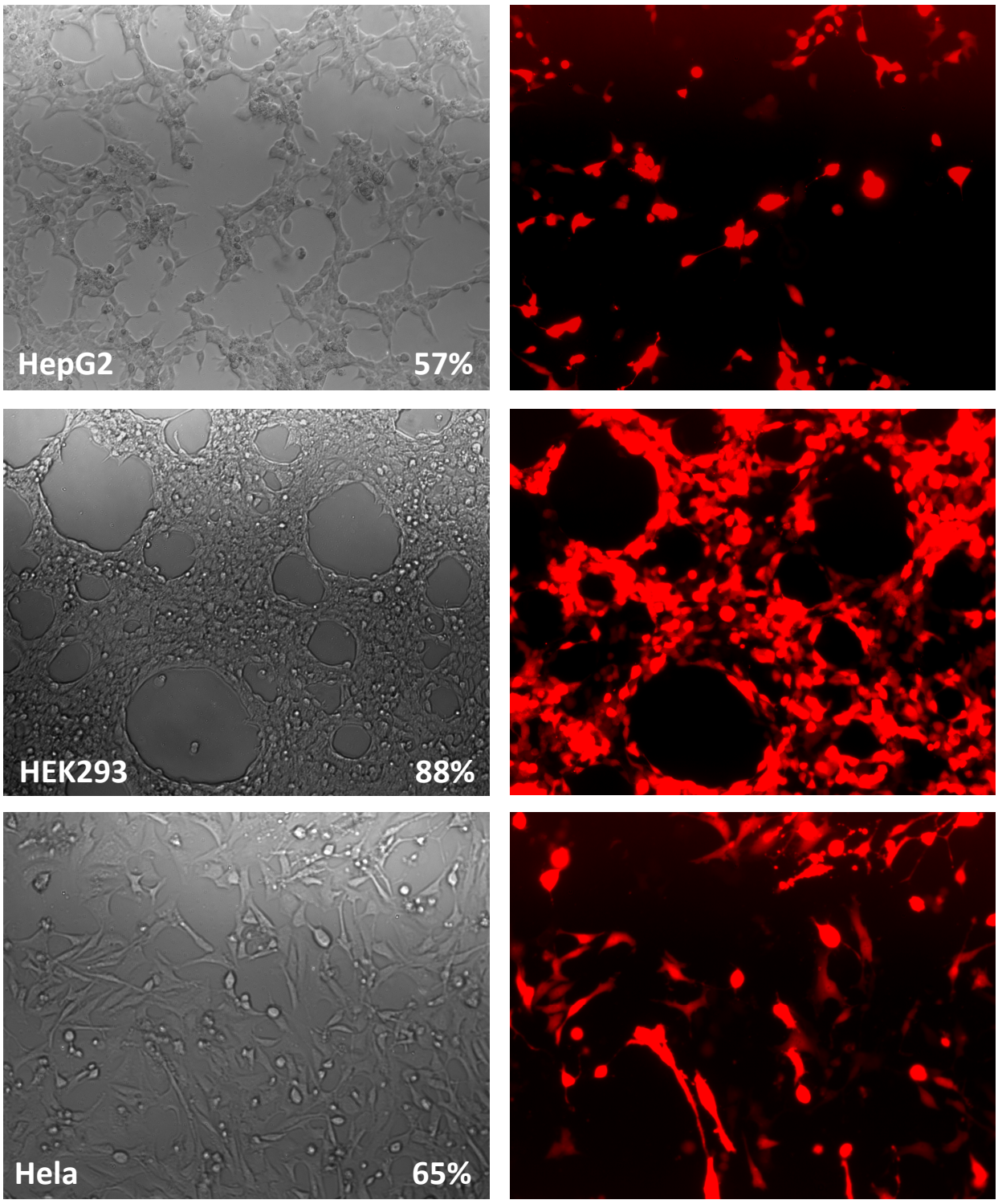

Fig.13 Transfection efficiency of all target cells with pCpG-hCMVenh-EF1-mcherry

Target cell lines (Coga2, Coga12, LS174T, SW480, HepG2) and non-deregulated cell lines (Hela and HEK293) were transfected with 500ng of pDNA harbouring an EF1-driven mcherry expression cassette complexed with LPEI at an N/P ratio of 6. Fluorescence images (right panel) as well as brightfield images (left panel) were obtained 48 hours after transfection and subsequently cells were analyzed via flow cytometry for transgene expression. Representative brightfield and fluorescence image of all transfected cell lines are shown with percentage of mcherry-positive cells analyzed via flow cytometry.

4.4.2. AnnexinV flow cytometric apoptosis analysis of all target cells

After the specificity and leakiness of the CTP4 promoter had been determined in various cell lines (Fig.6 A, B), CpG-depleted plasmid DNAs were designed encoding two different cytotoxic proteins – Apoptin (protein of 121 AA encoded by chicken anemia virus) or DTA (Diptheria Toxin Subunit A). All transfections were conducted with 500ng of either pCpG-hCMVenh-CTP4-DTA, pCpG-hCMVenh-CTP4-Apoptin complexed with LPEI-PEG-GE11 at an N/P ratio of 6 per well of 10,000 seeded cells.

Apoptosis was determined using an AnnexinV flow cytometry based assay, where transfected cells were counterstained with FITC-labelled AnnexinV and DAPI. With DAPI marking necrotic or late apoptotic cells (R2), FITC positive cells represent (early) apoptotic cells (R4) and unstained cells correspond to the viable cell portion (R1) (see Fig.9). The selective killing potential of pDNA encoding for either Apoptin or DTA was shown in all target cells measured by flow cytometry and for the final analysis number of apoptotic cells will be normalized to the percentage of transfected cells. pCpG-hCMVenh-CTP4-DTA or -Apoptin transfected cells were appropriately gated based on HBG treated cells. For comparison a positive control with staurosporine treated cells (0.5 µM for 6h) was included. All target and control cell lines were subsequently incubated with AnnexinV-FITC and DAPI to distinguish between viable, apoptotic and necrotic cells. Untreated cells of all investigated cell lines exhibited all an apoptosis rate < 5%, this small number of AnnexinV positive cells in the untreated population likely represents a basal level of apoptosis expected to occur in these cell populations. Staurosporine treated cells showed an apoptosis rate of >65%. After transfection with pGL3 basic (mock transfected) the percentage of apoptotic cell increased up to 8% in all cell lines (see Fig. 14 A – F). In Fig.14, in the upper panel of each cell line, pCpG-CTP4-DTA as well as pCpG-CTP4-Apoptin transfected cells are shown. In DTA transfected cells 40% are apoptotic, compared to Apoptin transfected cells where only 24% undergo apoptosis (Fig.14 A). When normalized to transfected cells, DTA transfection results in 68% and Apoptin transfection in 42% apoptotic cells. In LS174T cells DTA-and Apoptin-transfection induces apoptosis in 39% and 28% of the entire cell population, respectively (Fig.14 B). If the percentage of actually transfected cells is taken into consideration, DTA triggers an apoptotic response in 99% of transfected cells. The apoptosis induction rate of Coga 2 cells results in 19% for DTA-transfected (88% of transfected cell fraction) and 6% for Apoptin-transfected (27% of transfected cell fraction). In comparison, Coga12 cells show apoptosis in 49% of DTA-transfected (98% when normalized to % transfected cells) and 17% of Apoptin-transfected (34% when normalized to % of transfected cells). HepG2 cells demonstrated a higher extent of apoptosis after DTA transfection resulting in 56% (99% of transfected cells) undergoing apoptosis compared to 28% (49% of transfected cells) induced by Apoptin transfection.

In contrast, the non-permissive control cell line Hela transfected either with DTA or Apoptin showed 9% and 2% apoptotic cells, respectively. This exceeds the mock transfected control only slightly, which proves a highly restrictive expression of both cytotoxic transgenes controlled by the CTP4-promoter. All in all, specific apoptosis-induction could be achieved in all wnt/β-catenin deregulated target cell lines (SW480, Coga12, Coga2, HepG2 and LS174T) without significant cell death in control cell lines (Hela and HEK293). This argues that pDNA encoding potent cytotoxic proteins under the control of the CTP4-promoter are functional and transcriptional targeting is feasible *in vitro*. To conclude, maximum selectivity could be achieved and pCpG-CTP4-DTA/Apoptin exclusively kills cells with a deregulated wnt/β-catenin pathway.

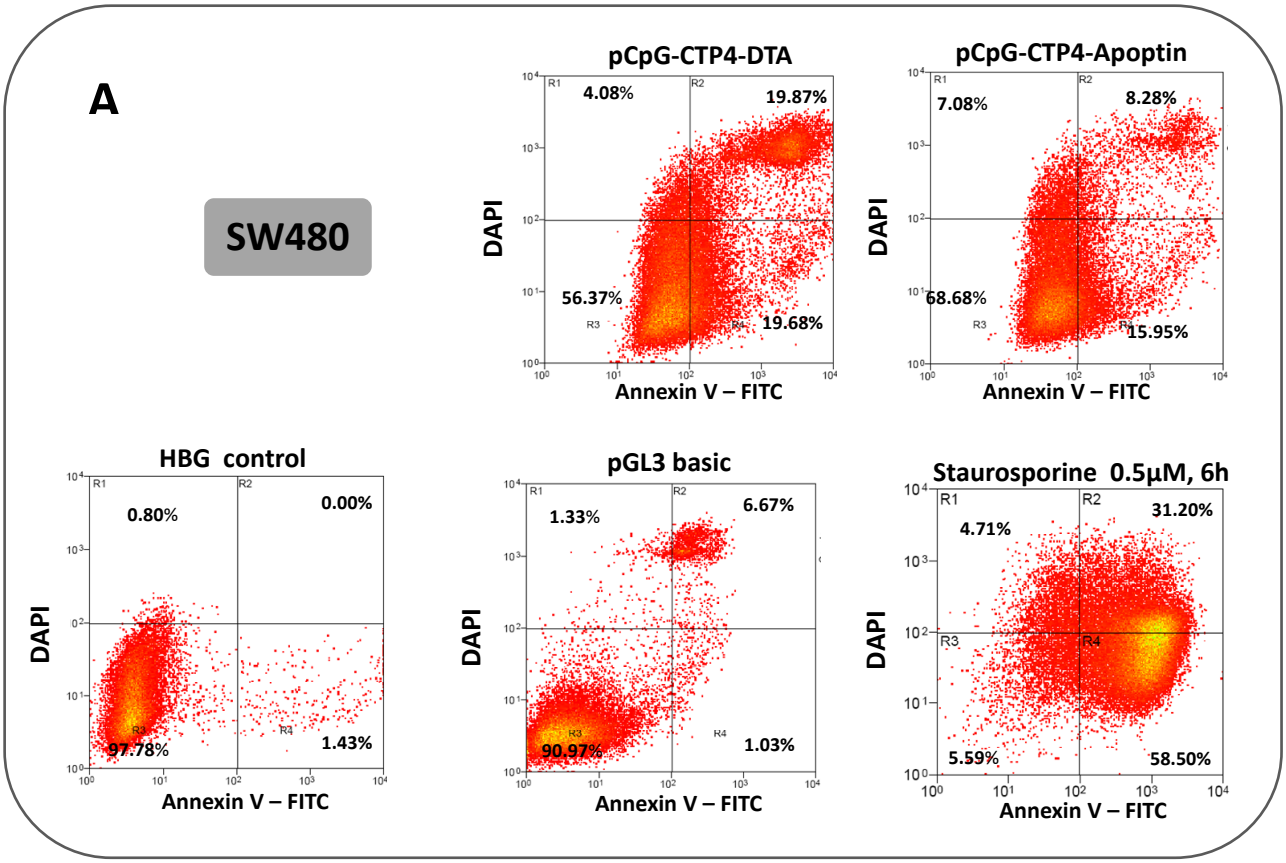

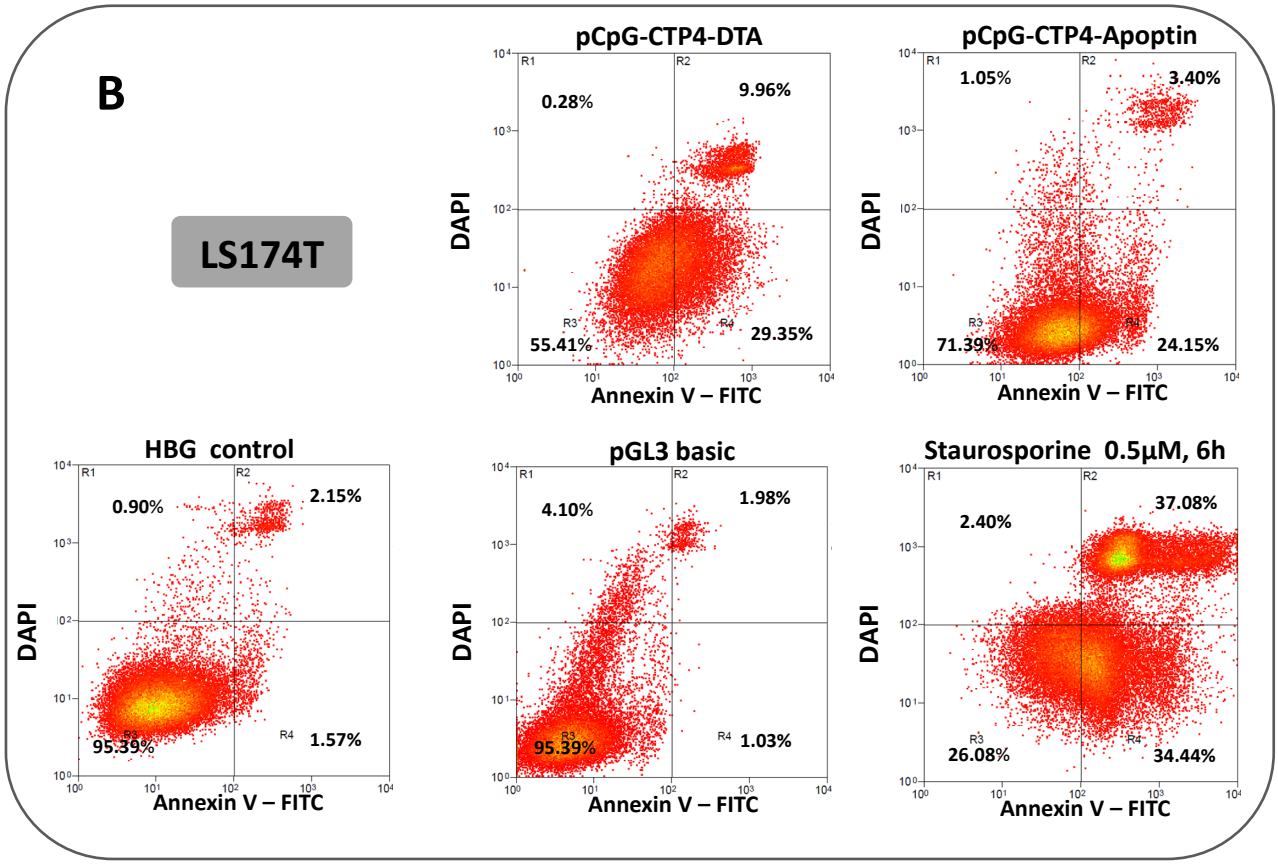
B
LS174T
pCpG-CTP4-DTA
0.28%
9.96%
55.41%
29.35%
pCpG-CTP4-Apoptin
1.05%
3.40%
71.39%
24.15%
HBG control
0.90%
2.15%
95.39%
1.57%
pGL3 basic
4.10%
1.98%
95.39%
1.03%
Staurosporine 0.5µM, 6h
2.40%
37.08%
26.08%
34.44%
DAPI
Annexin V – FITC

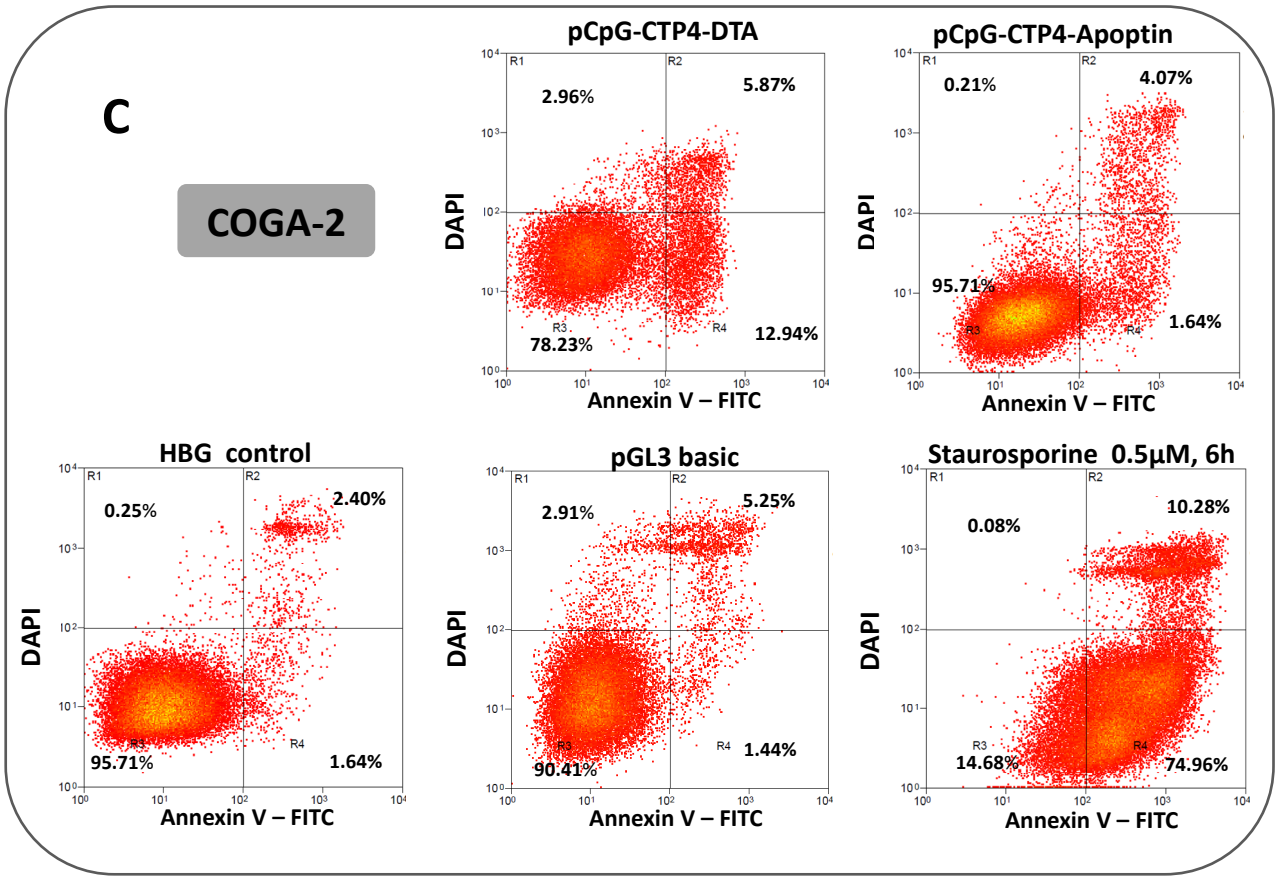
C
COGA-2
pCpG-CTP4-DTA
2.96%
5.87%
78.23%
12.94%
pCpG-CTP4-Apoptin
0.21%
4.07%
95.71%
1.64%
HBG control
0.25%
2.40%
95.71%
1.64%
pGL3 basic
2.91%
5.25%
90.41%
1.44%
Staurosporine 0.5µM, 6h
0.08%
10.28%
14.68%
74.96%
DAPI
Annexin V – FITC

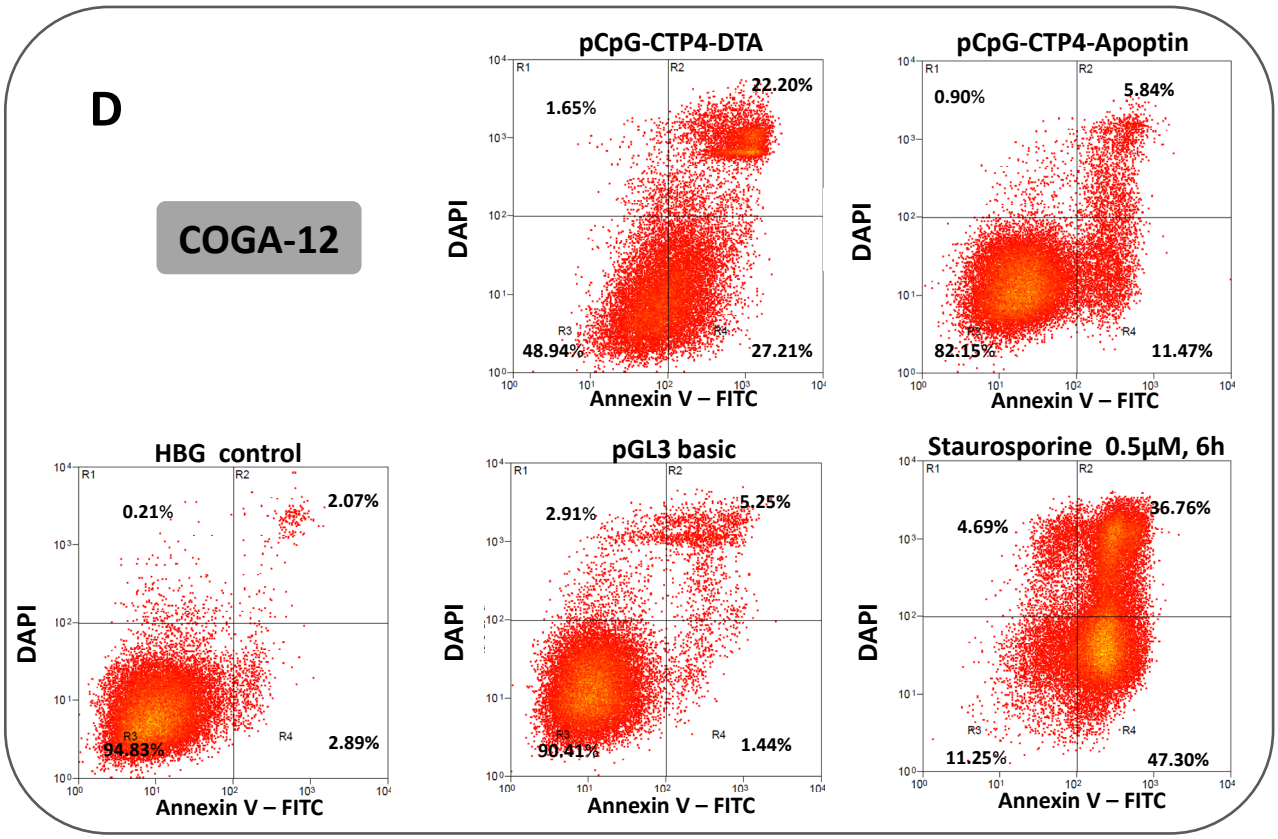
D
COGA-12
pCpG-CTP4-DTA
1.65%
22.20%
48.94%
27.21%
pCpG-CTP4-Apoptin
0.90%
5.84%
82.15%
11.47%
HBG control
0.21%
2.07%
94.83%
2.89%
pGL3 basic
2.91%
5.25%
90.41%
1.44%
Staurosporine 0.5µM, 6h
4.69%
36.76%
11.25%
47.30%
DAPI
Annexin V – FITC

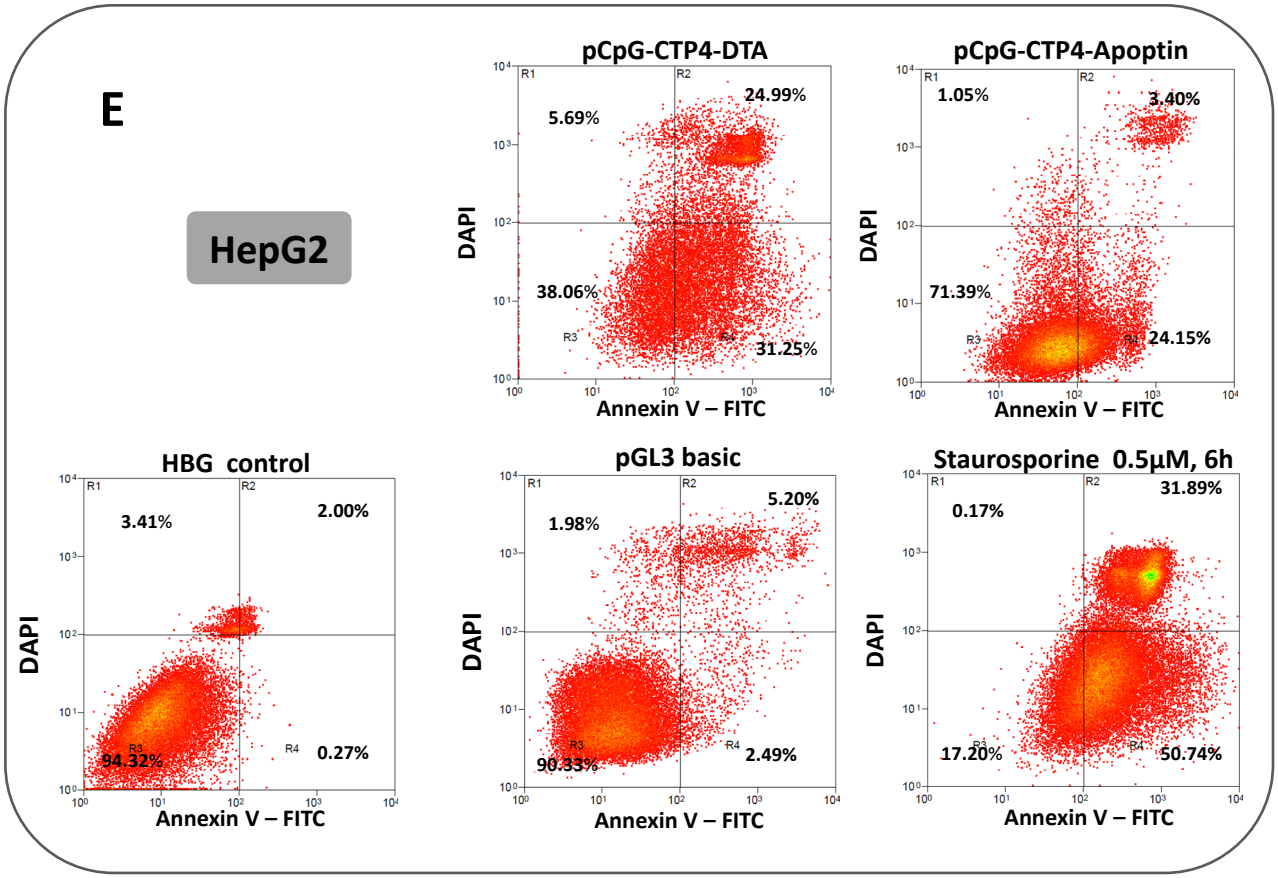
E
HepG2
pCpG-CTP4-DTA
5.69%
24.99%
38.06%
31.25%
pCpG-CTP4-Apoptin
1.05%
3.40%
71.39%
24.15%
HBG control
3.41%
2.00%
94.32%
0.27%
pGL3 basic
1.98%
5.20%
90.33%
2.49%
Staurosporine 0.5µM, 6h
0.17%
31.89%
17.20%
50.74%
DAPI
Annexin V – FITC

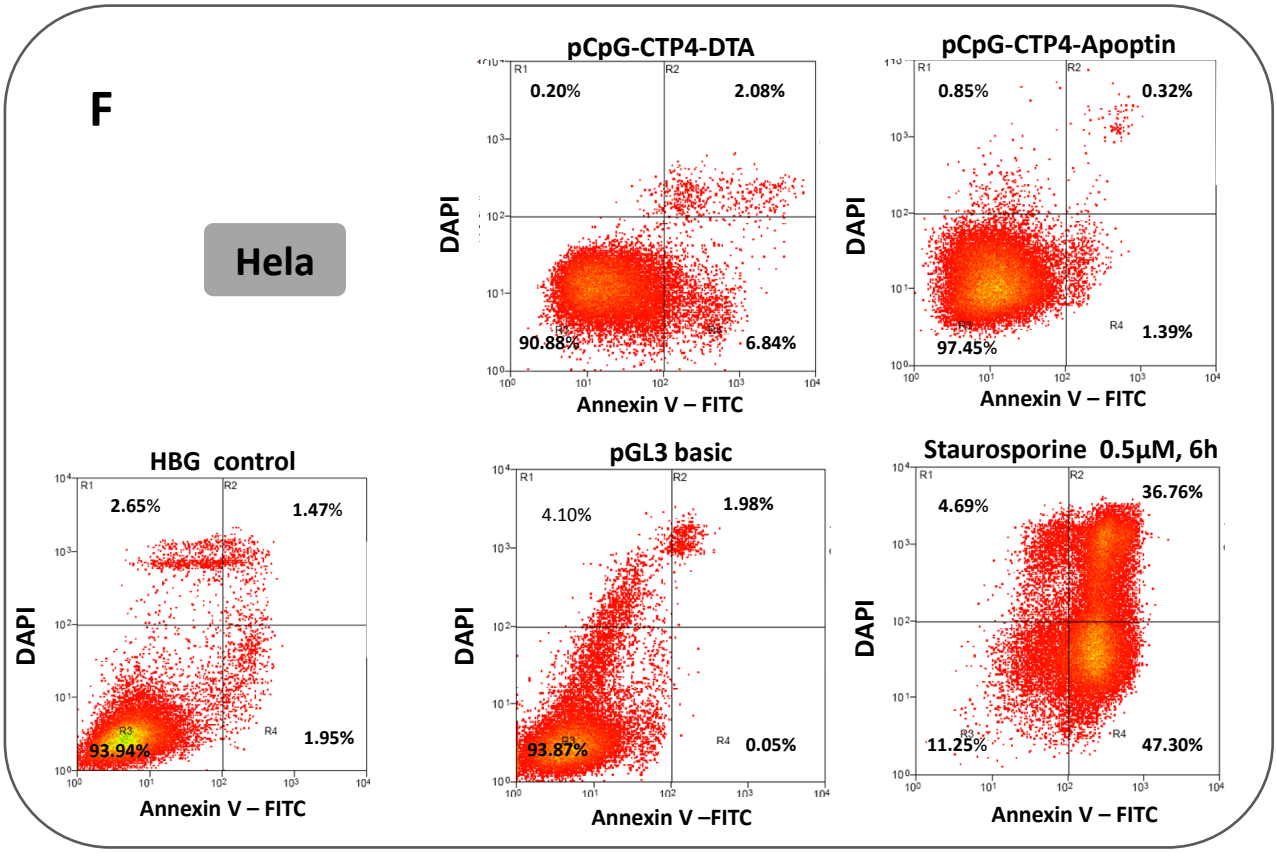

Fig.14 Flow cytometric analysis of DTA-and Apoptin-transfected target and control cells via a Annexin V-FITC and DAPI counterstaining

Target cell lines SW480 (A), LS174T (B), Coga2 (C), Coga12 (D) and HepG2 (E) as well as control cell line Hela (F) were either transfected with 500ng pCpG-CTP4-DTA, pCpG-CTP4-Apoptin or pGL3 basic using LPEI at an N/P ratio of 6 per 96-well. As positive controls for apoptosis, target cells were incubated with Staurosporine at a concentration of 0.5µM for 6h (A – F, lower panel, far left image). Untreated target cells were also included as an apoptosis negative control (A-F, lower panel, far right image). All target and control cell lines were then incubated with AnnexinV- FITC and DAPI simultaneously, analyzed 48 hours after transfection in a 96-well plate with 500ng of the indicated plasmids per 10,000 cells. Cells were transfected in quadruplicates and the combined cell suspension was analyzed via flow cytometry. Treated cell samples from all target cell lines were appropriately gated based on the untreated control cells (HBG control). The experiment was performed twice and data is presented as representative flow cytometry dot blots with at least 20,000 events gated per sample.

4.5. Orthotopic liver dissemination model for human CRC in NMRI nu/nu mice

The most common cause of death in patients is metastatic invasion of CRC cells from the primary tumor in the colon or rectum into the liver (stage IV)[133]. In order to mimic the malignant behavior of CRC-derived liver metastases, LS174T cells were utilized to establish a xenogeneic liver metastasis model by injecting tumor cells directly into spleen as described previously in numerous publications[134, 135]. Dr. Katarina Farkasova established this tumor model and performed all intrasplenic injections in the following experiments.

750,000 LS174T CTP4-Luc cells resuspended in 50µL PBS were injected directly into the spleen of NMRI-nude mice. Subsequently animals were monitored concerning weight, behavior and bioluminescent signal. In this tumor model the animals start losing weight at around day 8 after tumor inoculation, right around the time tumor masses in the abdominal cavity become palpable. At around day 9 after tumor inoculation the mice had shown an increased girth in the upper part of the abdominal cavity. At around day 10 after tumor inoculation we could observe the animals to arch the back, to walk more with caution and unwillingly stretching the body to the cratch[136]. An increase of the bioluminescence signal becomes evident between day 3 and day 10 after tumor inoculation, indicating progressive growth of the viable tumor mass. LS174T tumor metastases can be visualized at day 3 after tumor inoculation in all animals with a bioluminescent signal in the abdomen in an area of the spleen and liver. In the first attempts to establish indicated tumor model, starting at day six after tumor inoculation, the bioluminescent measurements were performed as sequence measurement so it was possible to determine the time point of maximal bioluminescence for this tumor model[136]. The pathological examination showed that all of the animals were tumor bearing. In all animals a primary tumor in the spleen was found which appeared more dense in texture than the metastases found in the liver, particularly at the rims of the liver small, almost granular in appearance (Fig. 15).

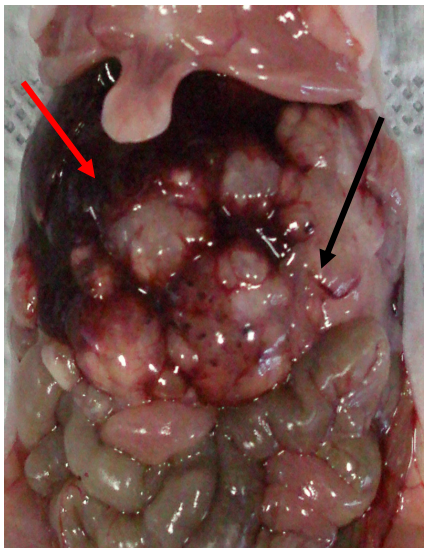

Fig. 15 LS174T CTP4-Luc liver metastases in NRMI nu/nu mice

Exemplary photographic image of a NMRI nude mouse bearing LS174T CTP4-Luc tumors 12 days after intrasplenic tumor inoculation. Red arrow marks non-malignant murine liver tissue, the black arrow marks LS174T tumor tissue.

Histological evaluation of LS174T CTP4-Luc i.s. tumors was carried out by cutting a 5-µm thick cross-section from paraffin embedded tumor tissue. Sections were embedded in paraffin, mounted on glass slides, and stained with an HRP-labeled anti-Firefly Luciferase antibody or a murine monoclonal β-catenin antibody (as described in 3.8.).

Histological studies provided qualitative results indicating highly distributed tumor growth with xenografts clearly distinguishable by the Luciferase staining (Fig.16). The growth of these human tumor xenografts in their respective hosts was also monitored by BLI of Luciferase activity and as can be seen in Fig.13. Luciferase expression is evenly distributed throughout the tumor tissue which shows the typical neoplastic morphology of a colorectal adenocarcinoma. After tumor implantation into the spleen, LS174T cells are redistributed into the liver and start growing as small, well-defined micro-tumors. When tumors exceed a certain size the center of the tumor nodule develops a necrotic center, which can be identified by absence of nuclear or luciferase staining. With an expanisve increase in size tumors develop almost similar to the morphology of colorectal villi.

All in all, representative immunohistochemical stainings of liver samples derived from untreated, yet tumor bearing animals, show strong FLuc expression sustained within each tumor and an evident necrotic center.

In the following, we utilized the previously identified therapeutic targets to analyze their potential in our established *in vivo* model. The orthotopic liver dissemination model utilizing LS174T CTP4-Luc cells is ideal for the delivery of wnt-related nucleic acid targets, since the defined microtumors are well vascularized and highly active in wnt/β-catenin signaling.

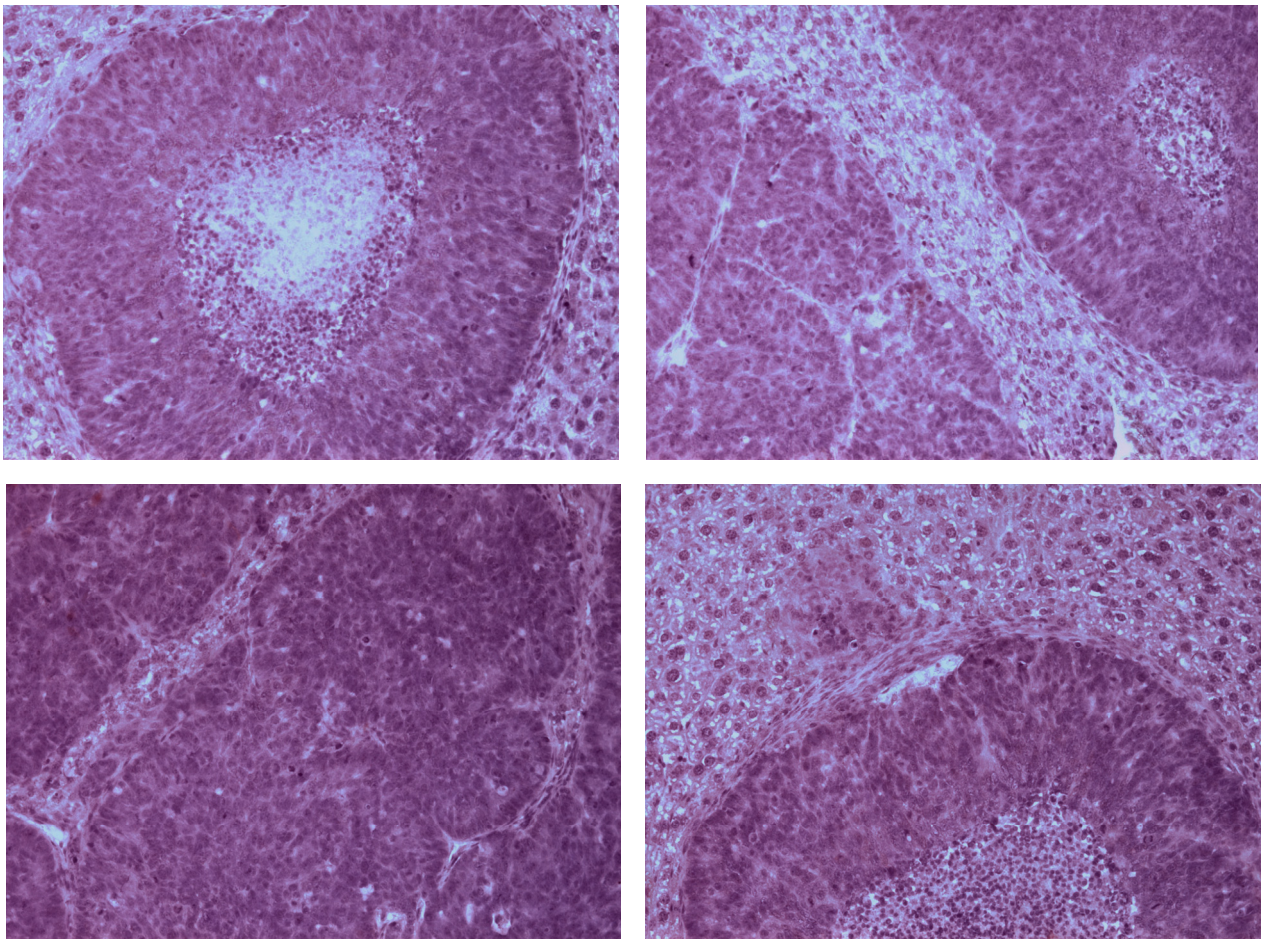

Fig.16 LS174T xenograft tumors stained for Firefly Luciferase

Staining of LS174T CTP4-Luc i.s. tumors was performed using a monoclonal HRP-labeled antibody against Firefly Luciferase. Paraffin-embedded tumor sections were treated with Pronase E for antigen retrival and endogenous peroxidase activity was quenched by treatment with 1% H_2O_2. Slides were incubated over night at 4°C with an anti-luciferase goat polyclonal horseradishperoxidase (HRP) conjugated antibody (1:50 in Tris-buffered saline (TBS)/0.3% BSA). Slides were evaluated on a Zeiss Axiovert 200 microscope (Carl Zeiss, Jena, Germany) using either a 20x or a 40x DIC objective.

Tumors were stained for β-catenin in untreated tumor specimen in order to evaluate wnt-activity in tumor tissue. Staining shows a strong nuclear and cytoplasmic distribution of β-catenin, with a particularly intense accumulation at the outer margin of single tumors the so-called „invasion front“ (Fig.17, black arrows in upper panel). The fluorescence staining of β-catenin shows a very similar staning pattern and distribution. The β-catenin staining marks on the one hand cells highly active in the wnt-signaling pathway (LS174T tumor tissue), on the other hand β-catenin is localized at the membrane in murine liver tissue since it is associated with E-cadherin and acts as part of a complex of proteins that constitute adherens junctions (murine tissue). The tumor stains strongly for β-catenin in the cytoplasm and nucleus, which concurs with HRP-staining (Fig.17, upper and lower panel).

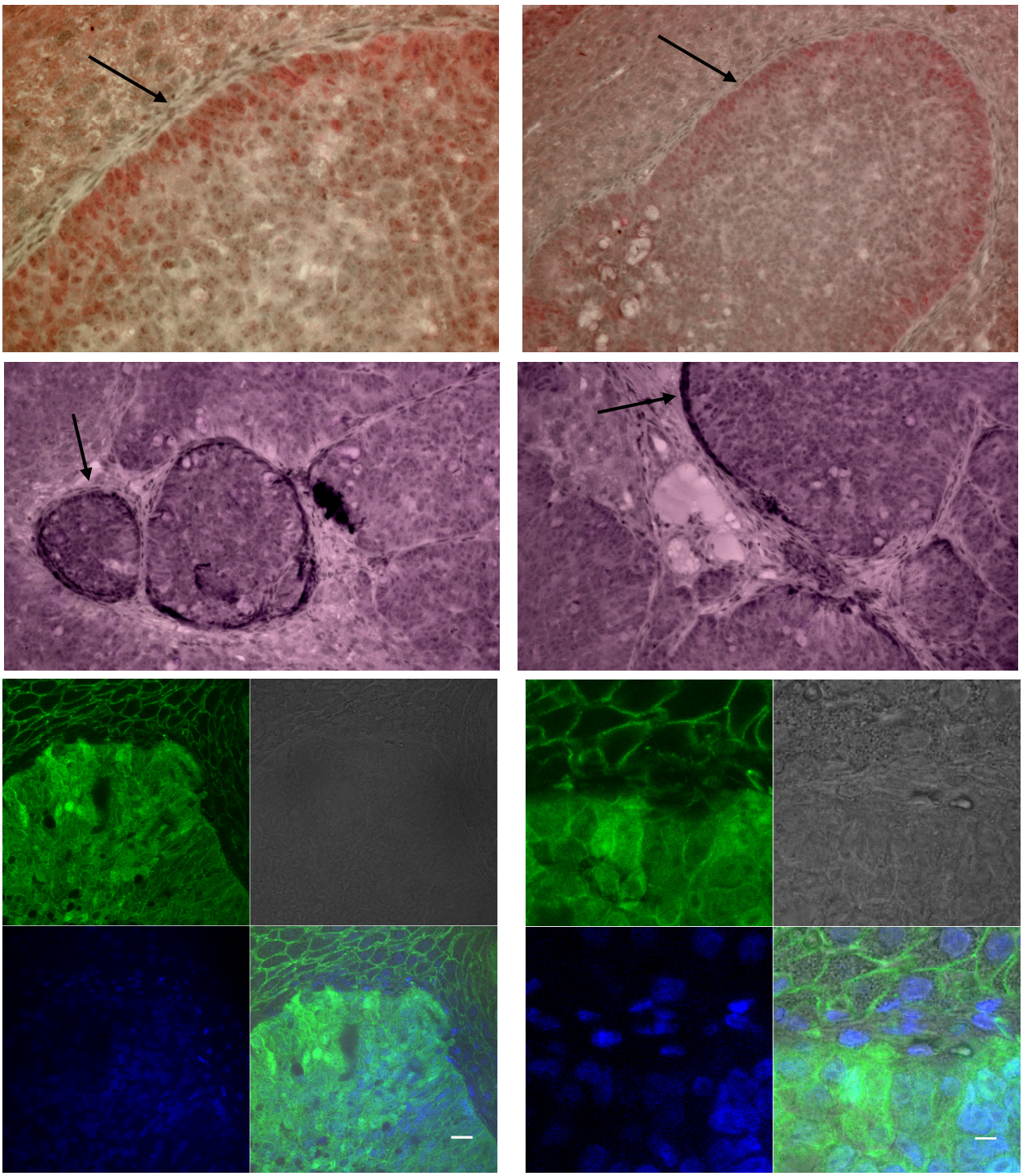

Fig.17 LS174T xenograft tumors stained for β-catenin (wnt-activity indicator)

Staining of LS174T tumors derived from the untreated group was performed using a murine monoclonal β-catenin antibody. Paraffin-embedded tumor sections were treated with Citrat for antigen retrival and endogenous peroxidase activity was quenched by treatment with 1% H_2O_2. Slides were incubated over night at 4°C with an anti-β-catenin mouse monoclonal antibody and subsequently incubated with either a HRP-labeled anti-mouse secondary antibody (upper panel) or a Alexa488-labeled anti-mouse secondary antibody (lower panel). Slides were evaluated on a Zeiss Axiovert 200 microscope (Carl Zeiss, Jena, Germany) using either a 20x or a 40x DIC objective.

4.5.1. *In vivo* pCpG-CTP4-DTA transfection an orthotopic liver dissemination model

LS174T cells marked with a CTP4-driven Firefly Luciferase were injected intrasplenically into NMRI nu/nu and after 4 days following tumor inoculation the treatment schedule was commenced. Three injections with 48 hours in between were performed with transfection complexes harbouring 50µg pCpG-hCMVenh-CTP4-DTA/LPEI-PEG-GE11 polyplexes at an N/P of 6 in HBG with 150µL - per injection (n= 7 per group). The control treated group received the same amount of nucleic acid combined with the indicated transfection reagent. The experiment was terminated 48h after the third and final injection (day 14). Particle size and zeta-potential of transfection complexes were determined before injection. Particles of 10µg/mL pCpG-hCMVenh-CTP4-DTA and LPEI-PEG-GE11 (N/P 6) had a size of 139,7 nm ± 3,8 nm and a zeta potential of +10,2 mV ± 0,5 mV.

All animals were given adequate care in compliance with institutional and state guidelines.

4.5.1.1. Bioluminescence imaging and Luciferase expression in tumor tissue

In order to verify tumor inoculation in the liver, mice from each group were analyzed for Luciferase expression in the abdomen by bioluminescence imaging (BLI). BLI is based on the sensitive detection of visible light produced during enzyme (luciferase)-mediated oxidation of the molecular substrate luciferin when the enzyme is expressed *in viv*o as a molecular reporter. The three groups (DTA transfected, control treated and untreated) with seven mice each were imaged before the first, second and third injection as well as 48 hours after final injection to monitor tumor growth. For live examination of Luciferase expression *in vivo* mice were anaesthetized by administration of isoflurane and injected i.p. with 100µl D-luciferin (60mg/ml, Promega) diluted in PBS. After 10 minutes the mice were imaged for bioluminescence in an IVIS Lumina device (Caliper Life Sciences, Mainz, Germany) in a light-tight chamber on an adjustable, heat-controlled stage.

Luciferase expression of DTA transfected mice decreased over the the course of treatment, the representative BLI images show reduced Luciferase expression particularly in the area of the liver (Fig. 18 A). This concurs with the transgene expression in liver lysates, where the reduction of Luciferase is evident in both control and DTA treated specimens. Compared to the control treated group the reduction in DTA transfected mice is more profound (Fig.18 C). In comparison, mice from the untreated group all showed unaccelerated tumor growth.

All in all, the treatement with a DTA-expressing construct reduced Luciferase expression which correlates with diminished tumor growth and the effect is verifiable via live imaging as well as in a functional assay measuring transgene expression in the liver lysates of all treated mice.

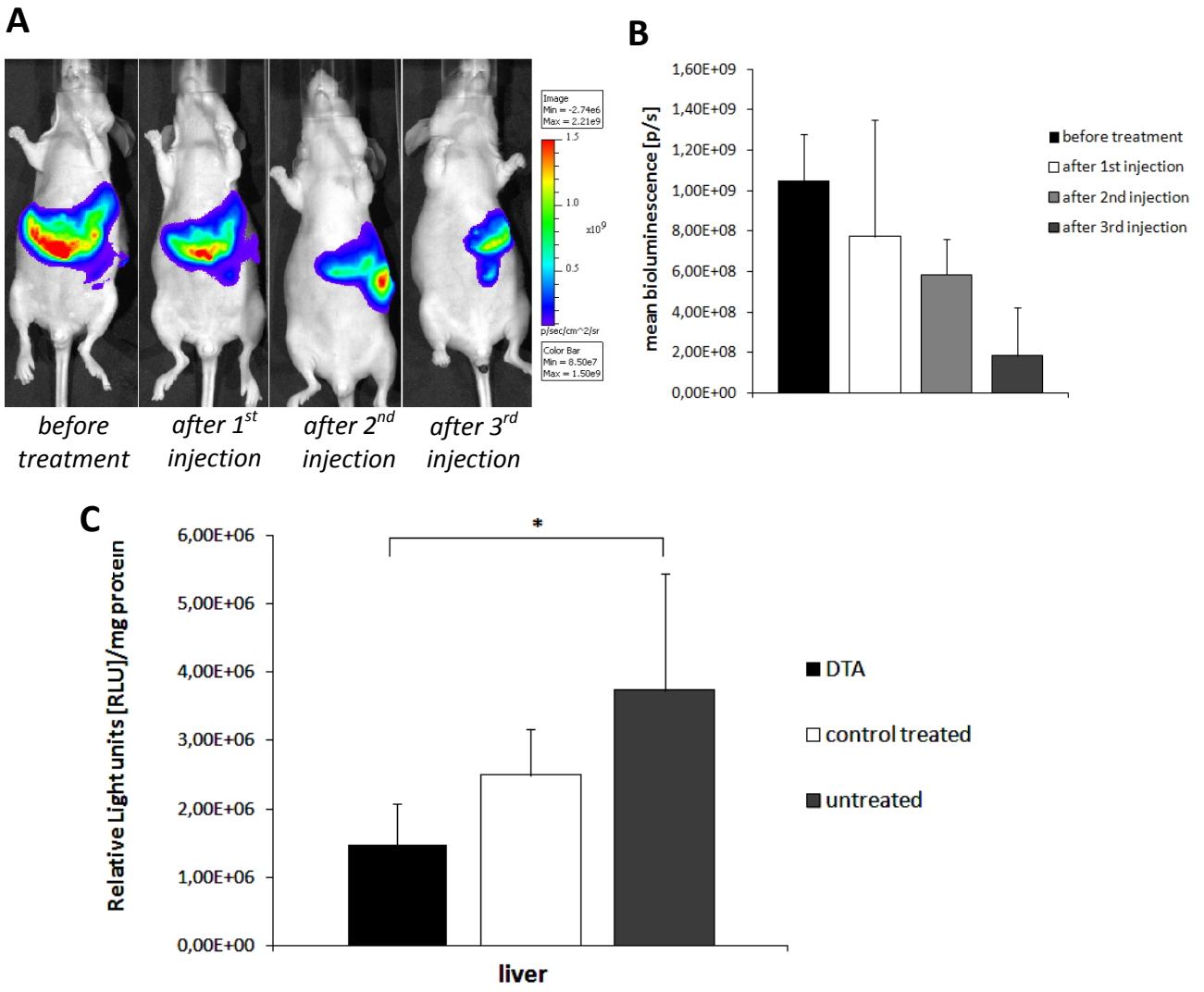

Fig.18 Monitoring of tumor growth in pCpG-CTP4-DTA and control treated tumor bearing mice

NMRI nu/nu were injected intrasplenically with CTP4-driven Firefly Luciferase marked LS174T cells (n=7 for each group). Animals from each group either received LPEI-PEG-GE11 (N/P 6) polyplexes with pDNA expressing DTA (2.5mg/kg) or control nucleic acid (scrambled sticky siRNA, 2.5mg/kg) i.v. on day 5, 7 and 9. Mice were sacrificed on day 13. (A) Representative BLI images of one animal from the DTA transfected group over the course of treatment are shown; a reflected light image (black-white) is overlaid by the color codes BLI signal. (B) The correlating quantification of the total flux of bioluminescence (expressed as photons per seconds [p/s]) of all DTA treated mice are shown. The mean bioluminescence of DTA transfected mice (n=7) are stated as mean ± s.e.m. of relative light units (RLU) before treatement and subsequently after each injection (48h between treatments). (C) The liver of each animal was snap frozen, ground and the tissue powder lysed in 600µL lysis buffer. The lysate of each mouse was analyzed for Luciferase expression and normalized to the total amount of protein. The values are representative means of seven animals and are stated as mean ± s.e.m. of relative light units (RLU) per mg protein. For statistical analysis a paired student's t-test comparing the DTA-transfected to control scr sticky siRNA transfected and untreated specimen was performed * = significantly different from respective controls ($p<0.05$).

4.5.1.2. Organ weight for tumor load determination

Organ weight was determined immediatetly after removal when the experiment was terminated on day 14 post-tumor inoculation. The increase in organ weight is the result of tumor growth in the liver. Reduced tumor load and thus lower organ weights were determined for DTA treated livers, while the control treated mice still developed tumors but to a lesser extend than the untreated counterparts (Fig.19 A). In Fig.19 B, representative images of tumor-bearing livers of one mouse per group (DTA, control treated and untreated) are shown. The weight of untreated livers was higher than the corresponding treated groups, which correlates with the tumor load of the affected organ. In comparison, the DTA-treated livers show significantly less tumors and thus reduced organ weights. For the control treated specimen a reduction in tumor weight was evident which is due to the effect of the transfection polymer on tumor growth.

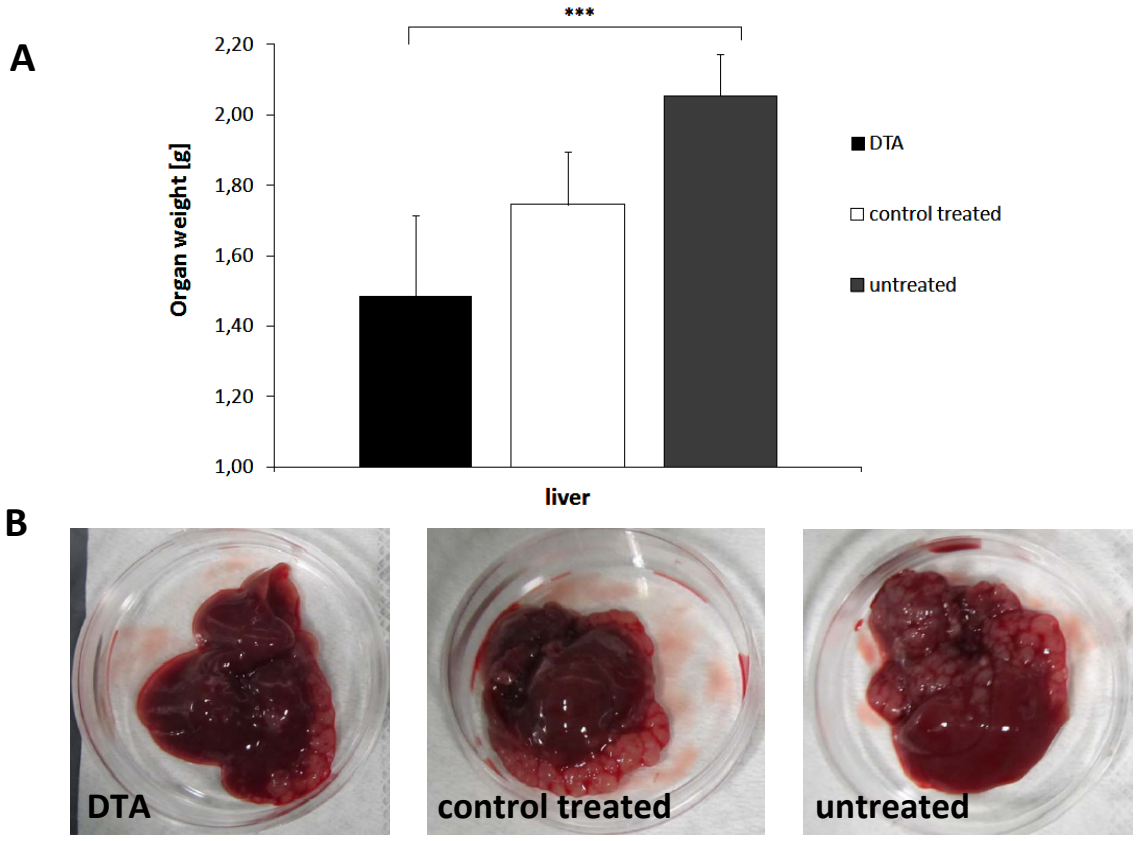

Fig.19 Tumor load determination in DTA-, control treated and untreated mice

After liver removal the organs of each mouse (n=7 per group) were weighed and snap frozen for further analysis. (A) Organ weight of seven animals of each group (DTA, scr sticky siNRA and untreated) are stated as means ± s.e.m. of g organ weight after liver removal. For statistical analysis a paired student's t-test comparing the DTA-transfected to control scr sticky siRNA transfected and untreated specimen was performed. * = significantly different from respective controls ($p<0.05$) and *** = $p < 0.0005$. (B) Representative images of one specimen per group are shown immediately after excision.

4.5.2 *In vivo* β-catenin siRNA knock-down in an orthotopic liver dissemination model

LS174T cells marked with a CTP4-driven Firefly Luciferase were injected in NMRI nu/nu intrasplenically and after 4 days following tumor inoculation the treatment regiment was commenced. Two injections with 72 hours in between were performed with transfection complexes harbouring 50µg β-catenin siRNA with brBPEI-Succ at a N/P of 15 in HBG with 150µL per injection (n= 6 per group). The control treated group received the same amount of control siRNA combined with the indicated transfection reagent. The experiment was terminated 48h after the final injection (day 12).

All animals were given adequate care in compliance with institutional and state guidelines.

4.5.2.1. Bioluminescence imaging and Luciferase expression in tumor tissue

In order to verify tumor inoculation in the liver, mice from each group were analyzed for Luciferase expression in the liver by bioluminescence imaging (BLI). The three groups (β-catenin transfected, control siRNA transfected and untreated) with six mice each were imaged before the first, second and finally 48 hours after final injection to monitor tumor growth. For live examination of Luciferase expression *in vivo* mice were anaesthetised by administration of isoflurane and injected i.p. with 100µl D-luciferin (60mg/ml, Promega) diluted in PBS. After 10 minutes the mice were imaged for bioluminescence in an IVIS Lumina device (Caliper Life Sciences, Mainz, Germany) in a light-tight chamber on an adjustable, heat-controlled stage.

Luciferase activity was monitored throughout the entire experimental procedure. As can be seen in representative images of BLI measurement (Fig.20 B, D) control siRNA treatment did not slow tumor growth significantly, whereas β-catenin siRNA transfection reduced Luciferase activity drastically. After the first round of control siRNA injections there is a short remission of Luciferase expression. This is only temporary, since the final BLI measurement showed a strong increase in Luciferase expression. In comparison, Luciferase expression of β-catenin siRNA transfected mice decreased over the course of treatment with the most significant decrease in transgene expression after final injection (Fig.20 A, C).
All in all, the treatment with β-catenin siRNA significantly and specifically reduced Luciferase expression over the course of treatment. In comparison, control siRNA treatment diminished Luciferase expression temporarily with a dramatic increase after the final injection.

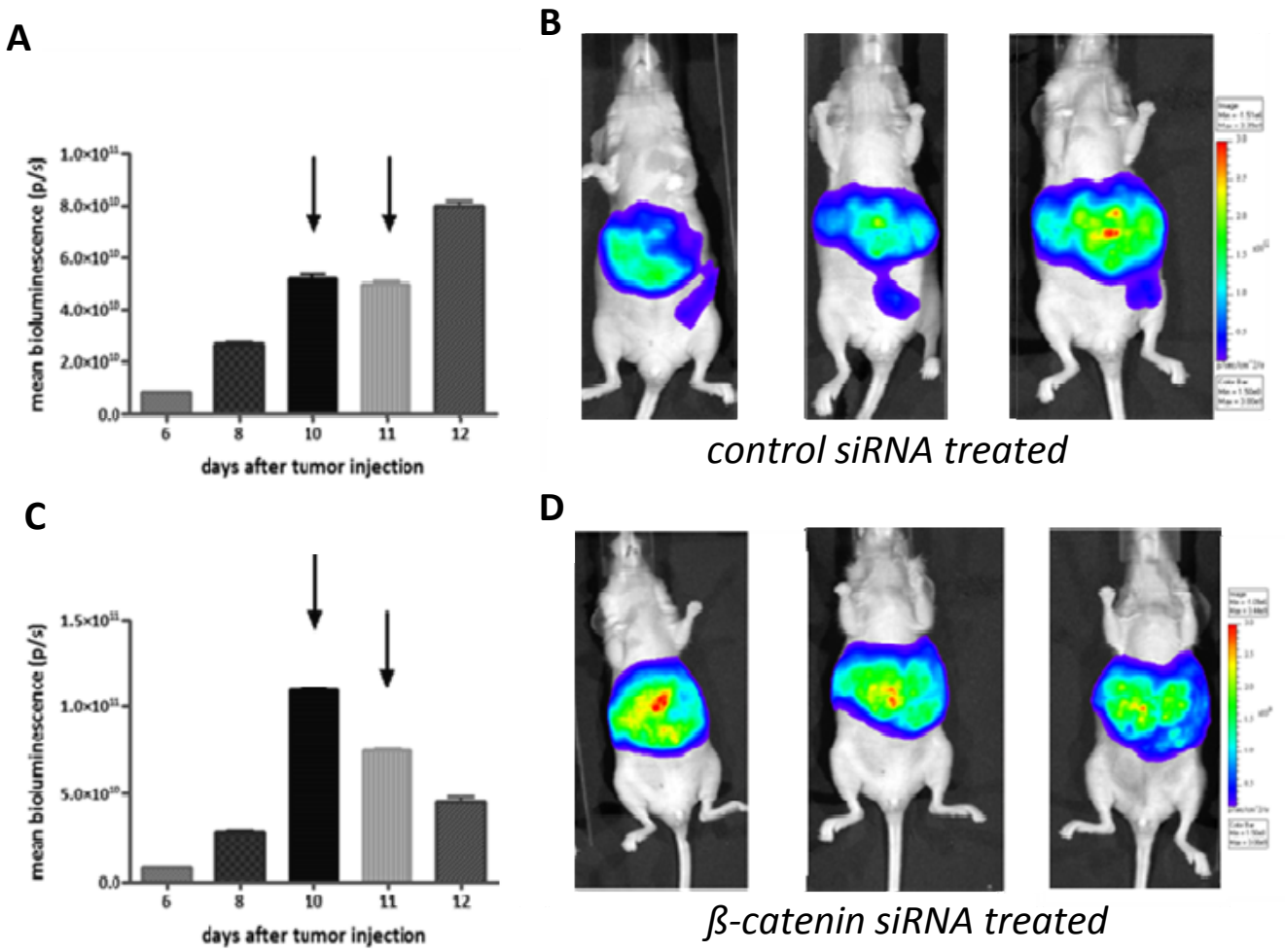

Fig.20 *In vivo* transfection of β-catenin siRNA and control siRNA for the treatment of an orthotopic dissemination human carcinoma tumor model

NMRI nu/nu were injected intrasplenically with CTP4-driven Firefly Luciferase marked LS17T cells, after initial tumor growth animal were either injected with either β-catenin siRNA or control siRNA (n=6 for each group). Animals from each group either received brPEISucc polyplexes with siRNA targeting β-catenin (2.5mg/kg) or control siRNA (2.5mg/kg) i.v. on day 8 and 10, Mice were sacrificed on day 12. (B,D) Representative BLI image of one specimen from the β-catenin transfected as well as control siRNA treated group are shown; a reflected light image (black-white) is overlaid by the color codes BLI signal. (A,C) The correlating quantification of the total flux of bioluminescence (expressed as photons per seconds [p/s]) of all treated mice are shown. The mean bioluminescence of β-catenin and control siRNA-transfected mice (n=6) are stated as mean ± s.e.m. of relative light units (RLU) over the course of treatment.

4.5.2.2. mRNA levels of β-catenin from liver samples

For qPCR analysis of relevant therapeutic targets, total RNA was isolated from all samples and 500ng each transcribed into cDNA. Samples were analyzed in duplicates from the same reverse transcriptase reaction and normalized to the housekeeping gene GAPDH.

The mRNA level of β-catenin in samples derived from each specimen showed a strong decrease in β-catenin levels (54% of untreated control), the control siRNA treated group had β-catenin levels in the range of the untreated control (Fig. 21). Thus, the control siRNA has no effect on the overall amount of β-catenin and reduced levels of β-catenin can be attributed to the specific RNA interference of siRNA targeting β-catenin.

In conclusion, mRNA level of β-catenin in all tumor samples showed overall a significant reduction compared to the siRNA treated and untreated samples.

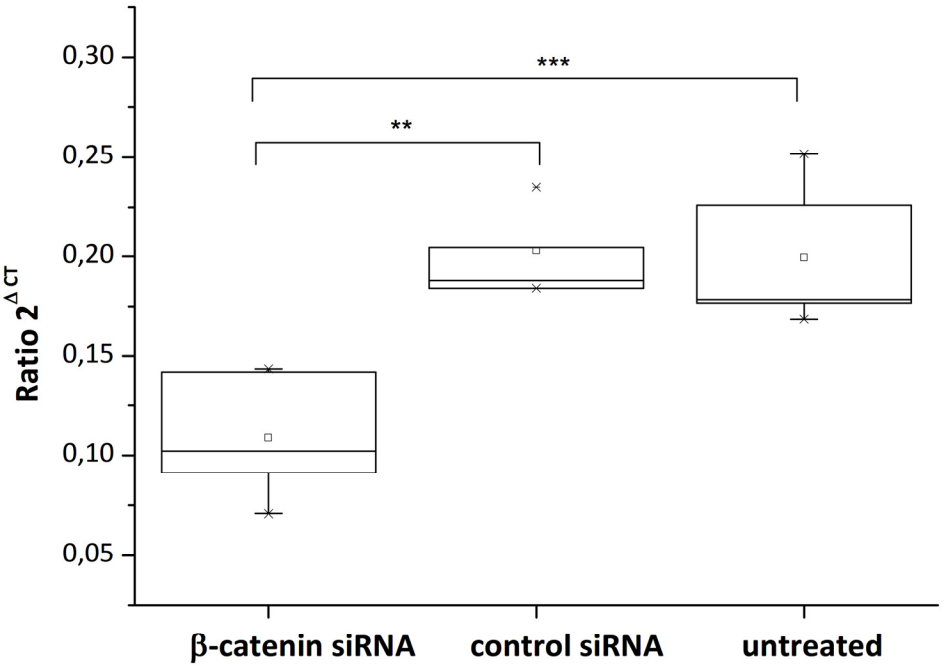

Fig.21 mRNA determination of β-catenin after siRNA-mediated transfection

Tumor bearing livers of each group from each animal were isolated, snap frozen and from the isolated total RNA after transcription into cDNA a RT-qPCR was performed analysing levels of β-catenin. For statistical analysis a paired student's t-test comparing the β-catenin transfected to control siRNA transfected and untreated specimen was performed. Data represent mean ± s.e.m with ** = significantly different from respective controls ($p<0.005$) and *** = $p < 0.0005$.

4.5.3. *In vivo* PAR-1 ssiRNA knock-down in an orthotopic liver dissemination model

LS174T cells marked with a CTP4-driven Firefly Luciferase were injected in NMRI nu/nu intrasplenically and after 4 days following tumor inoculation the treatment regiment was commenced. Three injections with 48 hours in between were performed with transfection complexes harbouring 50µg PAR-1 sticky siRNA (ssiRNA) with LPEI-PEG-GE11 at a N/P of 6 in HBG with 150µL - per injection (n= 7 per group). The control treated group received the same amount of scrambled PAR-1 sticky siRNA (ssiRNA) combined with the indicated transfection reagent. The experiment was terminated 48h after the third and final injection (day 14). Particle size and zeta-potential of transfection complexes were determined before injection. Particles of 10µg/mL PAR-1 ssiRNA and LPEI-PEG-GE11 (N/P 6) had a size of 168,4 nm ± 2,1 nm and a zeta potential of + 7,9 mV ± 0,8mV.

All animals were given adequate care in compliance with institutional and state guidelines.

4.5.3.1. Bioluminescence imaging and Luciferase expression in tumor tissue

In order to verify tumor inoculation in the liver, mice from each group were analyzed for Luciferase expression in the liver by bioluminescence imaging (BLI). The three groups (PAR-1 ssiRNA transfected, scr PAR-1 ssiRNA transfected and untreated) with seven mice each were imaged before the first, second and third injection as well as 48 hours after final injection to monitor tumor growth. For live examination of Luciferase expression *in vivo* mice were anaesthetised by administration of isoflurane and injected i.p. with 100µl D-luciferin (60mg/ml, Promega) diluted in PBS. After 10 minutes the mice were imaged for bioluminescence in an IVIS Lumina device (Caliper Life Sciences, Mainz, Germany) in a light-tight chamber on an adjustable, heat-controlled stage.

Luciferase expression of PAR-1 ssiRNA transfected mice decreased over the the course of treatment, the representative BLI images show reduced Luciferase expression particularly in the area of the liver (Fig. 22 A, B). In contrast, the Luciferase expression in the area of the spleen increased dramatically particularly after the second and third injection, indicating tumor growth in this area. This concurs with the transgene expression in liver lysates, where the reduction of Luciferase is evident in both PAR-1 scr and PAR-1 treated specimens, compared to the control treated group the reduction in PAR-1 transfected mice is more profound (Fig.22 C). In contrast, despite a clear reduction in Luciferase activity, the difference between PAR-1 ssiRNA treated and untreated spleen samples is not significant (Fig. 22 C). In the untreated group, all mice showed unaccelerated tumor growth (data not shown). All in all, the treatment with ssiRNA targeting PAR-1 reduced Luciferase expression which correlates with diminished tumor growth and the effect is verifiable via live imaging as well as in a functional assay measuring transgene expression in the liver lysates of all treated mice.

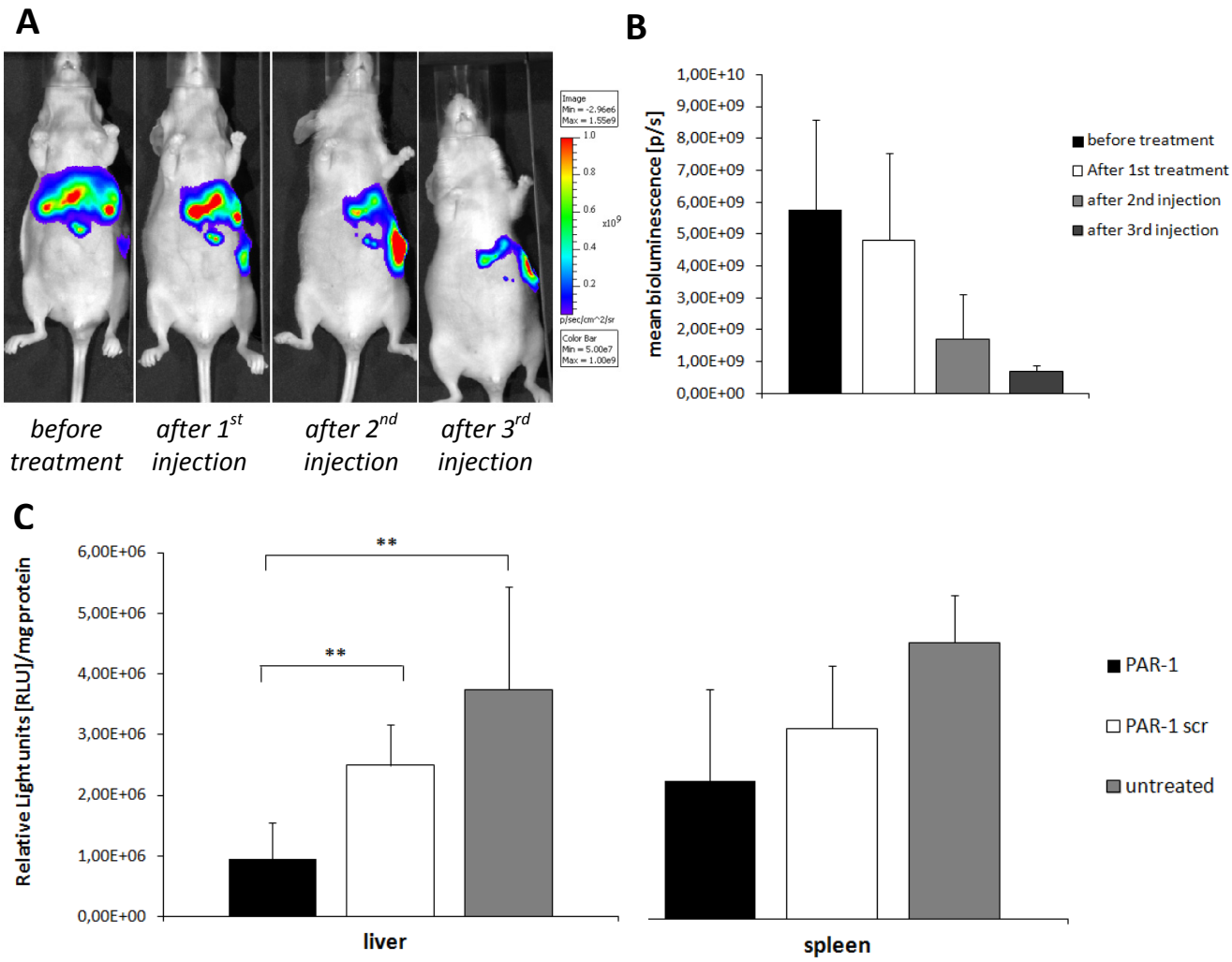

Fig.22 Monitoring of tumor growth in PAR-1 ssiRNA and scr PAR-1 ssiRNA treated tumor bearing mice

NMRI nu/nu were injected intrasplenically with CTP4-driven Firefly Luciferase marked LS17T cells (n=7 for each group). Animals from each group either received LPEI-PEG-GE11 (N/P 6) polyplexes with ssiRNA targeting PAR-1 (2.5mg/kg) or scr PAR-1 ssiRNA (2.5mg/kg) i.v. on day 5, 7 and 9. Mice were sacrificed on day 13. (A) Representative BLI image of one specimen from the PAR-1 ssiRNA transfected group are shown; a reflected light image (black-white) is overlaid by the color codes BLI signal. (B) The correlating quantification of the total flux of bioluminescence (expressed as photons per seconds [p/s]) of all treated mice are shown. The mean bioluminescence of PAR-1 ssiRNA transfected mice (n=7) are stated as mean ± s.e.m. of relative light units (RLU) during the course of treatement. (C) The livers of each specimen were snap frozen, ground and the tissue powder lysed in 600µL lysis buffer. The lysate of each mouse were analyzed for Luciferase expression and normalized to the total amount of protein. The values are representative means of seven specimens and are stated as mean ± s.e.m. of relative light units (RLU) per mg protein. For statistical analysis a paired student's t-test comparing the PAR-1 ssiRNA-transfected to scr PAR-1 ssiRNA transfected and untreated specimen was performed. ** = significantly different from respective controls ($p<0.005$).

4.5.3.2. Organ weight for tumor load determination

The average tumor weight of all livers removed from each mouse after the experiment was terminated on day 14 post-tumor inoculation. Organ weight was determined immediately after removal, the increase in organ weight is the result of tumor growth in the liver. Reduced tumor load and thus lower organ weights were determined for PAR-1 ssiRNA treated livers, while the scr PAR-1 ssiRNA treated mice still developed tumors but to a lesser extend than the untreated counterparts (Fig.23 A). In Fig.23 B, representative images of tumor-bearing livers of one mouse per group (PAR-1, scr PAR-1 and untreated) are shown. The weight of untreated livers was higher than the corresponding treated groups, which correlates with the tumor load of the affected organ. In comparison, PAR-1 ssiRNA-treated livers show significantly less tumors and thus reduced organ weights. For the control treated specimen a non-significant reduction in tumor weight was evident – compared to the untreated control - due to the effect of the transfection polymer on tumor growth.

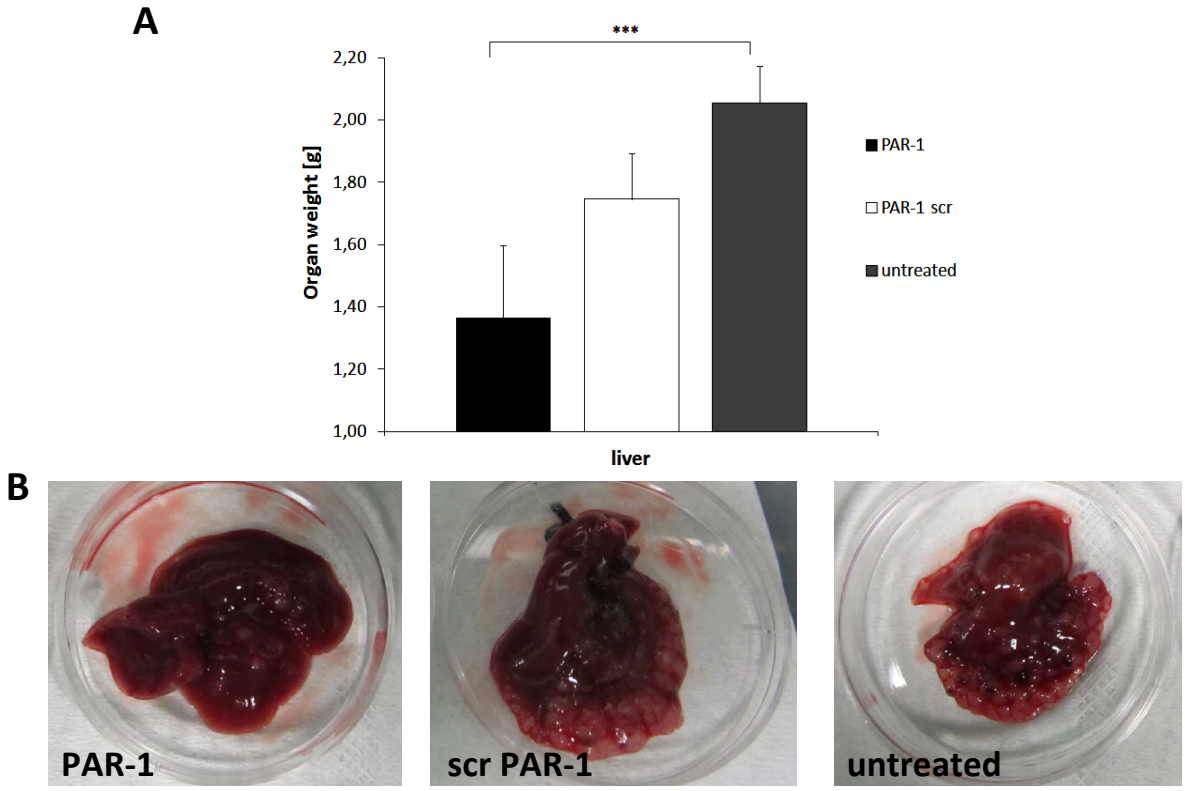

Fig.23 Tumor load determination in PAR-1 ssiRNA, scr PAR-1 ssiRNA and untreated mice

After liver removal the organs of each mouse (n=7 per group) were weighed and snap frozen for further analysis. (A) Organ weight of seven specimen from each group (PAR-1, scr PAR-1 and untreated) are stated as mean ± s.e.m. of g organ weight. For statistical analysis a paired student's t-test comparing the PAR-1 ssiRNA-transfected to scr PAR-1 ssiRNA transfected and untreated specimen was performed ** = significantly different from respective controls ($p<0.005$) and *** = $p < 0.0005$. (B) Representative images of one specimen per group are shown immediately after excision.

4.5.3.3. mRNA levels of PAR-1 from liver samples

For qPCR analysis of PAR-1 mRNA levels, total RNA from tumor bearing liver tissue of all three groups (untreated, scr PAR-1 ssiRNA and PAR-1 ssiRNA) was isolated and 500ng each transcribed into cDNA. Samples were analyzed in duplicates from the same reverse transcriptase reaction and normalized to the housekeeping gene GAPDH. The mRNA level of PAR-1 in samples derived from PAR-1 ssiRNA treated animals showed a strong decrease, in comparison to the untreated control PAR-1 levels were reduced by 35%. In contrast, when comparing PAR-1 ssiRNA treated liver speciment for their PAR-1 expression to control treated samples (scr PAR-1 ssiRNA) we can observe a reduction by 27%. The scr PAR-1 ssiRNA treated group had PAR-1 levels reduced by 11% compared to the untreated control (Fig.24). Thus, the scr PAR-1 ssiRNA has only a minor and not significant effect on the overall amount of PAR-1. This observation can be justified by transfection polymer-mediated toxicity. Thus, reduced levels of PAR-1 in PAR-1 ssiRNA treated samples can be attributed to the specific RNA interference of target ssiRNA. In conclusion, mRNA level of PAR-1 in tumor samples from PAR-1 ssiRNA treated animals showed overall a significant reduction compared to the scr PAR-1 ssiRNA treated and untreated samples.

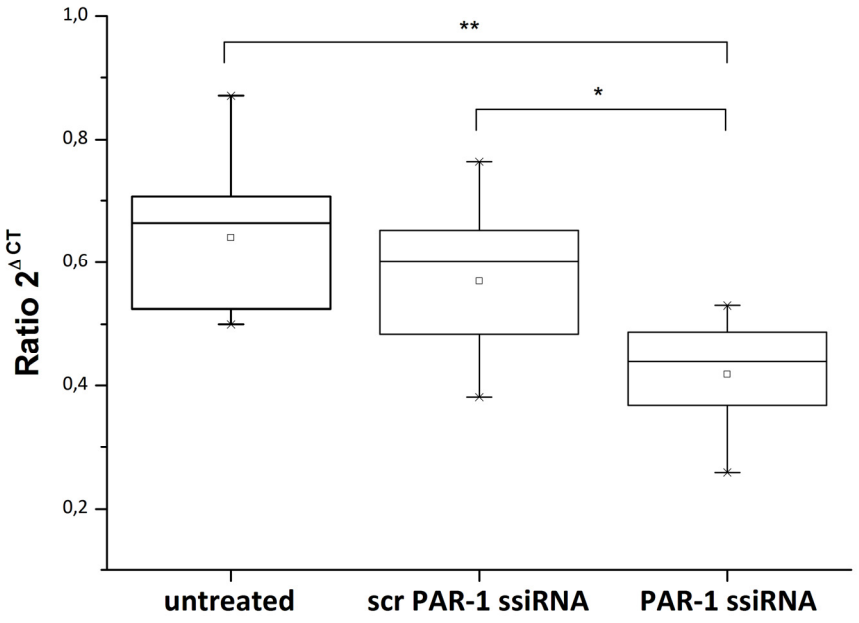

Fig.24 mRNA determination of PAR-1 after ssiRNA-mediated transfection

Tumor bearing livers of each group from each animal were isolated, snap frozen and from the isolated total RNA after transcription into cDNA a RT-qPCR was performed analysing levels of PAR-1. For statistical analysis a paired student's t-test comparing the PAR-1 ssiRNA-transfected to scr PAR-1 ssiRNA transfected and untreated specimen was performed. Data represents mean ± s.e.m with * = significantly different from respective controls ($p<0.05$) and ** = $p < 0.005$.

5. Discussion

5.1. Therapeutic siRNA target evaluation in wnt-deregulated cells

The incidence rate of cancers of the gastrointestinal tract, including the liver and colon is rising in all developed countries. Colorectal cancer is the third most common cancer in the world, with 1.24 million new cases diagnosed in 2008. Approximately 95 % of colorectal cancers are adenocarcinomas. Other types of cancer that can occur here include mucinous carinomas and adenosquamous carcinomas[45]. Generally they all have in common a chronic activation of the wnt pathway in common resulting in a continous expression of genes targeted by this pathway. Although improving early diagnostic and preventative measures are becoming more commonplace, the recurrence rate and 5-year survival of colorectal cancer in particular, is still very high. Combinatorial treatment approaches yield promising results, yet the side effects are still eminent and metastasis to other organs especially to the liver usually decreases survival rates even further. The treatement for highly aggressive malignant diseases remains challenging and standard treatment for metastasized disease are restricted to systemically applied radio- or chemotherapy. Thus, there is a considerable demand for more concised and targeted therapies. For targeted therapy cancer specific gene expression is an important factor. Approximately 90% of colorectal tumors show a deregulated wnt/β-catenin pathway[80] caused by either activating mutations of β-catenin or inactivating mutations of key players in the destruction complex like APC or Axin2[137] and therefore nuclear accumulation of β-catenin leading to an increase in accessible TCF4/LEF1 binding sites, which in turn induces transcription of numerous wnt target genes. The CTP4-promoter was used for various purposes: transient transfection for first screening and identification of deregulated cell lines for further analysis, stable introduction of this promoter coupled to an EGFPLuc cassette in order to pinpoint in a therapeutic siRNA mediated screen, viable candidates for therapy and finally the option of expressing cytotoxic proteins with said promoter. The cell line screening for wnt/β-catenin deregulation performed in various cancer cell lines and low passage colon carcinoma cells (Coga) confirmed previous findings from Lars Gaedtke[138] and Vecesey-Semjen[69] regarding Coga cell lines. Transfection of Coga cell lines and cancer cell lines of different origin were conducted with a PEI transfection reagent targeting the EGFR with a GE11 peptide[108]. The advantage of GE11 is the absence of receptor activation upon EGFR binding, although GE11 demonstrates a 10-times lower binding affinity to the EGFR (compared to murine EGF)[108], GE11 polyplexes demonstrated a very similar binding affinity for EGFR[108]. All Coga cells, as well as LS174T (Fig.S1), HepG2, SW480 and HEK293 cells have high levels of EGFR. The remaining cell lines that have been tested for CTP4-deregulation have either normal or low levels of EGFR (data not shown). Even though, an EGFR-targeting transfection reagent does increase transfection efficiency only in cell lines with high levels of EGFR, transfection efficiency in EGFR

low cells is not negatively affected by transfection using LPEI-PEG-GE11. Data from previous transfections indicate that $EGFR^{low}$ cell lines are equally well transfected using either a modified LPEI conjugate or LPEI alone (data not shown). Furthermore, increased overall transfection efficiency does not influence CTP4-regulated transgene expression compared to CMV-Luc expression. Despite the wide range and organs of origin for the investigated cell lines, the transient transfection of a CTP4-regulated Luciferase (CTP4-FLuc) only yielded high levels of transgene expression in colorectal cancer cell lines (SW480 and LS174T) and one hepatocellular carcinoma cell line (HepG2). The remaining cell lines showed no significant Luciferase expression for CTP4-FLuc, with quantified relative light units in the range of the promoterless control construct transfected cell specimens. Transiently transfected with CTP4-FLuc, SW480, LS174T, HepG2, COGA-2 as well as COGA-12 show strong Luciferase-activity usually even higher than the CMV-driven Luciferase signal (as a non-deregulated control Hela cells were used). The total protein levels for β-catenin as well as local concentration in the nuclear in these cell lines (Fig.S4) correlated well with the transactivation levels expressed as CTP4-driven Luc expression. Additionally, the mRNA levels of β-catenin can also be associated with CTP4-activity compared to CMV-controlled transgene expression (Fig.S2). The CTP4 promoter is highly specific in its expression, which is among others evident in Hela cells, a non-colorectal control cell line, where Firefly Luciferase levels are in the same range as the promoterless control construct pGL3 basic, in agreement with published results by Gaedtke and Lipinski[138]. The low passage colon cancer cell lines Coga are as expected all highly active in CTP4-driven transgene expression (Fig.6). Nonetheless only two Coga cell lines exhibit a higher transgene activity transfected with a CTP4-FLuc construct compared to the CMV-FLuc plasmid (Fig.6 A). Overall differences of CTP4 promoter activity could be directly correlated with differences in morphology, the number of mutations, either wnt- or more generally tumorigenicity-related and transfectability. The overall CTP4-transactivity peaks in the SW480 cell line, which shows a poorly differentiated morphology and harbours APC, p53, Kras and EGFR mutations[139]. Similarly the Coga2 cells as poorly differentiated colon cancer cell lines also display aberrant nuclear location of β-catenin caused by an APC mutation, additionally p53 and Kras mutations occur in this cell line. Coga12 cells also harbour an APC mutation, but unlike Coga2 have a tendency to grow in clumps with a more “piled-up” morphology and elevated but diffusely distributed β-catenin and show slightly decreased expression levels. LS174T and HepG2 both, unlike the previously described cell lines, have a β-catenin stabilizing mutation causing chronic wnt-activation. Literature search yielded several siRNA targets of interest, as for β-catenin and TCF4 being the obvious choice, published data for TNIK, OPG and PAR-1 implicated these structures as attractive therapeutic targets[117-119, 123, 124, 140-143]. Sox2 has a postulated role in various malignancies, but very little is known about its role in the tumorigenesis of colorectal cancer[121, 122, 144, 145]. In order to test the value of these molecular targets, siRNA-mediated knock down on stably

transduced target cell lines was performed. Prior to the cell-based screening, the overall mRNA levels of aforementioned genes were determined. OPG was only strongly upregulated in SW480 cells, additionally β-catenin levels were the highest in the same cell line. As for all remaining genes, the LS174T cells showed exceeding amounts of Sox2, TNIK, TCF4 and PAR-1. All in all, the non-colorectal control cell line (Hela), compared to the remaining target cell lines exhibited very low levels in all potentially therapeutic structures (Fig.7). Only Sox2 showed strong expression levels in Hela cells which is compliant with literature[146], since Sox2 acts as an important factor in tumorigenesis of cervical cancer. Despite the fact that there are a variety of routes used by human cancers to aberrantly activate the wnt pathway, a common feature of all these cancers is the constant presence of Tcf/β-catenin complexes in their nuclei, leading to chronic activation of a genetic program considered to promote cancer formation by stimulating cell growth, blocking apoptosis and altering cell movement. In order to establish a cell-based screening system for nucleic acids interfering with the wnt-pathway, previously identified target cell lines were stably transduced with a CTP4-EGFPLuc and an ubiquitous promoter PGK combined with the same expression cassette and treated with siRNA specifically targeting genes with a postulated influence on invasiveness, aggressiveness and proliferation of cancer cells. With this screening method the wnt pathway can be mined for potential cancer therapeutics, in this case in particular nucleic acids as therapeutic reagents. This *in vitro* screening system may be utilized as a prevalidation tool for therapeutically relevant targets. By treating both cell lines (CTP4- vs PGK-cells) with the same amount of siRNA simultaneously we can pinpoint specific influcences on the wnt pathway as well as non-specific effects on Firefly Luciferase activity, which can be explained with temporary toxicity by the transfection reagent but to the most part by reduced levels of proliferation serving as a measure of cell viability (Fig.8). The fact should not be overlooked that knock down of wnt-inducing/regulating factors will have an effect on proliferation rates, since many wnt target genes promote cell growth and survival. Direct comparison between CTP4-EGFPLuc and the PGK-EGFPLuc cells revealed a specific reduction in Luciferase expression levels for CTP4-cells with β-catenin, TCF4 and PAR-1 showing the strongest effect overall. From these screening results only OPG did not have a significant effect on transgene expression which would otherwise suggest a strong influence in wnt/β-signaling. As a proof of principle, the LS174T cells transfected with siRNA targeting β-catenin were further analyzed for specific knock-down effects on mRNA and protein level. The exempelary qPCR and Western Blot analysis of LS174T CTP4 cells confirmed actual target gene knock-down, thus reduced Firefly Luciferase levels reflect the actual knock-down of the gene targeted (Fig.9). Although, literature regarding β-catenin localization in wnt-deregulated cells suggests a clear nuclear accumulation, particularly the LS174T cells do not exhibit a homogenous but rather a very heterogenous intracellular distribution of β-catenin (Fig.9). Nonetheless, the overall amount of β-catenin is very high (Fig.7) and only exceeded by the SW480. The findings of

Vermeulen et al. suggest that only a subset of tumors cells show strong nuclear localization of β-catenin and thus increased wnt-activity („β-catenin paradoxon“)[78]. The wnt signaling model predicts that each tumor cell within a colorectal cancer initiated by mutations in APC or β-catenin should exhibit intracellular and/or nuclear β-catenin accumulation. Our findings support the β-catenin-paradoxon theory in LS174T cells, which would explain the highly aggressive growth behaviour *in vivo*, in comparison to SW480 or HepG2 cells, which despite their highler levels of β-catenin with high amounts of nuclear β-catenin (Fig.S4) are less tumorigenic than LS174T cells.

5.2. Contribution of therapeutic targets to colony formation and migration potential

We examined the effect of the inhibition of β-catenin, PAR-1, TNIK, Sox2, TCF4 and OPG by siRNA in human CRC and HCC cell lines along with the functional consequences, including effects on anchorage independent growth, proliferation and invasion. After the initial read-out of all target cell lines with six potentially therapeutic siRNAs, the biological effect of these targets had to be validated. For a possible treatment attempt, the biological effect of the siRNA mediated knock-down was determined with a number of established assays. For this purpose a colony formation and cell motility/migration assay was conducted for all relevant target cell lines and all previously defined siRNA targets which are involved in the wnt-pathway. The experimental approach to determine the effect of siRNA-mediated knock-down of PAR-1, TNIK, β-catenin, Sox2 and OPG on proliferation rates, was identical to the therapeutic target screen with the sole difference that target cell lines were stably transduced with a PGK-EGFPLuc casette instead of CTP4-EGFPLuc. In this scenario reduced transgene levels after siRNA-mediated knock-down correlate with diminished proliferation rates. Apart from OPG, all potentially therapeutic targets had a significant effect on cell growth and proliferation. From the therapeutic target screen, the mere reduction of FLuc levels provides a hint about the relevance of a gene within the wnt/β-catenin pathway, nonetheless it remains unclear if a stronger reduction in FLuc expression is due to a better knock-down efficiency of different targets or if the targeted gene has a stronger involvement in the wnt-pathway and thus causes a stronger activation of the CTP4-promoter. From this inital screen the targets further downstream of the wnt-pathway, β-catenin and TCF4, emerged as most interesting with at least 80% reduced transgene levels after knockdown. Additionally, a dramatic decrease in TNIK and PAR-1 expression was evident with a concomitant decrease in soft agar growth and reduced invasion behavior. The extent of the decrease in these biologic events was fairly robust in these cells. The evaluation of anchorage independent growth and migrative potential revealed for the most part, results which correlate well with the outcome of the siRNA screen in stably transduced cell lines. Therapeutic targets with a strong reducing effect on CTP4-Luc expression had also a significant impact on invasive behavior

as well as anchorage independent growth. This indicates that knock down by siRNA against β-catenin, TCF4, PAR-1 as well as TNIK along with its functional consequences, shown in reduction of anchorage independent growth and diminished migration, can be achieved. The extent of the decrease in these biologic events was fairly robust in all investigated target cells and indicated the clinical relevance of the transcriptional downregulation of these genes.

Based on the above findings, there appears to be an obvious merit of β-catenin, PAR-1 and TNIK suppression in wnt-deregulated CRC and HCC cell lines. All three targets have a profound inductive effect on the wnt/β-catenin signaling pathway and sustained suppression of either of these targets in wnt-deregulated tumors would have promising biologic consequences on tumor cell viability, proliferation and invasive potential.

5.3. Wnt-signaling as driving force of tumorigenesis

The wnt-signaling pathway has been described and analyzed in many publications[75, 76, 137], as the driving force of tumorigenesis and metastatic behavior, and the interference in the deregulation of this pathway has promising therapeutic implications. Inducing wnt-signaling and initiating the specific gene program associated with this pathway, is caused by a number of well defined mutations. In order to further analyze wnt-signaling we transactivated control cell lines Hela and HEK293 cells as well as target cell lines. Into all investigated cell lines a CTP4-driven transgen was stably introduced and expression levels monitored in untreated controls (HBG), cells either treated with 25mM LiCl, wnt3a protein (recombinant or supernatant from a wnt3a-producing cell line) or transfected cells with three different plasmids encoding for either mcherry, dnTCF4 or β-catenin S'33Y.

As predicted, the GSK-3 (glycogensythasekinase 3) inhibitor LiCl increased Luciferase expression immensely and in a time-dependent manner, particularly in the non-deregulated control cell lines. In a similar way, the transfection with pDNA encoding for a mutant β-catenin protein which is not susceptible to phosphorylation and thus can not be inactivated, as well as treatment with recombinant wnt3a protein, led both to a significant increase in Luciferase levels. Transactivation of wnt-signaling was feasible in cell lines without wnt-activity, but in part also in cell lines with deregulated wnt-pathway. Using wnt signaling activity as readout enabled us to determine the degree of deregulation and unterstand the role of this pathway in tumorigenesis. Wnt signalling is crucially important in tumor growth and malignant behavior and is a common pathway that is deregulated in most colon cancers. Mutations mimicking wnt stimulation—generally inactivating *APC* mutations or activating β-catenin mutations—result in nuclear accumulation of β-catenin which subsequently complexes with T-cell factor/lymphoid enhancing factor (TCF/LEF) transcription factors to activate gene transcription. The

suppression on various potentially therapeutic targets resulted into dramatic decrease in anchorage independent growth and invasion – both vital characteristics of malignant growth of tumor cells. Theoretically, transactivation of the wnt-pathway in otherwise non-permissive control cell lines, should also increase proliferation, invasive behavior and anchorage independent growth. Certain published data suggests, that inducing wnt-signaling levels in a variety of settings, does indeed have a strong influence on cell proliferation, differentiation and survival[147, 148]. Since the genetic programming regulated by β-catenin/TCF controlling the transcription of a range of genes promoting cellular proliferation and carcinogenesis[76], can be controlled by important regulators of the wnt-pathway, we investigated the contribution of PAR-1, TNIK and β-catenin in wnt-signaling as well as the effect of their knock-down. Taken together, these observations therefore confirm that the wnt signaling pathway, which leads to tumor formation when chronically activated, prompts uncontrolled cell growth and is thus crux of the matter regarding the development of therapeutic strategies.

5.4. Targeted delivery of cytotoxic proteins of target cells with pCpG-CTP4-DTA *in vivo*

Nonviral DNA delivery strategies for gene therapy are generally limited by a lack of specificity and efficacy: this can be avoided by transcriptional targeting using highly efficient plasmids. The basis for all plasmids utilized in this thesis, were CpG-depleted DNA constructs, which ensure prolonged transgene expression together with the human CMV enhancer and an S/MAR (scaffold/matrix attachment) region. CpG sequences are usually targeted for epigenetic silencing and induce an immune response, both relevant for *in vivo* applications[127, 149]. Another vital part of plasmid design is the promoter region, for specific wnt-related expression, a β-catenin/TCF-responsive promoter CTP1 has recently been developed by Lipinski and co-workers[114] and was further optimized for its specificity and activity later on, resulting in the promoter CTP4. This artificial promoter proved to be very effective in colon cancer cell lines like SW480 and in other tumor cell types[113]. For the delivery of this optimized constructs we utilized EGFR targeting transfection polymers, an addtitional targeting of tumor cells, since the LS174T cells overexpress the EGFR (Fig.S1) and thus the majority of transfection polyplexes are taken up by the tumor[150]. The transcriptional targeted gene vectors not only enabled high tumor specific expression of reporter genes like Firefly Luciferase or EGFP.

After the specificity and leakiness of the CTP4 promoter has been determined in various cell lines, pDNA was designed with expression casettes encoding for two different cytotoxic proteins – Apoptin (VP3 subunit of chicken anemia virus, 121 AA) or DTA (Diptheria Toxin Subunit A). Apoptin resides in the cytoplasm in normal cells, whereas in cancerous cells it translocates into the nucleus after phosphorylation. In tumor cells, apoptin redirects survival signals into cell death responses by

accumulating survival kinases including Akt in the nucleus, which is the phosphorylated by CDK2. Thereby, apoptin redirects survival signals into cell death responses. The proapoptotic signal of apoptin is then transduced from the nucleus to cytoplasm by Nur77, which triggers a p53-independent mitochondrial death pathway[151]. In contrast, the DTA peptide catalyzes ADP-ribosylation at the dipthamide residue of the cellular translation elongation factor 2 (eEF-2), inhibiting protein synthesis and causing cell death[152]. The major limiting factor to the apoptosis induction ability is the transfection efficiency of the target cell lines, but with improved transfection polymers and optimized pDNA killing efficacy could be enhanced. So far, the most important target cell lines have been transfected and induction of apoptosis was determined (AnnexinV/DAPI staining). Killing efficiency using the CTP4-DTA construct was very high for LS174T, SW480 and HepG2 with a normalized apoptosis rate over 95%, compared to the Coga2 and Coga12 with apoptosis induction around 90% when taking transfection efficiency into account. In contrast, in HeLa cells the expression of DTA and Apoptin controlled by the CTP4 promoter was insufficient to induce apoptosis compared to control transfection. This indicates an enhanced and specific transgene expression obtained by the CTP4 promoter in permissive cell lines and a considerably lower or no expression in non-permissive HeLa cells. The selective expression of cytotoxic proteins resulting in tumor-specific lethality will be shown in all target cells. Consequently, gene vectors that target unusual activation of the wnt pathway have vast prospective as novel cancer therapeutics.

The therapeutic potential of vectors encoding therapeutic genes could also be shown in an *in vivo* approach, the β-catenin paradoxon described in previous publications[78, 153], argues that only a small subset of tumor cells have high intrinsic wnt-activity with nuclear β-catenin and tumor-initiating potential. These cells have been referred to as cancer stem cells (CSC). In Bandapalli et al.[154] the transcriptional activation of the β-catenin gene at the invasion front of colorectal liver metastases could be shown and the histological evaluation of LS174T tumor sections stained for β-catenin as a „wnt-indicator“ supports this hypothesis. The increased expression and nuclear accumulation of β-catenin at the tumor margins in LS174T tumors, offer an ideal model for the transfection of DTA regulated by CTP4 in a CpG-depleted construct. Theoretically, since the highest expression is achieved in strongly wnt-deregulated cells, DTA induced apoptosis affects the invasion margin with high wnt-activity and also potential CSC. The effect of DTA treatment was evident in significantly reduced tumor-load compared to the control treated and untreated specimen. Taken all these observations into account, the targeted expression of CTP4-regulated cytotoxic proteins in tumors in a colorectal liver dissemination model was viable *in vitro* and *in vivo*. This approach could be used to potentially target CSCs which have been shown to be relatively resistant to therapy. Present strategies are aimed at developing tumor and CSC selective therapies, thereby attacking the tumor at its root.

5.5. Small interfering RNA and sticky siRNA knock-down of β-catenin and PAR-1 *in vivo*

Based on the above findings, we utilized a nude mouse/LS174T cell xenograft model of colorectal liver metastases model which induces tumor growth of a high number of small and well-vascularized tumor lesions in the liver[155]. The localization of β-catenin at the invasion front indicates strong wnt-activity at the tumor margins. It has been shown that the accessibility of the nodules in the liver is exceptionally high on the surface, thus nucleic acid delivery in this tumor model is viable.

The overall knock-down of β-catenin achieved in the tumor-bearing livers reaches 47% compared to control siRNA treated mice. Although antisense modalities being tested preclinically and clinically are still in its infancy, new strategies for cancer prevention and treatment are being developed[156]. We observed increased overall levels of β-catenin concentrated at the outer margin of liver metastases as well as enhanced levels of nuclear β-catenin, which complies with previously published data [154, 157, 158]. Certain data suggests dynamic transcriptional activation of the β-catenin promoter which in turn controls nuclear localization and transcriptional activation of wnt-target genes primarily at the invasion front of colorectal liver metastases[154]. We observed very similar β-catenin distribution, which suggests a very distinct regulation of wnt-related target genes during dissemination of tumor cells. This concentration of β-catenin and the expansive growth of tumor cells are only observed in liver metastases[154]. LPEI and its conjugates, although successfully employed for DNA delivery, are less effective for siRNA mediated transfections[159]. For siRNA transfection we used a branched PEI conjugate, which has been modified by introducing succinic acid groups as previously described[106]. This modification yields less toxicity and high transfection efficiency (80% knock-down relative to untreated cells *in vitro*) when utilized for siRNA transfection[106]. Especially the low polymer toxicity of brPEISucc renders it a promising transfection reagent for *in vivo* applications. Therefore, we used brPEISucc for transfection of siRNA targeting β-catenin in the liver nodules. Despite the lack of a targeting compound incorporated into the transfection polymer, the accessibility of the nodules and the strong concentration of β-catenin at the invasion margins are responsible for the successful siRNA mediated knock-down.

Although the knock down of β-catenin was successful and can be regarded as „proof-of-principle“, the ultimate goal will be to find other siRNA targets interfering with the wnt-pathway. The challenge will be to identify potent inhibitors of the wnt/β-catenin pathway with high selectivity to limit potential for side effects caused by direct interference with the cell's natural β-catenin pool, since other β-catenin complexes are vital for maintaining cell adhesion and regulation of the wnt-pathway in non-transformed

tissue. The applicability of this approach will depend on the identification of target genes whose functions are crucial for cancer cell survival, but are dispensable for normal cell growth.

As for β-catenin, which is a protein with multiple inherent functions interacting with other proteins such as E-cadherin, APC and Axin, therapeutic approaches must be selectively disrupting expression of wnt-related target genes while leaving other β-catenin complexes intact. The current study provides a proof of principle that β-catenin inhibition is feasible, is of clinical relevance, and has functional consequences in CRC and HCC cells, which show β-catenin overexpression and/or activation. Moreover, since the effect of β-catenin localization at invasion can only be observed *in vivo*, it can be argues that the microenvironement of the tumor directs wnt activation. This suggests a framework in which stromal components stimulate CSC features of cancer cell populations mainly at the tumor edges and simultaneously promote the invasion and spread of the malignancy into the surrounding tissue, as has also been suggested previously[78]. Thus, targets like PAR-1 and TNIK represent two genes which would fulfil these requirements and siRNA-mediated knock down would pose an attractive treatement option. The transfection of sticky siRNA targeting PAR-1 was successful and could reduce transgene levels by 35%. Interestingly this knock down rate was sufficient to significantly reduce tumor growth (Fig.23). The delivery of ssiRNA has one clear advantage: the possibility of utilizing exisiting LPEI conjugates targeting the EGFR. Furthermore the stability of ssiRNA, especially *in vivo*, can be ensured as has been described previously[42]. Thus, the LPEI-PEG-GE11 transfection of sticky siRNA is a highly promising therapeutic attempt. The contribution of PAR-1 to the wnt-pathway appears to be similarly strong when compared to the results from siRNA-mediated β-catenin knock-down. Therefore targeting PAR-1 reduces wnt-activity strongly.

As has been described previously, high wnt activity – in theory – functionally designates the colon cancer stem cell population. These alleged cancer stem cells may retain the capacity to self-renew and differentiate, allowing them to transiently trans-differentiate and to invade adjacent tissues more efficiently and eventually to form metastases in distant organs. Taking previous observations from all *in vivo* approaches into account, the non-random distribution of tumor cells with intracellular β-catenin accumulation suggests a scenario where differential wnt signaling activation regulates tumorigenesis and invasive behavior: the initiating APC or β-catenin mutation is necessary but insufficient for fullblown wnt activation and only tumor cells located at the invasive front are exposed to growth factors and cytokines able to further enhance β-catenin nuclear translocation[154]. Additionaly, somatic mutations in other tumor suppressors and oncogenes (e.g. KRAS or p53 mutation) may act synergistically in promoting wnt signaling. Overall, both intrinsic (tumor cell-autonomous) and extrinsic (secreted by the tumor microenvironment) factors are likely to play rate-limiting roles in local invasion and metastasis as well as cancer stemness and tumor growth by differentially modulating wnt/β-catenin signaling.

Considering the high activity of wnt-signaling in CSCs, the TCF-dependent CTP4 promoter as the driving force for a potent cytotoxic protein would elevate the idea of transcriptional targeting. Not only will the expression be solely restricted to tumor tissue, but the potentially most tumorigenic subpopulation of cells is particularly affected. Taken together, the *in vivo* data in particular show most promising results for targeted cancer gene therapy – on the one hand using siRNA targeting β-catenin as well as sticky siRNA against PAR-1, on the other hand utilizing pDNA encoding for the DTA protein – making full use of the wnt signalling pathway in an orthotopic xenograft colorectal metastasis model.

6. Summary

In this work, we were able to take advantage of a deregulated wnt signaling pathway – a condition which is found in most gastrointestinal cancers, in particular in colorectal carcinomas. In order to restrict reporter gene expression to the desired cell type, we utilized the β-catenin dependent CTP4-promoter to restrict the expression of Firefly Luciferase and enhanced green fluorescent fusion protein (EGFPLuc) to cell lines with deregulated wnt signaling including SW480, LS174T, HepG2, Coga2 and Coga12. Stable cell lines containing this CTP4-driven EGFPLuc construct were established with the help of a lentiviral vector to monitor wnt activity by transgene expression. With these stably transduced cell lines, we performed a therapeutic target screen via siRNA-mediated knock-down of a number of potentially therapeutic targets within the wnt pathway – osteoprotegerin (OPG), Traf2 and Nck-interacting kinase (TNIK), SRY-related HMG-box (Sox2), protease-activated receptor 1 (PAR-1), β-catenin and transcription factor 4 (TCF4). The *in vitro* screening system was utilized as a prevalidation tool for therapeutically relevant targets. The degree of interference of our novel targets was determined and the search for a suitable siRNA target in colorectal cancer cells was narrowed down to β-catenin, PAR-1 and TNIK. As proof of principle the siRNA-mediated knock down of β-catenin was verified on mRNA and protein level in LS174T cells. After the initial read-out of various cell lines with different siRNAs has been established via the reduction of Luciferase expression levels, the biological effect of these targets were validated. For this purpose colony formation and cell motility/invasion assays were conducted for all relevant target cell lines. Furthermore in the *in vitro* experiments, the tumor-selectivtiy of the CTP4-promoter was employed in the delivery of the cytotoxic protein diphteria toxin A (DTA) in colorectal cancer target cells. Data evaluation of all *in vitro* assays pointed at reduced levels of proliferation, invasive behavior and aggressiveness, which yielded three candidates (PAR-1, TNIK and β-catenin) considered as viable for a treatment attempt *in vivo*. In the *in vivo* experiments, systemic delivery of siRNA against β-catenin, sticky siRNA targeting PAR-1 and plasmid DNA encoding for CTP4 controlled DTA were evaluated in a disseminated liver metastasis model of LS174T colorectal cancer. Specific knock-downs of β-catenin and PAR-1 were achieved which was confirmed via mRNA analysis. As for CTP4-DTA pDNA delivery the overall tumor load of the liver was reduced without any significant systemic toxicity, indicating specific DTA expression in tumor tissue. Also knock down of PAR1 using sticky siRNA significantly reduced tumor growth. All in all, the therapeutic effect of PAR-1 and β-catenin knock-down could be verified in various *in vitro* assays analyzing invasive behavior and anchorage independent growth and ultimately also *in vivo.* The tumor-specific expression of DTA pDNA could also be confirmed *in vitro* and was further investigated in an orthotopic liver dissemination model in NMRI nude mice.

7. References

1. Schaffert, D. & Wagner, E. Gene therapy progress and prospects: synthetic polymer-based systems. *Gene therapy* **15**, 1131-1138 (2008).
2. Friedmann, T. & Roblin, R. Gene therapy for human genetic disease? *Science* **175**, 949-955 (1972).
3. Tatum, E.L. Molecular biology, nucleic acids, and the future of medicine. *Perspectives in biology and medicine* **10**, 19-32 (1966).
4. Blaese, R.M. & Culver, K.W. Gene therapy for primary immunodeficiency disease. *Immunodeficiency reviews* **3**, 329-349 (1992).
5. Blaese, R.M. et al. T lymphocyte-directed gene therapy for ADA- SCID: initial trial results after 4 years. *Science (New York, N.Y* **270**, 475-480 (1995).
6. Hacein-Bey-Abina, S. et al. Sustained correction of X-linked severe combined immunodeficiency by ex vivo gene therapy. *The New England journal of medicine* **346**, 1185-1193 (2002).
7. Aiuti, A. et al. Correction of ADA-SCID by stem cell gene therapy combined with nonmyeloablative conditioning. *Science (New York, N.Y* **296**, 2410-2413 (2002).
8. http://www.wiley.com/legacy/wileychi/genmed/clinical/.
9. Kircheis, R. et al. Tumor-targeted gene delivery of tumor necrosis factor-alpha induces tumor necrosis and tumor regression without systemic toxicity. *Cancer gene therapy* **9**, 673-680 (2002).
10. Raty, J.K., Pikkarainen, J.T., Wirth, T. & Yla-Herttuala, S. Gene therapy: the first approved gene-based medicines, molecular mechanisms and clinical indications. *Current molecular pharmacology* **1**, 13-23 (2008).
11. Raj, L. et al. Selective killing of cancer cells by a small molecule targeting the stress response to ROS. *Nature* **475**, 231-234 (2011).
12. Hemminki, A. From molecular changes to customised therapy. *Eur J Cancer* **38**, 333-338 (2002).
13. Bauerschmitz, G.J., Barker, S.D. & Hemminki, A. Adenoviral gene therapy for cancer: from vectors to targeted and replication competent agents (review). *International journal of oncology* **21**, 1161-1174 (2002).
14. Goldstein, I. et al. Understanding wild-type and mutant p53 activities in human cancer: new landmarks on the way to targeted therapies. *Cancer gene therapy* **18**, 2-11 (2011).
15. Guinn, B.A. & Mulherkar, R. International progress in cancer gene therapy. *Cancer gene therapy* **15**, 765-775 (2008).
16. Elbashir, S.M. et al. Duplexes of 21-nucleotide RNAs mediate RNA interference in cultured mammalian cells. *Nature* **411**, 494-498 (2001).
17. Fire, A. et al. Potent and specific genetic interference by double-stranded RNA in Caenorhabditis elegans. *Nature* **391**, 806-811 (1998).
18. Caplen, N.J., Fleenor, J., Fire, A. & Morgan, R.A. dsRNA-mediated gene silencing in cultured Drosophila cells: a tissue culture model for the analysis of RNA interference. *Gene* **252**, 95-105 (2000).
19. Tuschl, T. RNA interference and small interfering RNAs. *Chembiochem : a European journal of chemical biology* **2**, 239-245 (2001).
20. Meister, G. et al. Human Argonaute2 mediates RNA cleavage targeted by miRNAs and siRNAs. *Molecular cell* **15**, 185-197 (2004).
21. Song, J.J., Smith, S.K., Hannon, G.J. & Joshua-Tor, L. Crystal structure of Argonaute and its implications for RISC slicer activity. *Science* **305**, 1434-1437 (2004).
22. Mahato, R.I., Kawabata, K., Takakura, Y. & Hashida, M. In vivo disposition characteristics of plasmid DNA complexed with cationic liposomes. *Journal of drug targeting* **3**, 149-157 (1995).

23. Kawabata, K., Takakura, Y. & Hashida, M. The fate of plasmid DNA after intravenous injection in mice: involvement of scavenger receptors in its hepatic uptake. *Pharmaceutical research* **12**, 825-830 (1995).
24. Gao, S. et al. The effect of chemical modification and nanoparticle formulation on stability and biodistribution of siRNA in mice. *Molecular therapy* **17**, 1225-1233 (2009).
25. Boussif, O. et al. A versatile vector for gene and oligonucleotide transfer into cells in culture and in vivo: polyethylenimine. *Proceedings of the National Academy of Sciences of the United States of America* **92**, 7297-7301 (1995).
26. Aigner, A. Gene silencing through RNA interference (RNAi) in vivo: strategies based on the direct application of siRNAs. *Journal of biotechnology* **124**, 12-25 (2006).
27. Goula, D. et al. Size, diffusibility and transfection performance of linear PEI/DNA complexes in the mouse central nervous system. *Gene therapy* **5**, 712-717 (1998).
28. Merdan, T., Kunath, K., Fischer, D., Kopecek, J. & Kissel, T. Intracellular processing of poly(ethylene imine)/ribozyme complexes can be observed in living cells by using confocal laser scanning microscopy and inhibitor experiments. *Pharmaceutical research* **19**, 140-146 (2002).
29. Akinc, A., Thomas, M., Klibanov, A.M. & Langer, R. Exploring polyethylenimine-mediated DNA transfection and the proton sponge hypothesis. *The journal of gene medicine* **7**, 657-663 (2005).
30. Wiseman, J.W., Goddard, C.A., McLelland, D. & Colledge, W.H. A comparison of linear and branched polyethylenimine (PEI) with DCChol/DOPE liposomes for gene delivery to epithelial cells in vitro and in vivo. *Gene therapy* **10**, 1654-1662 (2003).
31. Dif, F., Djediat, C., Alegria, O., Demeneix, B. & Levi, G. Transfection of multiple pulmonary cell types following intravenous injection of PEI-DNA in normal and CFTR mutant mice. *The journal of gene medicine* **8**, 82-89 (2006).
32. Hassani, Z. et al. A hybrid CMV-H1 construct improves efficiency of PEI-delivered shRNA in the mouse brain. *Nucleic acids research* **35**, e65 (2007).
33. Vernejoul, F. et al. Antitumor effect of in vivo somatostatin receptor subtype 2 gene transfer in primary and metastatic pancreatic cancer models. *Cancer research* **62**, 6124-6131 (2002).
34. Liao, H.W. & Yau, K.W. In vivo gene delivery in the retina using polyethylenimine. *BioTechniques* **42**, 285-286, 288 (2007).
35. Ohana, P. et al. Regulatory sequences of H19 and IGF2 genes in DNA-based therapy of colorectal rat liver metastases. *The journal of gene medicine* **7**, 366-374 (2005).
36. Ohana, P.G., O.; Ayesh, S.; Al-Sharef, W.; Mizrahi, A.; Birman, T.; Schneider, T.; Matouk, I.; de Groot, N.; Tavdy, E.; Ami Sidi, A.; Hochberg,A. Regulatory sequences of the H19 gene in DNA based therapy of bladder cancer. *Gene Therapy and Molecular Biology* **8**, 181-192 (2004).
37. Lisziewicz, J. et al. DermaVir: a novel topical vaccine for HIV/AIDS. *The Journal of investigative dermatology* **124**, 160-169 (2005).
38. Lisziewicz, J. et al. Control of viral rebound through therapeutic immunization with DermaVir. *AIDS* **19**, 35-43 (2005).
39. Sonawane, N.D., Szoka, F.C., Jr. & Verkman, A.S. Chloride accumulation and swelling in endosomes enhances DNA transfer by polyamine-DNA polyplexes. *The Journal of biological chemistry* **278**, 44826-44831 (2003).
40. http://www.polyplus-transfection.com/therapeutics/clinical-pipeline/.
41. Bonnet, M.E., Erbacher, P. & Bolcato-Bellemin, A.L. Systemic delivery of DNA or siRNA mediated by linear polyethylenimine (L-PEI) does not induce an inflammatory response. *Pharmaceutical research* **25**, 2972-2982 (2008).
42. Bolcato-Bellemin, A.L., Bonnet, M.E., Creusat, G., Erbacher, P. & Behr, J.P. Sticky overhangs enhance siRNA-mediated gene silencing. *Proceedings of the National Academy of Sciences of the United States of America* **104**, 16050-16055 (2007).
43. Cohen, M.M., Jr. Molecular dimensions of gastrointestinal tumors: some thoughts for digestion. *American journal of medical genetics. Part A* **122A**, 303-314 (2003).

44. Reissfelder, C. et al. A randomized controlled trial to investigate the influence of low dose radiotherapy on immune stimulatory effects in liver metastases of colorectal cancer. *BMC cancer* **11**, 419 (2011).
45. www.wcrf.org.
46. Kinzler, K.W. & Vogelstein, B. Lessons from hereditary colorectal cancer. *Cell* **87**, 159-170 (1996).
47. Jass, J.R. Pathogenesis of colorectal cancer. *The Surgical clinics of North America* **82**, 891-904 (2002).
48. Weitz, J. et al. Colorectal cancer. *Lancet* **365**, 153-165 (2005).
49. Yu, J.L. et al. Oncogenic events regulate tissue factor expression in colorectal cancer cells: implications for tumor progression and angiogenesis. *Blood* **105**, 1734-1741 (2005).
50. Fearon, E.R. & Vogelstein, B. A genetic model for colorectal tumorigenesis. *Cell* **61**, 759-767 (1990).
51. Knudson, A.G. Antioncogenes and human cancer. *Proceedings of the National Academy of Sciences of the United States of America* **90**, 10914-10921 (1993).
52. Smalley, M.J. & Dale, T.C. Wnt signaling and mammary tumorigenesis. *Journal of mammary gland biology and neoplasia* **6**, 37-52 (2001).
53. Fodde, R. et al. Mutations in the APC tumour suppressor gene cause chromosomal instability. *Nature cell biology* **3**, 433-438 (2001).
54. Fodde, R. The APC gene in colorectal cancer. *Eur J Cancer* **38**, 867-871 (2002).
55. Henderson, B.R. Nuclear-cytoplasmic shuttling of APC regulates beta-catenin subcellular localization and turnover. *Nature cell biology* **2**, 653-660 (2000).
56. Rosin-Arbesfeld, R., Townsley, F. & Bienz, M. The APC tumour suppressor has a nuclear export function. *Nature* **406**, 1009-1012 (2000).
57. Rosin-Arbesfeld, R., Cliffe, A., Brabletz, T. & Bienz, M. Nuclear export of the APC tumour suppressor controls beta-catenin function in transcription. *The EMBO journal* **22**, 1101-1113 (2003).
58. Bienz, M. & Clevers, H. Linking colorectal cancer to Wnt signaling. *Cell* **103**, 311-320 (2000).
59. Polakis, P. The adenomatous polyposis coli (APC) tumor suppressor. *Biochimica et biophysica acta* **1332**, F127-147 (1997).
60. He, T.C. et al. Identification of c-MYC as a target of the APC pathway. *Science* **281**, 1509-1512 (1998).
61. Shtutman, M. et al. The cyclin D1 gene is a target of the beta-catenin/LEF-1 pathway. *Proceedings of the National Academy of Sciences of the United States of America* **96**, 5522-5527 (1999).
62. Tetsu, O. & McCormick, F. Beta-catenin regulates expression of cyclin D1 in colon carcinoma cells. *Nature* **398**, 422-426 (1999).
63. Huber, O. et al. Nuclear localization of beta-catenin by interaction with transcription factor LEF-1. *Mechanisms of development* **59**, 3-10 (1996).
64. Porfiri, E. et al. Induction of a beta-catenin-LEF-1 complex by wnt-1 and transforming mutants of beta-catenin. *Oncogene* **15**, 2833-2839 (1997).
65. Miyaki, M. & Kuroki, T. Role of Smad4 (DPC4) inactivation in human cancer. *Biochemical and biophysical research communications* **306**, 799-804 (2003).
66. Liu, F. SMAD4/DPC4 and pancreatic cancer survival. Commentary re: M. Tascilar et al., The SMAD4 protein and prognosis of pancreatic ductal adenocarcinoma. Clin. Cancer Res., 7: 4115-4121, 2001. *Clinical cancer research* **7**, 3853-3856 (2001).
67. Leslie, A., Carey, F.A., Pratt, N.R. & Steele, R.J. The colorectal adenoma-carcinoma sequence. *The British journal of surgery* **89**, 845-860 (2002).
68. Selivanova, G. p53: fighting cancer. *Current cancer drug targets* **4**, 385-402 (2004).
69. Vecsey-Semjen, B. et al. Novel colon cancer cell lines leading to better understanding of the diversity of respective primary cancers. *Oncogene* **21**, 4646-4662 (2002).

70. Angers, S. & Moon, R.T. Proximal events in Wnt signal transduction. *Nature reviews. Molecular cell biology* **10**, 468-477 (2009).
71. MacDonald, B.T., Tamai, K. & He, X. Wnt/beta-catenin signaling: components, mechanisms, and diseases. *Developmental cell* **17**, 9-26 (2009).
72. Nusse, R. The Wnt Homepage. *http://www.stanford.edu/~rnusse/wntwindow.html.* (2009).
73. Mosimann, C., Hausmann, G. & Basler, K. Beta-catenin hits chromatin: regulation of Wnt target gene activation. *Nature reviews. Molecular cell biology* **10**, 276-286 (2009).
74. Fearon, E.R. PARsing the phrase "all in for Axin"- Wnt pathway targets in cancer. *Cancer cell* **16**, 366-368 (2009).
75. Polakis, P. Wnt signaling and cancer. *Genes & development* **14**, 1837-1851 (2000).
76. Clevers, H. Wnt/beta-catenin signaling in development and disease. *Cell* **127**, 469-480 (2006).
77. Vogelstein, B. et al. Genetic alterations during colorectal-tumor development. *The New England journal of medicine* **319**, 525-532 (1988).
78. Vermeulen, L. et al. Wnt activity defines colon cancer stem cells and is regulated by the microenvironment. *Nature cell biology* **12**, 468-476 (2010).
79. Reya, T. & Clevers, H. Wnt signalling in stem cells and cancer. *Nature* **434**, 843-850 (2005).
80. Korinek, V. et al. Constitutive transcriptional activation by a beta-catenin-Tcf complex in APC-/- colon carcinoma. *Science* **275**, 1784-1787 (1997).
81. Miyaki, M. et al. Characteristics of somatic mutation of the adenomatous polyposis coli gene in colorectal tumors. *Cancer research* **54**, 3011-3020 (1994).
82. Miyoshi, Y. et al. Somatic mutations of the APC gene in colorectal tumors: mutation cluster region in the APC gene. *Human molecular genetics* **1**, 229-233 (1992).
83. Morin, P.J. et al. Activation of beta-catenin-Tcf signaling in colon cancer by mutations in beta-catenin or APC. *Science* **275**, 1787-1790 (1997).
84. Lammi, L. et al. Mutations in AXIN2 cause familial tooth agenesis and predispose to colorectal cancer. *American journal of human genetics* **74**, 1043-1050 (2004).
85. Sansom, O.J. et al. Loss of Apc in vivo immediately perturbs Wnt signaling, differentiation, and migration. *Genes & development* **18**, 1385-1390 (2004).
86. Pinto, D. & Clevers, H. Wnt, stem cells and cancer in the intestine. *Biology of the cell / under the auspices of the European Cell Biology Organization* **97**, 185-196 (2005).
87. Ilyas, M., Straub, J., Tomlinson, I.P. & Bodmer, W.F. Genetic pathways in colorectal and other cancers. *Eur J Cancer* **35**, 1986-2002 (1999).
88. Vogelstein, B. The Genetic Basis of Human Cancer. *McGraw-Hill Professional*, 821 (2002).
89. Powell, S.M. et al. APC mutations occur early during colorectal tumorigenesis. *Nature* **359**, 235-237 (1992).
90. Groden, J. et al. Identification and characterization of the familial adenomatous polyposis coli gene. *Cell* **66**, 589-600 (1991).
91. Kinzler, K.W. et al. Identification of FAP locus genes from chromosome 5q21. *Science* **253**, 661-665 (1991).
92. Munemitsu, S., Albert, I., Souza, B., Rubinfeld, B. & Polakis, P. Regulation of intracellular beta-catenin levels by the adenomatous polyposis coli (APC) tumor-suppressor protein. *Proceedings of the National Academy of Sciences of the United States of America* **92**, 3046-3050 (1995).
93. Rubinfeld, B. et al. Stabilization of beta-catenin by genetic defects in melanoma cell lines. *Science* **275**, 1790-1792 (1997).
94. Satoh, S. et al. AXIN1 mutations in hepatocellular carcinomas, and growth suppression in cancer cells by virus-mediated transfer of AXIN1. *Nature genetics* **24**, 245-250 (2000).
95. Behrens, J. et al. Functional interaction of an axin homolog, conductin, with beta-catenin, APC, and GSK3beta. *Science* **280**, 596-599 (1998).
96. Aberle, H., Bauer, A., Stappert, J., Kispert, A. & Kemler, R. beta-catenin is a target for the ubiquitin-proteasome pathway. *The EMBO journal* **16**, 3797-3804 (1997).

97. Marikawa, Y. & Elinson, R.P. beta-TrCP is a negative regulator of Wnt/beta-catenin signaling pathway and dorsal axis formation in Xenopus embryos. *Mechanisms of development* **77**, 75-80 (1998).
98. Ha, N.C., Tonozuka, T., Stamos, J.L., Choi, H.J. & Weis, W.I. Mechanism of phosphorylation-dependent binding of APC to beta-catenin and its role in beta-catenin degradation. *Molecular cell* **15**, 511-521 (2004).
99. Huber, A.H. & Weis, W.I. The structure of the beta-catenin/E-cadherin complex and the molecular basis of diverse ligand recognition by beta-catenin. *Cell* **105**, 391-402 (2001).
100. Graham, T.A., Weaver, C., Mao, F., Kimelman, D. & Xu, W. Crystal structure of a beta-catenin/Tcf complex. *Cell* **103**, 885-896 (2000).
101. Cox, R.T., Pai, L.M., Kirkpatrick, C., Stein, J. & Peifer, M. Roles of the C terminus of Armadillo in Wingless signaling in Drosophila. *Genetics* **153**, 319-332 (1999).
102. Felgner, P.L. et al. Lipofection: a highly efficient, lipid-mediated DNA-transfection procedure. *Proceedings of the National Academy of Sciences of the United States of America* **84**, 7413-7417 (1987).
103. Godbey, W.T., Wu, K.K. & Mikos, A.G. Poly(ethylenimine) and its role in gene delivery. *Journal of controlled release***60**, 149-160 (1999).
104. Kircheis, R., Wightman, L. & Wagner, E. Design and gene delivery activity of modified polyethylenimines. *Advanced drug delivery reviews* **53**, 341-358 (2001).
105. Liu, D., Ren, T. & Gao, X. Cationic transfection lipids. *Current medicinal chemistry* **10**, 1307-1315 (2003).
106. Zintchenko, A., Philipp, A., Dehshahri, A. & Wagner, E. Simple modifications of branched PEI lead to highly efficient siRNA carriers with low toxicity. *Bioconjugate chemistry* **19**, 1448-1455 (2008).
107. Klutz, K. et al. Image-guided tumor-selective radioiodine therapy of liver cancer after systemic nonviral delivery of the sodium iodide symporter gene. *Human gene therapy* **22**, 1563-1574 (2011).
108. Schafer, A. et al. Disconnecting the Yin and Yang Relation of Epidermal Growth Factor Receptor (EGFR)-Mediated Delivery: A Fully Synthetic, EGFR-Targeted Gene Transfer System Avoiding Receptor Activation. *Human gene therapy* **22**, 1463-1473 (2011).
109. Kim, H. & Muller, W.J. The role of the epidermal growth factor receptor family in mammary tumorigenesis and metastasis. *Experimental cell research* **253**, 78-87 (1999).
110. Spano, J.P. et al. Impact of EGFR expression on colorectal cancer patient prognosis and survival. *Annals of oncology* **16**, 102-108 (2005).
111. Zhu, Z.B. et al. Transcriptional targeting of tumors with a novel tumor-specific survivin promoter. *Cancer gene therapy* **11**, 256-262 (2004).
112. Ma, X.J., Huang, R. & Kuang, A.R. AFP promoter enhancer increased specific expression of the human sodium iodide symporter (hNIS) for targeted radioiodine therapy of hepatocellular carcinoma. *Cancer investigation* **27**, 673-681 (2009).
113. Lipinski, K.S. et al. Optimization of a synthetic beta-catenin-dependent promoter for tumor-specific cancer gene therapy. *Molecular therapy* **10**, 150-161 (2004).
114. Lipinski, K.S. et al. High-level, beta-catenin/TCF-dependent transgene expression in secondary colorectal cancer tissue. *Molecular therapy* **4**, 365-371 (2001).
115. Miller, N. & Whelan, J. Progress in transcriptionally targeted and regulatable vectors for genetic therapy. *Human gene therapy* **8**, 803-815 (1997).
116. Robson, T. & Hirst, D.G. Transcriptional Targeting in Cancer Gene Therapy. *Journal of biomedicine & biotechnology* **2003**, 110-137 (2003).
117. Mahmoudi, T. et al. The kinase TNIK is an essential activator of Wnt target genes. *The EMBO journal* **28**, 3329-3340 (2009).
118. Shitashige, M. et al. Traf2- and Nck-interacting kinase is essential for Wnt signaling and colorectal cancer growth. *Cancer research* **70**, 5024-5033 (2010).

119. De Toni, E.N. et al. OPG is regulated by beta-catenin and mediates resistance to TRAIL-induced apoptosis in colon cancer. *Clinical cancer research***14**, 4713-4718 (2008).
120. Takahashi, K. et al. Induction of pluripotent stem cells from adult human fibroblasts by defined factors. *Cell* **131**, 861-872 (2007).
121. Saigusa, S. et al. Correlation of CD133, OCT4, and SOX2 in rectal cancer and their association with distant recurrence after chemoradiotherapy. *Annals of surgical oncology* **16**, 3488-3498 (2009).
122. Fang, X. et al. ChIP-seq and functional analysis of the SOX2 gene in colorectal cancers. *Omics : a journal of integrative biology* **14**, 369-384 (2010).
123. Turm, H. et al. Protease-activated receptor-1 (PAR1) acts via a novel Galpha13-dishevelled axis to stabilize beta-catenin levels. *The Journal of biological chemistry* **285**, 15137-15148 (2010).
124. Sun, T.Q. et al. PAR-1 is a Dishevelled-associated kinase and a positive regulator of Wnt signalling. *Nature cell biology* **3**, 628-636 (2001).
125. Yam, P.Y. et al. Design of HIV vectors for efficient gene delivery into human hematopoietic cells. *Molecular therapy* **5**, 479-484 (2002).
126. Ogris, M. et al. The size of DNA/transferrin-PEI complexes is an important factor for gene expression in cultured cells. *Gene therapy* **5**, 1425-1433 (1998).
127. Navarro, G. et al. Low generation PAMAM dendrimer and CpG free plasmids allow targeted and extended transgene expression in tumors after systemic delivery. *Journal of controlled release* **146**, 99-105 (2010).
128. Egeblad, M. & Werb, Z. New functions for the matrix metalloproteinases in cancer progression. *Nature reviews. Cancer* **2**, 161-174 (2002).
129. Albini, A. et al. A rapid in vitro assay for quantitating the invasive potential of tumor cells. *Cancer research* **47**, 3239-3245 (1987).
130. Repesh, L.A. A new in vitro assay for quantitating tumor cell invasion. *Invasion & metastasis* **9**, 192-208 (1989).
131. Terranova, V.P. et al. Use of a reconstituted basement membrane to measure cell invasiveness and select for highly invasive tumor cells. *Proceedings of the National Academy of Sciences of the United States of America* **83**, 465-469 (1986).
132. Liotta, L.A. Tumor invasion and metastases: role of the basement membrane. Warner-Lambert Parke-Davis Award lecture. *The American journal of pathology* **117**, 339-348 (1984).
133. Harrington, W. et al. HIV Nef-M1 Effects on Colorectal Cancer Growth in Tumor-induced Spleens and Hepatic Metastasis. *Molecular and cellular pharmacology* **1**, 85-91 (2009).
134. Li, H. et al. Adenovirus-mediated delivery of a uPA/uPAR antagonist suppresses angiogenesis-dependent tumor growth and dissemination in mice. *Gene therapy* **5**, 1105-1113 (1998).
135. Hamada, K. et al. Liver metastasis models of colon cancer for evaluation of drug efficacy using NOD/Shi-scid IL2Rgammanull (NOG) mice. *International journal of oncology* **32**, 153-159 (2008).
136. Farkasova, K. *Dissertation* (2010).
137. Barker, N. & Clevers, H. Mining the Wnt pathway for cancer therapeutics. *Nature reviews. Drug discovery* **5**, 997-1014 (2006).
138. Gaedtke, L., Pelisek, J., Lipinski, K.S., Wrighton, C.J. & Wagner, E. Transcriptionally targeted nonviral gene transfer using a beta-catenin/TCF-dependent promoter in a series of different human low passage colon cancer cells. *Molecular pharmaceutics* **4**, 129-139 (2007).
139. Trainer, D.L. et al. Biological characterization and oncogene expression in human colorectal carcinoma cell lines. *International journal of cancer. Journal international du cancer* **41**, 287-296 (1988).
140. Pettersen, I., Bakkelund, W., Smedsrod, B. & Sveinbjornsson, B. Osteoprotegerin is expressed in colon carcinoma cells. *Anticancer research* **25**, 3809-3816 (2005).
141. Darmoul, D., Gratio, V., Devaud, H., Peiretti, F. & Laburthe, M. Activation of proteinase-activated receptor 1 promotes human colon cancer cell proliferation through epidermal growth factor receptor transactivation. *Molecular cancer research: MCR* **2**, 514-522 (2004).

142. Shi, X., Gangadharan, B., Brass, L.F., Ruf, W. & Mueller, B.M. Protease-activated receptors (PAR1 and PAR2) contribute to tumor cell motility and metastasis. *Molecular cancer research: MCR* **2**, 395-402 (2004).
143. Darmoul, D., Gratio, V., Devaud, H., Lehy, T. & Laburthe, M. Aberrant expression and activation of the thrombin receptor protease-activated receptor-1 induces cell proliferation and motility in human colon cancer cells. *The American journal of pathology* **162**, 1503-1513 (2003).
144. Park, E.T. et al. Aberrant expression of SOX2 upregulates MUC5AC gastric foveolar mucin in mucinous cancers of the colorectum and related lesions. *International journal of cancer. Journal international du cancer* **122**, 1253-1260 (2008).
145. Papailiou, J., Bramis, K.J., Gazouli, M. & Theodoropoulos, G. Stem cells in colon cancer. A new era in cancer theory begins. *International journal of colorectal disease* **26**, 1-11 (2011).
146. Ji, J. & Zheng, P.S. Expression of Sox2 in human cervical carcinogenesis. *Human pathology* **41**, 1438-1447 (2010).
147. Fuerer, C. & Nusse, R. Lentiviral vectors to probe and manipulate the Wnt signaling pathway. *PloS one* **5**, e9370 (2010).
148. Asciutti, S., Akiri, G., Grumolato, L., Vijayakumar, S. & Aaronson, S.A. Diverse mechanisms of Wnt activation and effects of pathway inhibition on proliferation of human gastric carcinoma cells. *Oncogene* **30**, 956-966 (2011).
149. Magnusson, T., Haase, R., Schleef, M., Wagner, E. & Ogris, M. Sustained, high transgene expression in liver with plasmid vectors using optimized promoter-enhancer combinations. *The journal of gene medicine* **13**, 382-391 (2011).
150. Klutz, K. et al. Epidermal growth factor receptor-targeted (131)I-therapy of liver cancer following systemic delivery of the sodium iodide symporter gene. *Molecular therapy : the journal of the American Society of Gene Therapy* **19**, 676-685 (2011).
151. Los, M. et al. Apoptin, a tumor-selective killer. *Biochimica et biophysica acta* **1793**, 1335-1342 (2009).
152. Sorin, V. et al. Regional therapy with DTA-H19 vector suppresses growth of colon adenocarcinoma metastases in the rat liver. *International journal of oncology* **39**, 1407-1412 (2011).
153. Fodde, R. & Brabletz, T. Wnt/beta-catenin signaling in cancer stemness and malignant behavior. *Current opinion in cell biology* **19**, 150-158 (2007).
154. Bandapalli, O.R. et al. Transcriptional activation of the beta-catenin gene at the invasion front of colorectal liver metastases. *The Journal of pathology* **218**, 370-379 (2009).
155. Zirvi, K.A., Najjar, T.A. & Slomiany, B.L. Sensitivity of human colon tumor metastases to anticancer drugs in athymic (nude) mice. *Cancer letters* **72**, 39-44 (1993).
156. Pillay, V., Dass, C.R. & Choong, P.F. The urokinase plasminogen activator receptor as a gene therapy target for cancer. *Trends in biotechnology* **25**, 33-39 (2007).
157. Brabletz, T. et al. Variable beta-catenin expression in colorectal cancers indicates tumor progression driven by the tumor environment. *Proceedings of the National Academy of Sciences of the United States of America* **98**, 10356-10361 (2001).
158. Hlubek, F. et al. Heterogeneous expression of Wnt/beta-catenin target genes within colorectal cancer. *International journal of cancer. Journal international du cancer* **121**, 1941-1948 (2007).
159. Grayson, A.C., Doody, A.M. & Putnam, D. Biophysical and structural characterization of polyethylenimine-mediated siRNA delivery in vitro. *Pharmaceutical research* **23**, 1868-1876 (2006).

8. Appendix

8.1. Supplementary data

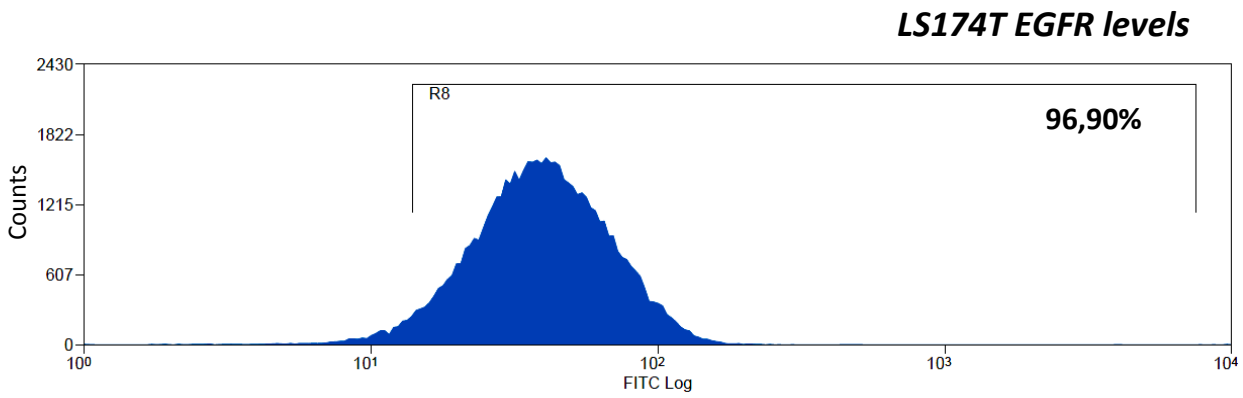

Fig.S1. LS174T EGFR determination via FACS analysis

Levels of EGFR on the surface of LS174T were analyzed via flow cytometry where $2x10^6$ LS174T cells were trypsinized and washed twice with PBS. Cells were incubated with a murine anti-EGFR IgG antibody for 2 hours at room temperature and subsequently with a compatible anti-IgG-Alexa488 antibody for 45 min at room temperature in the dark. The IgG control sample was used to calibrate cell scattering in the non-fluorescent range and for final analysis 50 000 events were gated.

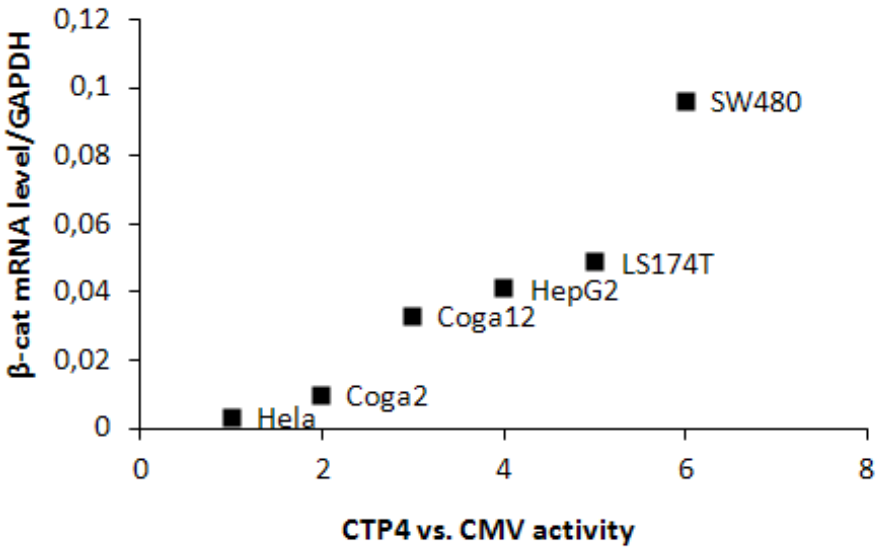

Fig.S2. Correlation of specific CTP4-activity and β-catenin mRNA levels

Coga2, Coga12, HepG2, LS174T, SW480 and Hela cells were transfected with a CTP4-regulated FLuc as well as a CMV-Luc construct, ratio of fold-increase in CTP4 activity over the CMV promoter was compared to the overall β-catenin levels determined with qPCR.

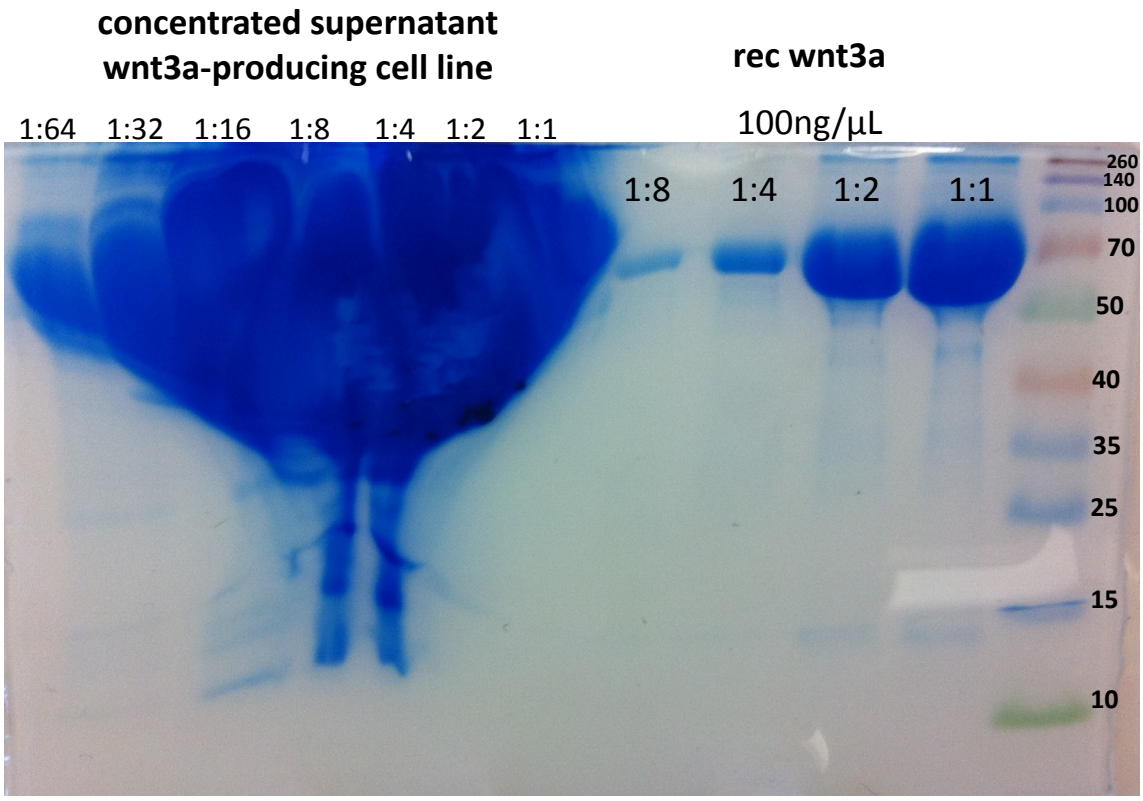

Fig.S3. Coomassie Blue stained polyacrylamidegel for L-wnt3A supernatant and recombinant wnt3a

The supernatant of L-wnt3A, a wnt3a-producing cell line, was concentrated and resuspended in RPMI medium, additionally recombinant wnt3a protein was dissolved in cell culture media at a concentration of 100ng/µL. Serial dilutions of both were loaded onto a polyacrylamide gel and stained with coomassie blue. Size of wnt3a protein is 37kDa (dimerization on gel).

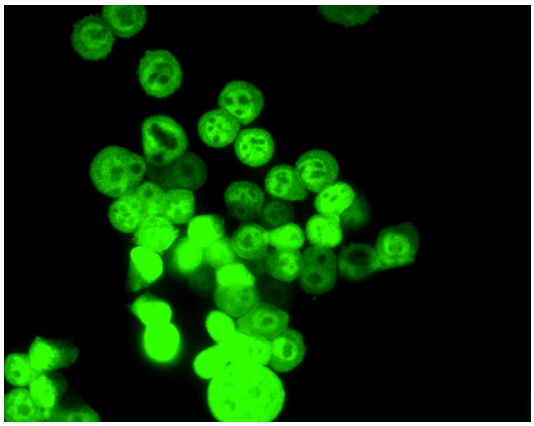

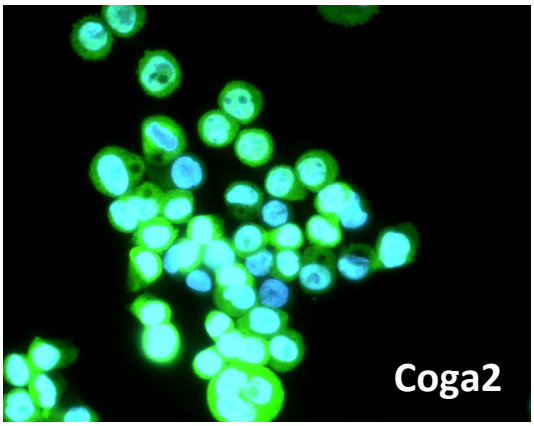
Coga2

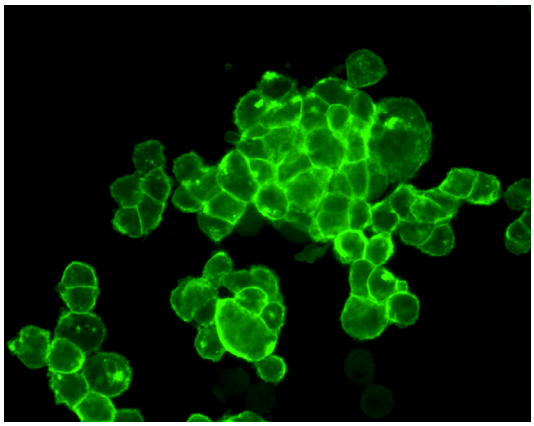

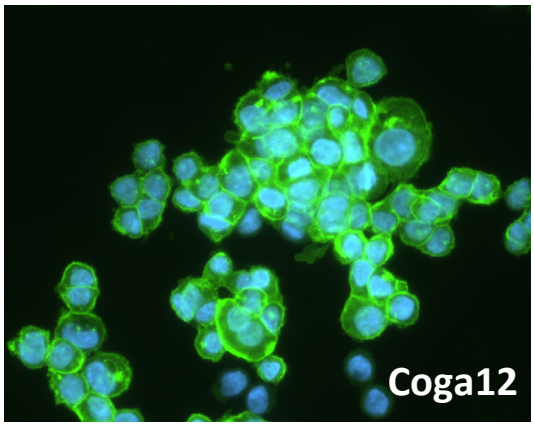
Coga12

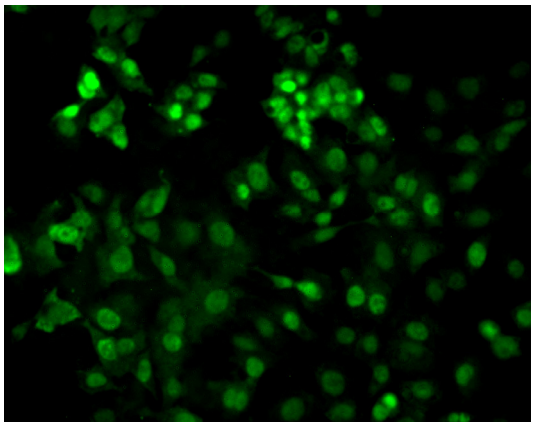

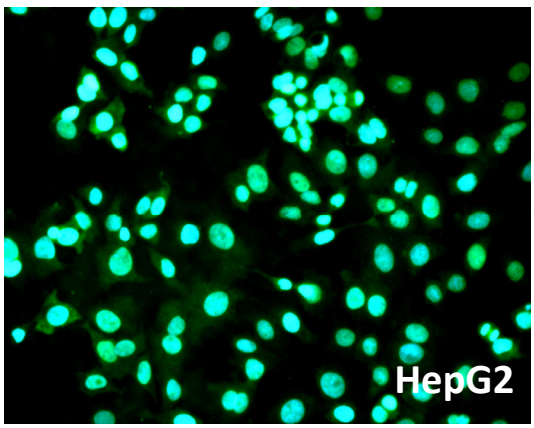
HepG2

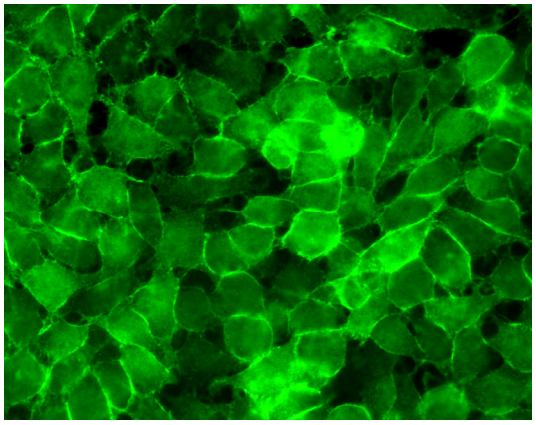

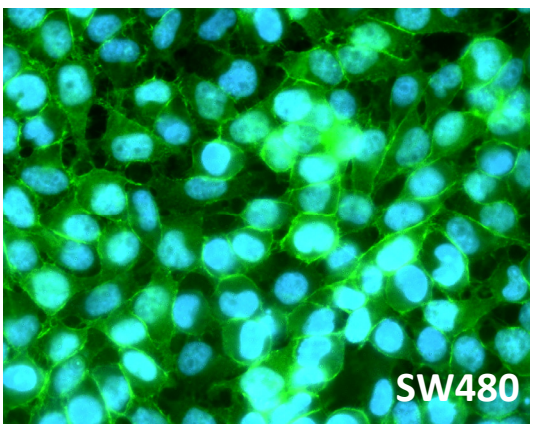
SW480

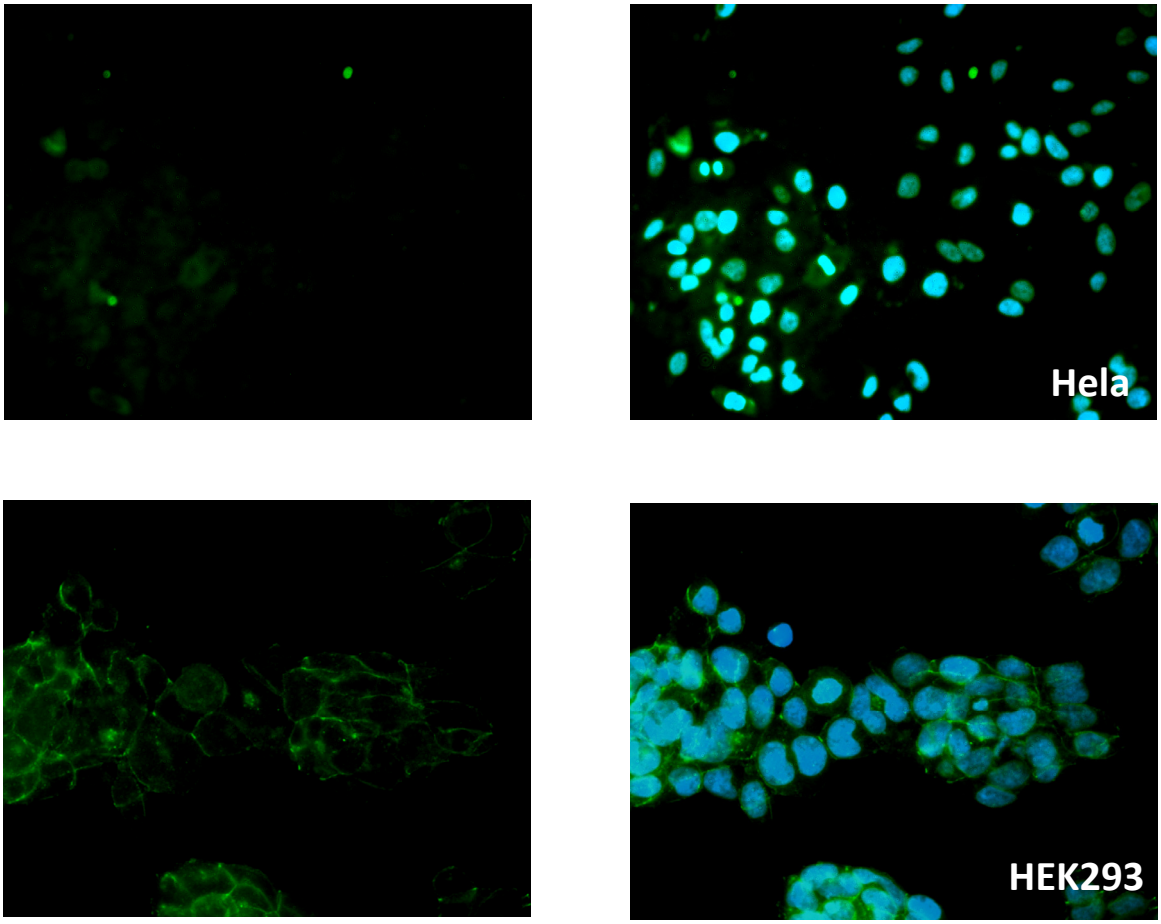

Fig.S4. Target cells stained for β-catenin level

Immunofluorescence of β-catenin in Coga2, Coga12, HepG2, SW480, Hela and HEK293 cells stained with an Alexa488 labelled secondary antibody. Cells were grown in chamber slides for 24 hours, fixed with 4% PFA and permeabilzed with methanol. After incubation with the primary β-catenin antibody, cells were stained with an Alexa488-secondary antibody and counterstained with DAPI. Two separate images are shown with β-catenin staining alone (left panel) or overlay of β-catenin and DAPI staining (right panel).

NMRI nu/nu	heart	liver	spleen	lung	kidneys	body weight [g]
Mouse 1	193,2 mg	1647,4 mg	233,5 mg	189,4 mg	464,6 mg	27,8
Mouse 2	141,1 mg	1571,2 mg	203,1 mg	193,8 mg	392,6 mg	27,0
Mouse 3	135,9 mg	1366,1 mg	147,7 mg	175,7 mg	389,5 mg	25,5
Mouse 4	149,8 mg	1527,3 mg	244,5 mg	191,8 mg	421,9 mg	27,5
Mouse 5	166,7 mg	1543,1 mg	224,8 mg	193,6 mg	413, 5 mg	26,3
Mouse 6	196,5 mg	1612,9 mg	188,9 mg	200,6 mg	415,0 mg	27,7
Mouse 7	145,1 mg	1402,1 mg	176,1 mg	177,9 mg	385,3 mg	26,0
mean	**161,19 mg**	**1524,30 mg**	**202,66 mg**	**188,97 mg**	**411,48 mg**	26,8

Fig.S5 Organ weight control of non-tumor bearing wt NMRI nu/nu mice

Heart, liver, spleen, lung and kidneys of seven female NMRI nu/nu mice (7 weeks old) were removed and weighed. Before organ removal body weight of all mice was determined.

8.2. List of siRNA and qPCR primer sequences

siRNA sequences	
ß-catenin (Thermo Scientific, Waltham/MA, USA)	5‘-ACAAGUAGCUGAUAUUGAUUU-3‘
PAR-1 (Ambion, Austin/TX, USA)	5‘-GCAUUUUACUGUAACAUGUdTdT-3‘
OPG (Ambion, Austin/TX, USA)	5‘-GUACCUUCAUUAUGACGAAdTdT-3‘
TNIK (Ambion, Austin/TX, USA)	5‘-GCUAGUUGAUCUCACGGUAdTdT-3‘
TCF4 (Ambion, Austin/TX, USA)	5‘-GCUCUGAGAUCAAAUCCGAdTdT-3‘
Sox2 (Thermo Scientific, Waltham/MA, USA)	5‘-GCUCGCAGACCUACAUGAAdTdT-3‘
control siRNA (Thermo Scientific, Waltham/MA, USA)	5‘-AUGUAUUGGCCUGUAUUAGUU-3‘

qPCR primer sequences		
ß-catenin (Probe # 8)	FWD 5’-TGTTAAATTCTTGGCTATTACGACA-3’	REV 5’-CCACCACTAGCCAGTATGATGA-3’
TCF4 (Probe # 79)	FWD 5’-TGGGTTGAGAACTGCTACTCG-3’	REV 5’-GCCCGTCCAAGAGATAATGT-3’
PAR-1 (Probe # 68)	FWD 5’-ATCTGGGCTTTGGCCATC-3’	REV 5’-ACCTGGATGGTTTGCTCCT-3’
TNIK (Probe #63)	FWD 5’-GCGGAGCATGAACAGGAA-3’	REV 5’-GCTGCTGCAAGATCTCTAACTGAT-3’
OPG (Probe #17)	FWD 5’-GAAGGGCGCTACCTTGAGAT-3’	REV 5’-GCAAACTGTATTTCGCTCTGG-3’
Sox2 (Probe #35)	FWD 5’-TTGCTGCCTCTTTAAGACTAGGA-3’	REV 5’-CTGGGGCTCAAACTTCTCTC-3’

8.4. Plasmid maps

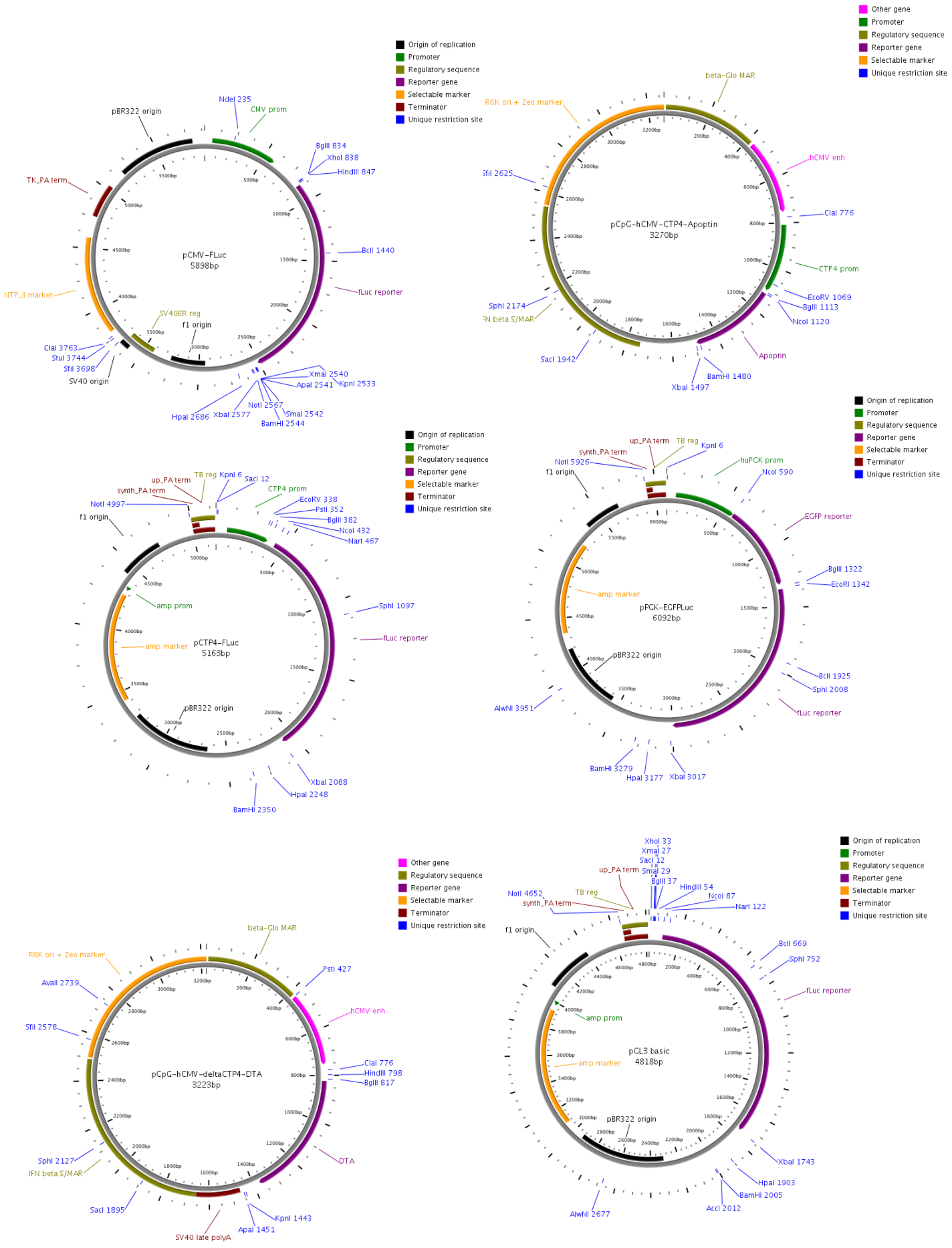

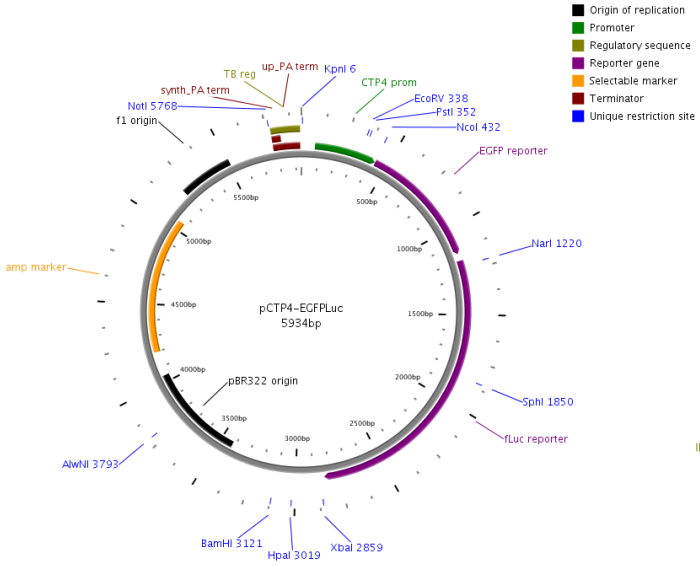
Origin of replication
Promoter
Regulatory sequence
Reporter gene
Selectable marker
Terminator
Unique restriction site
pCTP4-EGFPLuc
5934bp
up_PA term
Kpnl 6
TB reg
synth_PA term
NotI 5768
f1 origin
CTP4 prom
EcoRV 338
PstI 352
NcoI 432
EGFP reporter
NarI 1220
SphI 1850
fLuc reporter
BamHI 3121
HpaI 3019
XbaI 2859
AlwNI 3793
amp marker
pBR322 origin

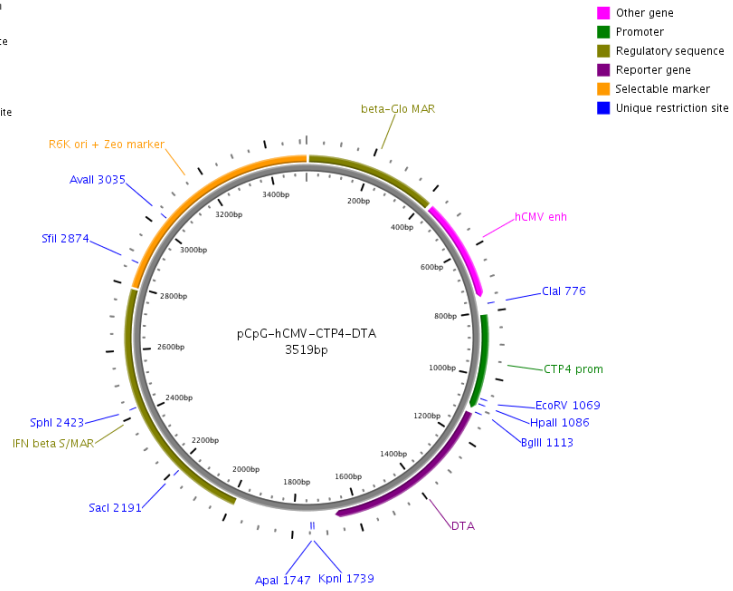
Other gene
Promoter
Regulatory sequence
Reporter gene
Selectable marker
Unique restriction site
pCpG-hCMV-CTP4-DTA
3519bp
beta-Glo MAR
R6K ori + Zeo marker
AvaII 3035
SfiI 2874
hCMV enh
ClaI 776
CTP4 prom
EcoRV 1069
HpaII 1086
BglII 1113
DTA
SphI 2423
IFN beta S/MAR
SacI 2191
ApaI 1747
KpnI 1739

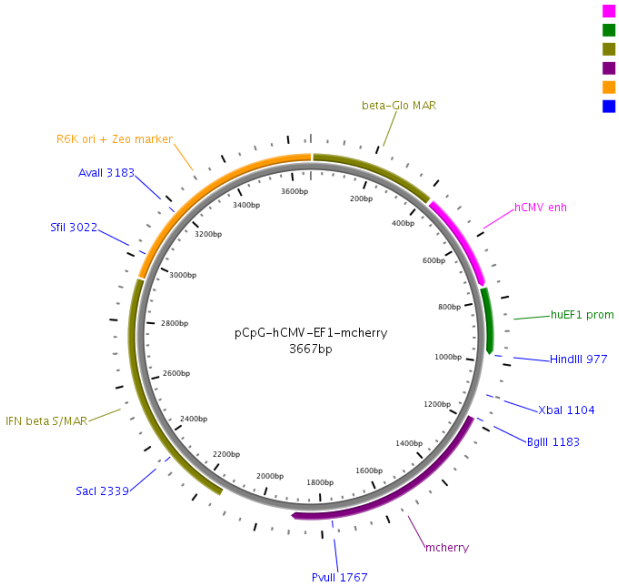
Other gene
Promoter
Regulatory sequence
Reporter gene
Selectable marker
Unique restriction site
pCpG-hCMV-EF1-mcherry
3667bp
beta-Glo MAR
R6K ori + Zeo marker
AvaII 3183
SfiI 3022
hCMV enh
huEF1 prom
HindIII 977
XbaI 1104
BglII 1183
mcherry
PvuII 1767
SacI 2339
IFN beta S/MAR

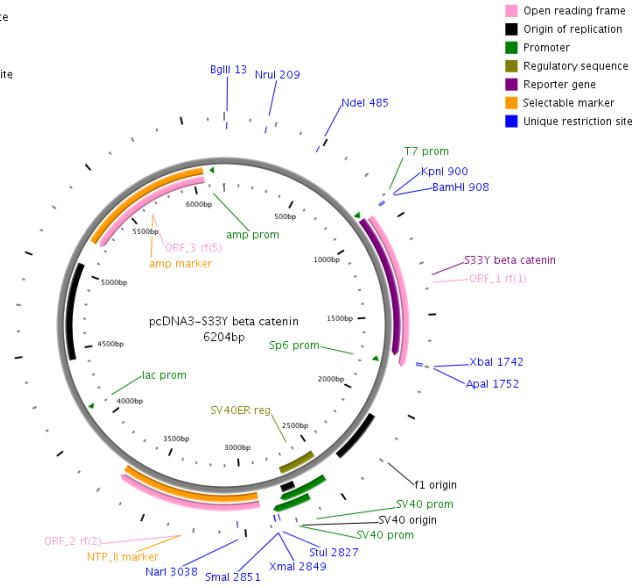
Open reading frame
Origin of replication
Promoter
Regulatory sequence
Reporter gene
Selectable marker
Unique restriction site
pcDNA3-S33Y beta catenin
6204bp
BglII 13
NruI 209
NdeI 485
T7 prom
KpnI 900
BamHI 908
amp prom
ORF_3 rf(5)
amp marker
S33Y beta catenin
ORF_1 rf(1)
Sp6 prom
lac prom
XbaI 1742
ApaI 1752
SV40ER reg
f1 origin
SV40 prom
SV40 origin
SV40 prom
StuI 2827
XmaI 2849
SmaI 2851
NarI 3038
ORF_2 rf(2)
NTP_II marker

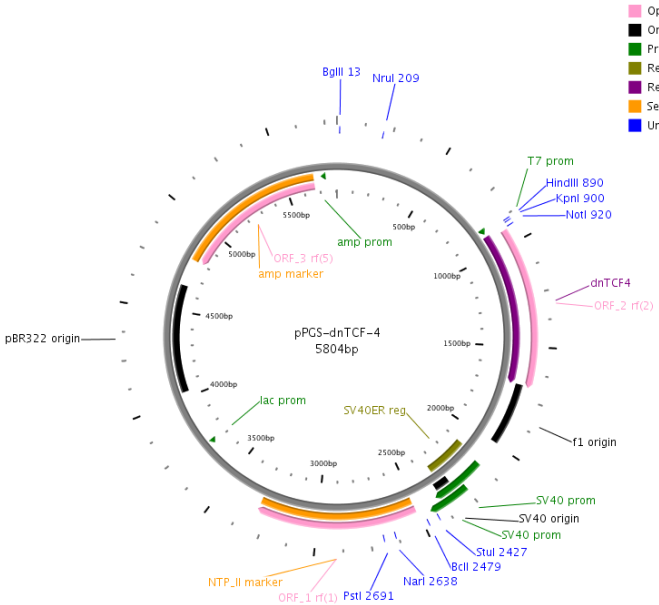
Open reading frame
Origin of replication
Promoter
Regulatory sequence
Reporter gene
Selectable marker
Unique restriction site
pPGS-dnTCF-4
5804bp
BglII 13
NruI 209
T7 prom
HindIII 890
KpnI 900
NotI 920
amp prom
ORF_3 rf(5)
amp marker
dnTCF4
ORF_2 rf(2)
pBR322 origin
lac prom
SV40ER reg
f1 origin
SV40 prom
SV40 origin
SV40 prom
StuI 2427
BclI 2479
NarI 2638
PstI 2691
ORF_1 rf(1)
NTP_II marker

8.4. List of Abbreviations

°C	Degree Celsius
Amp	Ampicillin
APC	Adenomatosis polyposis coli
ATCC	American type culture collection
bp	Base pairs
brPEI	Branched polyethylenimine
BSA	Bovine serum albumin
CMV	Cytomegalovirus
DAPI	4',6-Diamidino-2-phenylindole
DMEM	Dulbecco's Modified Eagle Medium
DMSO	Dimethyl sulfoxide
DNA	Desoxyribonucleic acid
DSMZ	German collection of microorganisms and cell cultures
E.coli	Escherichia coli
EGFP	Enhanced green fluorescent Protein
EGFR	Epidermal growth factor receptor
ELISA	Enzyme linked Immunosorben Assay
FACS	Fluorescence associated cell sorting
FBS	Fetal bovine serum
FITC	Fluorescein isothiocyanate
g	Relative centrifugal force
GFP	Green fluorescence protein
GSK-3β	Glycogen synthase kinase 3β
HBG	HEPES-buffered glucose
HEPES	4-(2-hydroxyethyl)-1-piperazineethanesulfonic acid
Kb	Kilo base pairs
kDa	Kilo Dalton
LB	Lysogeny broth
LEF	lymphoid enhancer-binding factor
Luc	*Photinus pyralis* Luciferase
LPEI	Linear polyethylenimine
MTT	(3-(4,5-Dimethylthiazol-2-yl)-2,5-diphenyltetrazolium bromide

MW	Molecular weight
NaCl	Sodium chloride
N/P	ratio number of protonable nitrogens to phosphates
OD	Optical density
pDNA	Plasmid DNA
PCR	polymerase chain reaction
PBS	Phosphate buffered saline
PEG	Polyethylene glycol
PEI	Polyethylenimine
PGK	Phosphoglycerate kinase
PVDF	Polyvinylidene fluoride
RISC	RNA-induced silencing complex
RLU	Relative light units
RNA	Ribonucleic acid
RNAi	RNA interference
rpm	Revolutions per minute
RPMI	Roswell Park Memorial Institute
RT	Room temperature
s.e.m.	standard error of the mean
siRNA	Small interfering RNA
Succ	Succinyl
TCF	tumor cell factor
Tris	Tris(hydroxymethyl)aminomethane
UV	Ultraviolet
V	Volt
v/v	Volume for volume
w/w	Weight for weight
WB	Western-Blot

8.5. Curriculum Vitae and publications

PERSONAL DATA

Address:	Arzu Cengizeroglu
	Karl-Richter-Strasse 3
	80939 München
Marital status:	unmarried
Date of birth:	07.10.1982
Place of birth:	Augsburg

EDUCATION

08/1993 – 06/2002	A.B. von Stettensches Institut, Augsburg Final secondary-school examination (Abitur), Grade awarded: 1,8
10/2003 – 08/2006	Technical University Munich (TUM), Munich Biology studies (B.Sc.), overall grade awarded: 1.5
09/2006 – 12/2006	Hong Kong University of Science and Technology (HKUST), HK SAR Semester abroad with LAOTSE exchange programme as full-time student
01/2007 – 04/2007	Ludwig Institute of Cancer Research (LICR), Melbourne Internship as visiting student, overall grade awarded: A
04/2007 – 07/2008	Technical University Munich (TUM), Munich Biology studies (M.Sc.), overall grade awarded: 1.2
09/2008 – 12/2011	Ludwig-Maximilians-Universität (LMU), München Dept. Pharmaceutical Biology-Biotechnology, Doctoral Thesis

EMPLOYMENT

09/2004 – 03/2005	Technical University Munich (TUM), Weihenstephan Working student (Hilfswerkstudent)
04/2007 – 07/2008	University Hospital of the Technical University Munich, Munich Working student (Hilfswerkstudent)
08/2008 – 12/2011	Nanosystem Initiative Munich (NIM), Munich Mentor at the NIM-mentoring program for pupils (age 16-19)
01/2010 – dato	Deutsches Museum, Munich Supervision of experimental courses in the DNA Visitors' Laboratory

PUBLICATIONS

Original Papers

Sanchez-Antequera Y, Mykhaylyk O, van Til NP, Cengizeroglu A, de Jong JH, Huston MW, Anton M, Johnston IC, Pojda Z, Wagemaker G, Plank C, *Magselectofection: an integrated method of nanomagnetic separation and genetic modification of target cells.* Blood, 2011 Apr 21; 117(16):e171-81. Epub 2011 Feb 28.

Su B, Cengizeroglu A, Farkasova K, Anton M, Ellwart J, Haase R, Wagner E, Ogris M, *Systemic TNF alpha gene therapy synergizes with liposomal doxorubicine in the treatment of metastatic cancer.* submitted

Manuscripts in Preparation

Cengizeroglu A, Farkasova K, Haase R, Anton M, Pagel J I, Bolcato-Bellemin AL, Ellwart J, Deindl E, Erbacher P, Wagner E, Ogris M, *siRNA based approach to study the influence of tumorigenicity-related wnt-targets*, in preparation

Farkasova K, Cengizeroglu A, Haase R, Ellwart J, Wagner E, Ogris M, *Luciferase-based dual bioluminescence imaging of tumor metastases after systemic transgene delivery with a synthetic gene carrier,* in preparation

Fröhlich T, Edinger D, Troiber C, Salcher E, Badgujar N, Martin I, Schaffert D, Cengizeroglu A, Hadwiger P, Vornlocher HP, Wagner E, *Structure-activity relationships of sequence-defined oligo (ethane amino) amides for siRNA delivery,* in preparation

Poster Presentation

Cengizeroglu A, Farkasova K, Deutsch D, Haase R, Anton M, Wagner E, Ogris M. (2010) *Harnessing Molecular Targets in Human Colon Cancer Cells for Tumor Specific RNAi and pDNA-based Therapies.* 7th Annual Meeting of German-Society-for-Gene-Therapy (DG-GT e.V.) OCT 07-09, 2010 LMU Campus Großhadern, Munich, GERMANY Human Gene Therapy 21: 1205 – 1205.

Farkasova K, Cengizeroglu A, Haase R, Anton M, Ellwart J, Wagner E, Ogris M. (2010) *Luciferase-Based Dual Bioluminescence Imaging of Tumor Metastases After Systemic Transgene Delivery with a Synthetic Gene Carrier.* 7th Annual Meeting of German-Society-for-Gene-Therapy (DG-GT e.V.) OCT 07-09, 2010 LMU Campus Großhadern, Munich, GERMANY Human Gene Therapy 21: 1186 – 1186.

8.6. Acknowledgements

The past three years which eventually resulted in the completion of my PhD thesis were both the most challenging and the most rewarding times of my life. With the next chapter of my life with new people and places to encounter, I feel obliged to look back and thank those without whom this piece of work would not have been possible. First and foremost, I want to thank with all my heart my direct supervisor Dr.Manfred Ogris for his support on every conceivable level. Without his constant guidance which put me back on track when necessary, his optimism and sense of humor I would not have been able to complete my work. He was the best supervisor any PhD student could ask for, even getting his „own hands dirty“ in the animal house. His generosity, scientific guidance and support will never be forgotten. I am very grateful to Prof.Dr.Ernst Wagner for giving me the opportunity to perform my work in his laboratories and giving me the scientific freedom to follow my project, although it seemed at times that the final destination was not always obvious. I could always rely on his honest, fair and scientifically sound input – for this I will always be deeply thankful. The most heart-felt thanks will have to go to my beloved friend Katarina Farkasova, it was her relentless optimism and support, sacrificing her free time to perform all my animal experiment, which made my thesis possible – without her my thesis could not be completed. The other person of utter importance to me and my work was Dr. Rudolf „Rudi“ Haase - my „cloning guru“ responsible for most plasmids utilized in this work. He was a great lab mate and I will not forget his professional input regarding the art of cloning.

Also, I would like to thank Dr. Martina Rüffer for her help with student courses and general organization issues. To Ursula Biebl and Anna Kulinyak I am grateful for taking care of all „last minute“ requests when there was more to do than time available. My special thanks go to Wolfgang Rödl for truly being a „jack of all trades“ and coming to my rescue more times than I can count. Finally I want to dearly thank Markus Kovac for his warm-hearted friendship, fascinating insights into the male psyche and being so openly candid especially after a couple of beers. Last but not least I want to thank Olga Brück for helping out with all administrative tasks. I would like to thank all PhD students and postdoctoral fellows I had the opportunity to work with. I was fortunate enough to work with many inspiring and kind colleagues, especially Christian Marfels, Edith Salcher and Kevin Maier were my dearest companions during the last three years and I will always cherish my time with them. Finally, I want to thank my friends and family for their love and trust in me, but also their patience during stressful times when I was preoccupied with my work. Especially the unconditional love of my parents gave me strength and patience to tackle all obstacles completing my PhD thesis. Without Lukas, my askim, I could not have done this, he always helped me to find inner peace and the will power to ignore those who were harmful and endure difficult times accepting them for what they are – an inevitability.

Without all of you I could not have done this.